



City Research Online

City, University of London Institutional Repository

Citation: Devi, P. (2025). Depth perception and depth-related visuomotor performance with normal, reduced, and absence of binocularity. (Unpublished Doctoral thesis, City St George's, University of London)

This is the accepted version of the paper.

This version of the publication may differ from the final published version.

Permanent repository link: <https://openaccess.city.ac.uk/id/eprint/35638/>

Link to published version:

Copyright: City Research Online aims to make research outputs of City, University of London available to a wider audience. Copyright and Moral Rights remain with the author(s) and/or copyright holders. URLs from City Research Online may be freely distributed and linked to.

Reuse: Copies of full items can be used for personal research or study, educational, or not-for-profit purposes without prior permission or charge. Provided that the authors, title and full bibliographic details are credited, a hyperlink and/or URL is given for the original metadata page and the content is not changed in any way.

Depth perception and depth-related visuomotor performance with normal, reduced, and absence of binocularity

Preetirupa Devi

*Department of Optometry & Visual Science,
City St George's, University of London, United Kingdom*

and

Hyderabad Eye Research Foundation, L V Prasad Eye Institute, India



Dissertation submitted to City St George's, University of London in fulfilment of the requirements for the degree of Doctor of Philosophy

March, 2025

Contents

Declaration	6
List of tables.....	7
List of Figures.....	8
Acknowledgement.....	13
Abstract	14
Chapter 1 Overview	16
1.1 General introduction	16
1.2 Disruption in binocularity	18
1.3 Outline of the dissertation.....	19
Chapter 2 Literature review.....	21
2.1 Depth perception	21
2.1.1 Types of depth perception	23
2.1.2 Perspective geometry	24
2.1.3 Depth from motion parallax.....	28
2.1.4 Similarities between depth perceived from retinal disparity and motion parallax.....	31
2.1.5 Bayesian framework of depth cues combination	35
2.2 Depth cues for visuomotor task.....	40
2.3 Evidence for plasticity of visual performance	44
2.4 Rationale and aim of the studies	48
Chapter 3 Depth-related visuomotor task performance in the absence of binocularity.....	53
3.1 Introduction	53
3.2 Methods.....	56
3.2.1 Participants	56
3.2.2 The buzz-wire apparatus	59
3.2.3 The buzz-wire task	59
3.2.4 Determination of the key outcome variables in the buzz-wire task.....	61

3.2.5	Determination of the error location in the buzz-wire task	62
3.2.6	Analysis of head movements.....	63
3.2.7	Statistical analysis	65
3.3	Results.....	67
3.3.1	Repeatability of error rate and speed across the three buzz-wire trials	67
3.3.2	Cohort-level task performance.....	69
3.3.3	Multivariate analysis of task performance in controls.....	69
3.3.4	Multivariate analysis of task performance in the uniocular cases ...	73
3.3.5	Analysis of the location of the error in the buzz-wire task.....	75
3.3.6	Analysis of head movements.....	76
3.4	Discussion.....	79
3.4.1	Summary of the results	79
3.4.2	Is the buzz-wire task sensitive enough to pick the differences in task performance with and without binocular disparity?	80
3.4.3	The effect of age on performance	81
3.4.4	Is the task performance of uniocular individuals better than expectations from chronological maturity?	83
3.4.5	Larger head movements but limited utility to dynamic visuomotor task performance.....	84
3.4.6	Role of proprioceptive feedback in the buzz-wire task performance	86
Chapter 4 Depth-related visuomotor performance in degraded binocularity ..		87
4.1	Introduction	87
4.2	Methods.....	89
4.2.1	Participants	89
4.2.2	The buzz-wire apparatus and task performance	91
4.2.3	Measurement of stereo threshold	91
4.2.4	Protocol	92
4.2.5	Schematic framework for data interpretation.....	93
4.2.6	Data analyses	95

4.2.7 Comparison of buzz-wire performance in cases with those of uncorrected myopes.....	96
4.3 Results.....	97
4.3.1 Buzz-wire task performance in controls and cases	97
4.3.2 Relationship between stereo threshold and binocular advantage in error rate	101
4.3.3 Impact of rigid contact lenses on the error rates of the cases	103
4.3.4 Buzz-wire task performance of uncorrected myopes	103
4.4 Discussion.....	105
4.4.1 Summary of results	105
4.4.2 Stereo threshold as a poor predictor of visuomotor task performance	106
4.4.3 Retinal image quality and its impact on visuomotor task performance	108
4.4.4 Clinical implications.....	111
Chapter 5 Exploration of usage of monocular cues for perception of depth..	113
General introduction	113
5.1 Part 1.....	113
5.1.1 Introduction	113
5.1.2 Method	115
5.1.3 Result	121
5.1.4 Discussion	125
5.2 Part 2.....	128
5.2.1 Introduction	128
5.2.2 Methods.....	130
5.2.3 Results.....	133
5.2.4 Discussion	135
Chapter 6 General summary and discussion.....	140
6.1 Summary of results.....	140
6.2 Contribution to science	142
6.3 Future direction.....	143

6.3.1 Neural Adaptation and Motion Parallax in the Absence of Binocularity.....	144
6.3.2 Compensatory Monocular Cues and Training Strategies	144
6.4 Conclusion	145
References	146
Appendix 1.....	155
A1. Demographic details	155
Appendix 2.....	156
A2.1 Ethic certificate (LVPEI).....	156
A2.2 Ethic certificate (City St. George’s University of London)	159

Declaration

I, Preetirupa Devi, confirm that the work presented in this thesis is my own. The work included in this thesis has not been submitted anywhere else for a degree/qualification.

Chapter 3 and 4 of the thesis has been published in Investigative Ophthalmology and Visual Science (Devi et.al., 2024, IOVS and Devi et al., 2025, IOVS).

Parts of the dissertation have been presented at various national and international conferences.

List of tables

<i>Table 3-1 Demographic details of controls and cases and the cause of uniocularly in cases that participated in the study. Chronological age and the age and duration of uniocularly are reported as median (25th – 75th quartiles).</i>	58
<i>Table 3-2 The results of five-way RM-MANOVA comparing the binocular and monocular task performance of controls. Multivariate test results are shown for the main effects and interaction between relevant independent variable pairs</i>	71
<i>Table 3-3 The results of step-wise multiple regression investigating the relationship between the error rate with uniocular participant's age alone and upon adding the duration of uniocularly into the regression model</i>	74
<i>Table 3-4 Results of the two-way MANOVA comparing the head movements made by controls under binocular and monocular conditions, and by uniocular participants</i>	79
<i>Table 4-1 Demographic and clinical details of study participants</i>	98
<i>Table 4-2 Results of the main statistical analyses conducted in this study</i>	100
<i>Table 5-1 Results of the main statistical analyses conducted for the perceptual buzz-wire task</i>	123

List of Figures

Figure 1.1 A and B can be cross-fused to see the depth of the desk. (C) The painting ‘The Montefeltro Altarpiece’ by Piero Della Francesca. (D) shows an enlarged portion of the suspended egg in the middle of the dome of (A). Taken from {Tyler, 2020 #185@@author-year}.	17
Figure 2.1 Schematic diagrams to represent the different types of depth. A. represents the hyperacuity where the two fronto-parallel planes are separated by a step. B. represents the super-resolution or pyknostereopsis where the surface appears thickened. C. represents the diastereopsis, where the two fronto-parallel surfaces appear to be separated by empty space between them. D and E. represent the shape of a surface in terms of slant (D) and curvature (E) using texture cue. Figure A-C is taken from {Stevenson, 1989 #60@@author-year}, D is adapted from {Saunders, 2015 #195@@author-year} and E is taken from {Landy, 1995 #113@@author-year}.	24
Figure 2.2 A, B, C, and D shows the schematic ray diagram for image formation on the retina. Panel A shows the basic projection geometry of an object OI on the image plane or the retina and forming the image $O'I'$. The dotted lines denote the projection lines. Panel B) Schematic of relative size depth cue. Object O_1I_1 at a farther distance (D) forms a relatively smaller image compared to object O_2I_2 placed at a closer distance of ΔD from the nodal point (P). Panel C) Schematic of binocular retinal disparity. The object O_1 and O_2 form their images on the non-corresponding points of the retina of the two eyes resulting in visual angle differences ($\theta_1 > \theta_2$). Panel D) Schematic of motion parallax. While the objects O_1 and O_2 are stationary, one eye moves from one position to the other, resulting in visual angle differences ($\theta_1 > \theta_2$).	26
Figure 2.3 Extent of perceived depth (A) and perceived motion (B) as a function of head movement (left-side bars) versus no head movement (right-side bars), 6" disparity (front bars) versus 1°52" disparity (back bars), and profile of the gradient (sine, triangle, saw, or square waveform). Taken from {Ono, 1990 #178@@author-year}.	30
Figure 2.4 Disparity (open symbols) and motion parallax (closed symbols) threshold as a function of spatial frequency for three subjects (A, B, C) Taken from {Rogers, 1982 #121@@author-year}.	32
Figure 2.5 Matched stereo-specified slant (A) and curvature (B) as a function of motion-specified slant. The dashed line gives the results expected when observers judge the slants of motion- and stereo-specified surface patches equal. The three curves represent three subjects. Error bars indicate the measurement error. Taken from {de Vries, 1995 #123@@author-year}.	33
Figure 2.6 Flow of signals from retina project through LGN to V1 and higher cortical regions. Taken from {Kandel, 2000 #125@@author-year}.	35
Figure 2.7 Flow diagram showing A. Strong fusion, B. Weak fusion, C. Modified weak fusion models. ‘d’ denotes depth represented by individual depth cues, and ‘r’ denotes the depth denoted by the ancillary cues. Taken from {Landy, 1995 #113@@author-year}.	39
Figure 2.8 Distribution of cells based on eye dominance. Categories 1 and 7 include neurons that respond exclusively to the left or right eye, respectively and 4 are equally influenced by both eyes. Panel A) neurons from normal monkeys. Panels B–D) neurons with right eye deprived of vision through lid sutures for different	

durations, all starting at four weeks of age. Panel E) neurons from a monkey with binocular deprivation via lid suture between the 2nd and 8th weeks of life. The ND (non-driven) column indicates the number of cells that did not respond to visual stimulation. Taken from Crawford et al. (1975). 46

Figure 2.9 The average stereo and motion parallax depth threshold values for binocular controls (normal) and amblyopes. Taken from Thompson and Nawrot (1999). 48

Figure 3.1 A) Buzz-wire experimental setup from the participant's view with key elements highlighted. B) The unbent buzz-wire used in this study. C) Representative stereoscopic image depicting the position of the metal loop and the wire track in depth. To view the stereogram in-depth, either fuse the left and middle panels by converging the eyes or fuse the middle and right panels by diverging the eyes. D) Representative screenshot of a spectrogram obtained using the Audacity software, with markings for completion time and the epochs of error time (high contrast tracks in the spectrogram). E – G) Representative images of the loop position during the straight (E), transition (F), and curved (G) portions of the wire track. H – J) Representative frames of head tracking performed by the OpenFace software: successful tracking in binocular (H) and monocular (I) views, and failed tracking (J). Consent was obtained from the participants shown above to use their pictures in this figure. 57

Figure 3.2 Bland-Altman plots for error rate (A) and speed (B) observed across the three trials of the buzz-wire task with depth modulation under head-free viewing for individual controls under binocular (green) and monocular (red) viewing conditions (top panel) and for the uniocular participants (bottom panel). The left columns compare data obtained from trials 1 and 2, the middle columns compare data obtained from trials 2 and 3 and the right columns compare data obtained from trials 1 and 3. In each panel, the solid black line represents the mean difference, with the value $\text{mean} \pm 1\text{SD}$ of the mean mentioned on the right side of the line. The upper and lower edge of the coloured box indicates the upper and lower limits of agreement, respectively, with the specific value specified on the right of the edges. 68

Figure 3.3 Violin plot pairs showing the distribution of the error rate (panel A) and speed (panel B) for the binocular and monocular viewing of controls and uniocular cases while they performed the buzz-wire tasks with depth modulation under head-free viewing conditions Each violin plot is constructed with a kernel density that was calculated by taking the maximum and minimum data range for each outcome variable in a given cohort and dividing it into ten equal bins. Superimposed within the violin plots are box and whisker plots, with the central yellow solid line within each plot, indicating the median value, the notch of the box indicating the 95% confidence interval of the median and the edges of the box indicating the 25th and 75th percentile. The violin plot is truncated at the 1st and 99th percentile. The circles, with random jittering along the abscissa, indicate the individual subjects' error rate, averaged over the three trials with the depth-modulated buzz-wire and under head-free conditions. The asterisk symbol indicates statistical significance at $p \leq 0.05$ 70

Figure 3.4 Panels A-C) Scatter diagrams of the square root of the error rate plotted as a function of the square root of the participant's age under binocular (panel A), monocular (panel B) and uniocular (panel C) viewing conditions. Panels D and E) Partial residual plots for children (panel D) and adults (panel E) demonstrating the impact of the duration of uniocularity on the error rate after adjusting for the effect of the participant's age, as shown in panel C. The solid and curved lines in each panel indicate the best-fit linear regression equation and

its $\pm 95\%$ confidence interval obtained for the data of children (closed symbols) and adults (open symbols), separately. The abscissa and ordinate of Panels A-C are relabelled for the untransformed age and duration of uniocularly for ease of interpretation. Similarly, the abscissa and ordinate of Panels D and E are relabelled for the untransformed duration of uniocularly and residuals of the error rate for ease of interpretation. 72

Figure 3.5 The error rate (panel A) and speed (panel B) obtained for buzz wires with depth modulation plotted against those without depth modulation in controls and cases in the free head condition. The diagonal line in each panel represents the line of equal performance. 73

Figure 3.6 Similar to Figure 3.3 but buzz-wire performance for the head-restricted viewing condition. 74

Figure 3.7 Panel A shows histograms of the proportion of errors made at the straight (S), transition (T), and curved (C) regions of the buzz-wire across the randomly selected error frames analysed under binocular (green) and monocular (red) viewing conditions of controls and uniocular viewing condition of cases (blue). Error bars indicate the upper and lower (95%) confidence interval of each proportion shown in this panel. Panel B shows box and whisker plots of the duration of errors made by controls under binocular and monocular viewing conditions and by uniocular participants in each of the locations of the wire. The middle black horizontal line in each box and whisker plot indicates the median value, the lower and upper horizontal lines indicate the 25th and 75th quartiles and the dotted vertical lines indicate the 1st and 99th percentile of the data distribution. The open circles represent the data of individual participants..... 76

Figure 3.8 Violin plot pairs showing the distribution of the translational [horizontal (panel A), vertical (panel B) and antero-posterior (panel C)] and rotational [pitch (panel D), yaw (panel E) and roll (panel F)] head movements for the binocular and monocular viewing of controls and uniocular cases while they performed the buzz-wire tasks with depth modulation under head-free viewing conditions. All other details are similar to Figure 3.3. Bubble plots showing the disparity available for depth computations in the buzz-wire task with depth modulations from horizontal head translation in the monocular viewing of controls (Panel G) and uniocular cases (Panel H). In both panels, the participants are arranged in ascending order of the disparity available to each participant in the cohort. Lighter-coloured and larger-sized bubbles indicate a larger velocity of head motion. The horizontal line with the green shaded area in each panel denotes the median with 25th and 75th quartile of binocular retinal disparity available for depth calculations under binocular viewing conditions. 78

Figure 4.1 A representative, cross-fusible, example of the random-dot stereogram used for estimating the stereo threshold. The fused stereogram shows a leftward tilted rectangular bar in crossed retinal disparity. 93

Figure 4.2 Schematics for the different pattern of results that may be obtained across controls and cases for the error rates in the buzz-wire task used in this study. Data clouds are assumed to have elliptical distributions. The solid circle is the centroid of the elliptical data cloud. The “smiley” face indicates statistically significant impact of the independent variable (i.e., viewing condition) on the dependent variable (i.e., error rate, in this case) while the “gloomy” face indicates no evidence of such a statistical significance. Panels B–I are described in the text..... 95

Figure 4.3 Scatter diagrams of the error rate (panel A) and speed (panel B) obtained from controls (green symbols) and cases (red symbols) while performing the buzz-wire task in this study. The coloured patches

represent the best-fit bivariate contour ellipse for the controls and cases datasets. The major and minor axes are shown for each ellipse, the intersection of which represents its centroid (see text inset for details). The diagonal line in each panel represents the line of equality for monocular and binocular performance. The gestalt obtained from these contours may be readily compared with the schematics described in Figure 4.2. The insets show Box and Whisker plots of the binocular advantage in error rate and speed obtained for controls and cases in this study (see figure insets in each panel). For each box and whisker plot, the horizontal line is the median, the edges are the 25th and 75th quartiles and the whiskers are the 1st and 99th quartiles. The black dots are the individual data points, jittered randomly along the X-axis for ease of visualization. 99

Figure 4.4 Binocular advantage in error rate plotted against the random-dot stereo threshold for controls (green), cases (red), and uncorrected myopes (blue). The transparency of the dots represents the 68% credible interval for the stereo thresholds. The vertical line indicates the disparity threshold (611 arcsec or 2.79 log arcsec) for diastereopsis. The horizontal line denotes the level where there was no binocular advantage. 102

Figure 4.5 Panels A and B show the stereo threshold and error rate, respectively, obtained with the spectacle and contact lens corrections in cases. The transparency on the right and left hemispheres in Panel A, represents the 68% credible interval for the spectacle and contact lens, respectively. Panel C shows the fold-change in stereo threshold from spectacles to contact lens wear plotted against the corresponding fold-change in error rates of the buzz-wire task. The region above the intersection of the vertical and horizontal lines indicates an improvement in both parameters with contact lens wear in this panel. The region diagonally opposite this indicates worsening of performance in both parameters with contact lens wear. 104

Figure 4.6 Scatter diagrams of the error rate (panel A) and speed (panel B) in uncorrected myopes (blue symbols) while performing the buzz-wire task plotted along the corresponding bivariate contour ellipses. The ellipses of the controls (green) and cases (red), identical to those in Figure 4.3, are also reproduced here for comparison purposes. All other details are the same as Figure 4.3 105

Figure 4.7 Panels A–H) Point-of-view optical simulations of the buzz-wire apparatus with clear vision (panel A), blurred vision from uncorrected myopia (panels B – D) and blurred vision from cases, whose severity is indicated on top of each panel by the root-mean-squared values of the higher-order aberrations (HORMS) (panels E–H). Panels I–K show cross-fusible zoomed-in stereoscopic image pairs of the buzz-wire apparatus illustrating the location of the loop relative to the wire when vision is clear in both eyes (panel I) and when vision is bilaterally (panel J) or unilaterally (panel K) blurred from keratoconus. The wavefront aberration values used to blur the right and left eye of the stereogram pair are indicated on top of each figure panel. 109

Figure 5.1 The static buzz-wire apparatus. A) One model from the participant's point of view. B) Top view of the 12 models on the turntable. C, D and E) Straight (S), transition (T) and curve (C) sections. 118

Figure 5.2 Scatter plot showing the average detection sensitivity (d') across different viewing durations (0.5, 1, 2, and 3 sec) for control participants under both binocular and monocular viewing conditions. Error bars denote the SEM. 120

Figure 5.3 A) Bar graph for the mean error rates obtained from the visuomotor task for the binocular and monocular viewing of controls and uniocular cases. B) Bar graph for the mean detection sensitivity for the binocular and monocular viewing of controls and uniocular cases obtained at the straight, transition and curve

sections of the perceptual buzz-wire task. The error bars represent the SEM. The circles represent the data of individual participants. The colour of the circle indicates the subject number. The circles with the same colours under the binocular and monocular viewing conditions represent the same subject, while the same colour under unocular bars indicates a different participant. The circles are jittered for better visibility of individual data points. The horizontal bar with the asterisk marks the group that showed significant differences ($p < 0.05$). 122

Figure 5.4 representative image showing a cross-sectional view of the triangular prism that would pop out of the monitor screen, when the stimulus starts to move. The base of the triangle was equivalent to the vertical width of the 14 rows of dots. The height of the triangle was based on depth seen with motion parallax..... 131

Figure 5.5 shows the depth modulation in percentage for the four depth criteria: depth detection, the height of the triangle = half the base of the triangle ($H=B/2$), the height of the triangle = base of the triangle ($H=B$), and height of triangle = double the base of the triangle ($H=2B$). Panel A-E, shows the results of the 5 control subjects. The y-axis limits are different to showcase the trend of increase in depth modulation with the increase in the depth criterion. 134

Acknowledgement

I would like to begin by expressing my gratitude to all the participants for dedicating their time to this study. Given the challenge of finding typically developing children within a tertiary eye care institute, I am especially thankful to Mr. Tejah Balantrapu, Associate Director – Science, Health Data and Storytelling, LVPEI, for connecting me to a school from where many parents and children volunteered to participate after school hours.

I am particularly grateful to two individuals whose contributions significantly shaped this study. Mr. Ashish Jain, Lead Design Consultant, LVPEI, casually mentioned the buzz-wire game in a conversation, sparking an idea that became central to my experimental setup. Dr. PremNandhini Satgunam, Scientist, LVPEI, introduced me to the OpenFace software during my upgrade examination, providing a crucial tool for tracking head movements.

I consider myself fortunate to have had an exceptional team of PhD supervisors. Dr. Shrikant Bharadwaj, for believing in me from the moment I applied for a Research Optometrist position at LVPEI in 2018, originally intending to gain just one year of research experience. Since then, he made me realise that science is fun but requires rigor and persistence to uncover the full story. Prof. Christopher Tyler's invaluable advice—"Hypotheses cannot be pulled out of thin air"—and Prof. Joshua Solomon's insistence on well-defined variables under testing, trained me to visualize all possible outcomes, both graphically and statistically even before data collection. Their guidance, quick responses, and support have been instrumental throughout this journey. I also acknowledge Prof. Solomon for the initial motion parallax code.

I am also deeply grateful to LVPEI for its incredible and supportive team of clinicians and ocularists, Ms. Mahima Bhengra and Mr. Deepak Kumar, who ensured a smooth data collection process. My sincere appreciation extends to Mr. Nabeel Quadri, Lead Designer, and Mr. Ayush Kumar, Electronics and Communication Engineer, for their invaluable help in developing the perceptual version of the buzz-wire. My sincere gratitude to City St George's University of London for the collaboration with LVPEI and its amazing library services.

Special thanks to my friends, Mrs. Monika Thakur for standing by me through every high and low of this journey and Ms. Ketakee Jain for sitting through endless experimental trials. I am grateful to my lab mates, Mr. Rahul Negi, Ms. Tithi Bhakta, Ms. Indrani Sirivella and Mr. Tai Jarkum for their support and to scientists - Drs. PremNandhini Satgunam, Pavan Kumar, Amithavikram Hathibelagal and Srinivas Marmamula for their valuable feedback during the journey.

Finally, a heartfelt thanks to my mother, Mrs. Jayashree Devi, my father, Mr. Probin Nath, and my sister, Mrs. Priyankita Devi, for their unwavering support — even if they don't quite understand what I do!

Abstract

Binocular disparity provides a strong depth cue, but when binocularity is absent or degraded, monocular depth cues such as motion parallax, occlusion, and perspective become critical. This thesis investigates how depth perception and depth-related visuomotor performance are affected in individuals with absent (uniocular) or degraded (keratoconus) binocularity and explores the role of monocular cues in perceptual and motor tasks. A pilot study also explores the ability of the uniocular participants to derive veridical 3D shapes from motion parallax.

A buzz-wire game assessed visuomotor performance where participants guided a loop along a convoluted wire, with errors triggering a buzzer. Uniocular individuals showed no evidence of reduced error rates relative to the monocularly occluded controls, despite making larger head movements, suggesting no adaptive changes of long-term reliance on monocular depth cues or inability to extract depth estimates from motion parallax.

In reduced binocularity — keratoconus — binocular advantages were associated with lower monocular error rates. Rigid gas-permeable lenses enhanced image quality and partially restored stereopsis and performance, though improvement in stereopsis did not correlate with task success. Uncorrected myopes with comparable loss of stereopsis continued to show binocular advantage.

Perceptual version of the game, involving detection of loop-wire contact, revealed that uniocular participants outperformed monocularly occluded controls, suggesting long-term uniocular experience may exploit monocular depth cues in perceptual tasks, but not for visuomotor tasks.

A final pilot study simulated motion parallax using moving dots to define a triangular prism. Controls adjusted velocity to construct prisms with varying height-width ratios, but uniocular participants reported no depth. This suggests a joint loss of the neural architecture: loss of binocular retinal disparity undermines depth from motion parallax.

These results underscore the importance of considering alternative training strategies to enhance depth-related visuomotor function in individuals with compromised binocularity.

Chapter 1 Overview

1.1 General introduction

Humans are naturalistically binocular organisms giving an added advantage for depth perception, which enables various depth-related tasks from navigation by breaking camouflage and judging looming objects, to performing manual dexterity tasks (Read et al., 2013). However, the image of the real world forms only a 2D image on the retina, yet, we perceive the world in 3D, indicating that the brain recreates the probable 3D space using the 2D information from the retina.

However, the world does not appear flat when one eye is closed. This can be experienced by the reader by closing one eye and looking around at the objects surrounding them. The monitor screen will still appear to be on a separate plane from the rest of the items on their desk no matter whether they are viewed with one or two eyes. Similarly, Figure 1.1A and B show the image of my desk taken from two camera locations separated by 6 cm, thus mimicking the different views that our two eyes usually receive. The reader can cross-fuse the two images and try to grab a cup of coffee before proceeding with reading the dissertation! By viewing either Figure 1.1A or B, with one eye, one can still perceive the depth but the vividness of the depth might be lost compared to the cyclopean view. For a long time, artists have identified the ability of the human brain to perceive 3D depth from 2D images and they have exploited this ability to depict depth in paintings with multiple pictorial cues. One example is the painting of “The Montefeltro Altarpiece’ by Piero Della Francesca (Figure 1.1C). Unlike the picture of my desk, a more pronounced sensation of depth

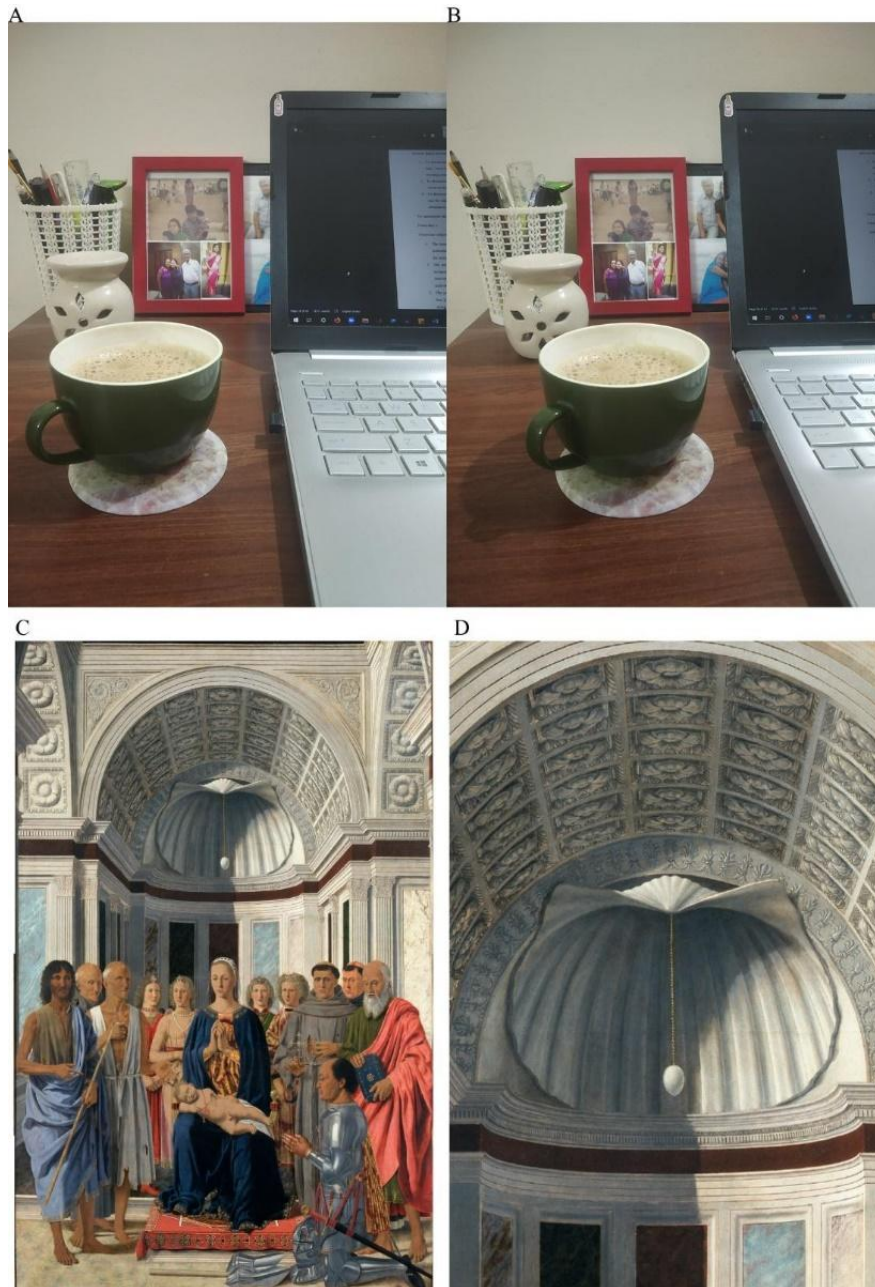


Figure 1.1 A and B can be cross-fused to see the depth of the desk. (C) The painting ‘The Montefeltro Altarpiece’ by Piero Della Francesca. (D) shows an enlarged portion of the suspended egg in the middle of the dome of (A). Taken from Tyler (2020).

(Tyler, 2020) can be appreciated in Figure 1.1D by viewing it with one eye which is an enlarged portion of the suspended egg near the dome of Figure 1.1C. The ability to perceive depth around us using the 2D image formed on only one eye (the other eye closed) or even on a flat surface of paintings is due to the presence of monocular

depth cues. These binocular and monocular depth cues normally interact with each other for the final depth estimates. And once the depth is estimated, either one just views it (perceptual task), or may need to interact with it (visuomotor task), for example, grabbing that cup of coffee in the cyclopean view of Figure 1.1A and B.

1.2 Disruption in binocularity

Disruption of binocularity can happen in 3 different ways. Firstly, it can be a temporary disruption due to the voluntary closure of one eye, and binocularity is restored immediately by opening both eyes. Secondly, it can be a permanent disruption that can occur when one of the eyes is either surgically removed, or when an eye fails to develop and the baby is born without an eye (anophthalmos) or an incompletely developed eye (microphthalmos). Based on data from tertiary eye care centres in India, 95% of enucleations (complete removal of the orbital content, except extraocular muscle) were performed on children, with retinoblastoma (eye cancer) being the leading cause of enucleation (Vemuganti et al., 2001). According to an editorial letter by Kivelä (2009), the incidence of retinoblastoma in Asia was estimated to be 18.8 cases per 1000 live births, while in northern America and Europe, it was 13.8 and 10.2 cases per 1000 live births, respectively. Other causes for enucleation or evisceration (removal of orbital content except for sclera and extraocular muscles) are acute trauma to the eye and anterior staphyloma, where the uveal tissue protrudes through thinned or weakened portion of sclera or cornea. Thirdly, the disruption in binocularity can be partial. This can be due to mechanical inability to lock fusion as seen in strabismus, optical degradation of images formed on the retina, as in post-refractive surgery, corneal ectasias, etc, or neurological conditions like amblyopia. Prevalence of keratoconus in particular is known to be higher in Asian and middle-eastern populations compared to Caucasians, ranging from 0.2 to 4790 per 1,000,000

population for the former compared to under 1000 per 1,000,000 population for the latter (Santodomingo-Rubido et al., 2022).

Due to this disruption in binocularity, depth from binocular disparity is either completely absent or substantially reduced. While it is assumed that a good visual input is required for proper visuomotor control, studies related to neurophysiology suggest that the visual processing system that mediates perception is (at least partly) separate from the processing system that mediates visuomotor control (Milner, 1998). This means that, while the perception of depth can be affected, the visuomotor control can remain intact or conversely, the perception of depth can be intact but the visuomotor control can be impaired. For example, an individual with ‘visual form agnosia’ has an incorrect perception of shape and orientation but the visuomotor responses remain unaffected, and in an individual with optic ataxia, the perception of shape and location is unaffected but visuomotor performance is impaired (Milner, 1998).

1.3 Outline of the dissertation

To orient readers with the flow of the dissertation, the next chapter provides a comprehensive review of the literature on depth cues — their functional roles, the mechanisms by which they contribute to veridical depth estimation, and the interplay among these cues. The chapter further compiles the literature on depth perception among unocular individuals, and the neurological changes that accompany with early loss of an eye.

The third chapter starts with a clear case of the long-term absence of binocularity in the form of one-eyed individuals and investigates its impact on depth-related visuomotor tasks. It also investigates if factors like the age at which an eye was lost, the duration of one-eye viewing, and the age of the participants have any impact on

the task performance. The chapter also dives into the head movement patterns and whether they are useful while performing the task.

The fourth chapter investigates the same on individuals with reduced binocularity due to optical degradation as in the case of keratoconus, and the impact on the task when the binocularity is improved. The chapter further investigates the relationship between the common clinical measures of stereopsis and depth-related visuomotor task performance.

The fifth chapter explores the perceptual ability of uniocular individuals to derive the depth estimates in a perceptual version of the visuomotor task and secondly determines if they can derive 3D shapes exclusively from motion parallax.

The last, sixth chapter summarizes the findings and suggests possible future studies to understand if any limitations in depth perception exist and how to improve it.

Chapter 2 Literature review

2.1 Depth perception

Depth is the perception of the fullness of an object and the empty spaces between the objects, like perceiving the roundness of pool balls and the empty space between two balls (Vishwanath, 2014). This enables us to break camouflage, judge looming objects, and assist in performing as mundane of a job as pouring a glass of water from a jug or performing intricate jobs like watchmaking or jewellery making (Fielder & Moseley, 1996; Read et al., 2013). This impression of depth is obtained from the binocular retinal disparity and monocular depth cues.

Due to the horizontal displacement between the two eyes, the visual fields of the two eyes overlap causing the retinal points of the two eyes to pair up in such a way that images formed on these corresponding points are perceived to originate from the same location in the visual space. The imaginary line connecting all the image locations originating from corresponding points forms the horopter. The image of objects in front or back of the horopter falls on the non-corresponding points causing a crossed and uncrossed disparity respectively (Howard & Rogers, 2002).

The various monocular depth cues are as follows (Howard & Rogers, 2002):

Linear perspective: Parallel lines appear to converge towards a single point at a farther distance.

Relative size: A familiar object of different sizes will appear to be located at a distance from the observer such that the normal-sized object would subtend the same angular size.

Texture: Texture elements undergo a uniform change in size with distance. Unlike relative size and linear perspective, texture not only estimates Z-dimensional depth but also cues for surface curvature.

Lighting, Shadows, and Shading: Similar to texture, lighting, and shading provide information about the surface curvature (shape) by indicating the surface normal at each location of the object.

Occlusion: An occluding contour confirms the ordinal depth cue's performance or provides information about relative depth differences at the borders of the occluding contour.

Aerial perspective: Farther objects appear hazy with a bluish tint due to atmospheric scattering of light.

Motion parallax: Translational movement of the observer's eye with respect to the visual field or movements of the visual field with respect to the observer's eyes results in a differential angular velocity on the retina (Bradshaw & Rogers, 1996; Gibson et al., 1959). This differential angular velocity causes objects farther away from the fixation object to move slower and along the same path as the observer's movement whereas objects closer to the fixation point move faster and in the opposite direction to the observer's movement resulting in motion parallax. There are different types of motion parallax:(Howard & Rogers, 2002)

- i. Absolute parallax: The magnitude of motion of a single image when it moves across the retina during head or object motion. The magnitude of the motion is inversely proportional to the viewing distance, i.e. the closer the object to the observer, the faster will be the magnitude of motion.

- ii. Linear parallax: As the observer makes translational movement or the objects move in the visual space, objects closer to the observer move faster while further objects move slower.
- iii. Kinetic depth effect (KDE): The outline of a 3D object when it moves around a vertical axis, the image configuration changes without changing the mean position in the visual space.
- iv. Stereokinetic effect (SKE): The outline of a radially asymmetric 3D object that rotates around the visual axis, providing the perception of depth.

2.1.1 Types of depth perception

The depth cue can indicate the distance of an object in space. Depth cues can either be a cue for an absolute depth — how far an object is from the observer's point of fixation, or relative depth estimations — relative to an object in space, the location of another object in space (Ding et al., 2024), or it can provide ordinal (depth order). While all the depth cues provide information regarding the relative depth, the binocular retinal disparity and motion parallax can provide absolute depth estimates (Johnston et al., 1994).

Within the relative depth, there can be three types of depth detection (Stevenson et al., 1989). The first is the detection of a step between two adjacent depth planes (Figure 2.1A). This is analogous to vernier acuity in the spatial domain. The threshold for detection of the step is around 3 arcsec. The second is a super-resolution task of discriminating flat surfaces from the surface with thickness (Figure 2.1B). The term pyknostereopsis is coined for this and its threshold lies at 15-30 arcsec. The third is the detection of the two overlapping surfaces with empty space between them (Figure 2.1C). This perception is called diastereopsis. This is analogous to the monocular grating acuity.

Depth provides information about the shape of an object in terms of its horizontal and vertical slant (Figure 2.1D) and the curvature of a surface (Figure 2.1E). A slant of an object causes a graded change in disparity; however, the horizontal disparity alone is not enough and needs vertical disparity for a veridical estimate of slant and viewing distance (Backus et al., 1999). Other cues to curvature in depth include parallel lines becoming curvilinear, and changes in density and aspect ratios of the texture pattern as seen in Figure 2.1E.

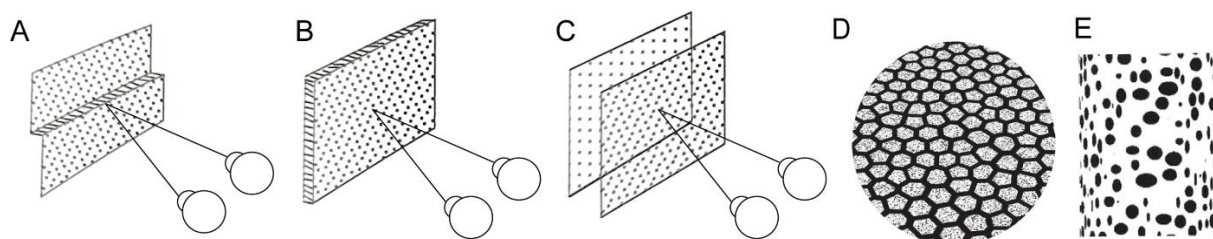


Figure 2.1 Schematic diagrams to represent the different types of depth. A. represents the hyperacuity where the two fronto-parallel planes are separated by a step. B. represents the super-resolution or pyknostereopsis where the surface appears thickened. C. represents the diastereopsis, where the two fronto-parallel surfaces appear to be separated by empty space between them. D and E. represent the shape of a surface in terms of slant (D) and curvature (E) using texture cue. Figure A-C is taken from Stevenson et al. (1989), D is adapted from Saunders and Chen (2015) and E is taken from Landy et al. (1995).

2.1.2 Perspective geometry

The first step in the perception of an object in space is that the object has to cast a 2D image on the retina, and the image formed on the retina represents the projection of the visual scene in front of the eyes (Howard & Rogers, 2002). A projection line is a line that connects the points of the object to the points on the image plane (Figure 2.2A). When the light source is at a faraway distance such that the projection lines are parallel to each other (parallel projection), the projection is independent of the viewing

distance and preserves the parallel lines and the ratio of the lengths of the objects, but the angles may get altered (Howard & Rogers, 2002). Under the polar projection, the projection lines are not parallel. The image thus formed on the retina does not retain the properties of the object like its parallel lines, lengths, and areas, but retains the object's collinearity, and concurrence of intersecting lines. The parallel lines of an object appear to recede towards a vanishing point. Commonly perspective is classified into one, two, or three-point perspective, depending on the orientation of the object with respect to the image plane. A one-point perspective consists of one vanishing point that provides a head-on view of a 3D object. A 3D object when viewed from an angle, consists of two vanishing points. The typical worm's eye view (horizon is high up) or a bird's eye view (horizon is below) from an oblique corner consists of three vanishing points. A complex scene can have multiple vanishing points. The deformation of parallel lines to appear like lines converging towards a vanishing point is termed *linear perspective*.

As the object O_1I_1 in Figure 2.2B is placed closer to the image plane, the angle subtended at the nodal point increases ($\alpha > \theta$ in Figure 2.2B), thus forming an enlarged image on the image plane (O_2I_2 Figure 2.2B), i.e. the angular size on the retina is inversely proportional to the distance to the object. This forms the basis for depth judgment from *relative size* and *perspective distortions*, where a familiar object forming an enlarged image on the retina is perceived to be closer than the same object when its retinal subtense is smaller. As the distance to the object changes, a textured surface undergoes deformation, causing compression of the textures at farther distances, thus changing the aspect ratios and density of the textures as noted in the slanted polygon textured surface in Figure 2.1D and a curved circular textured surface in Figure 2.1E.

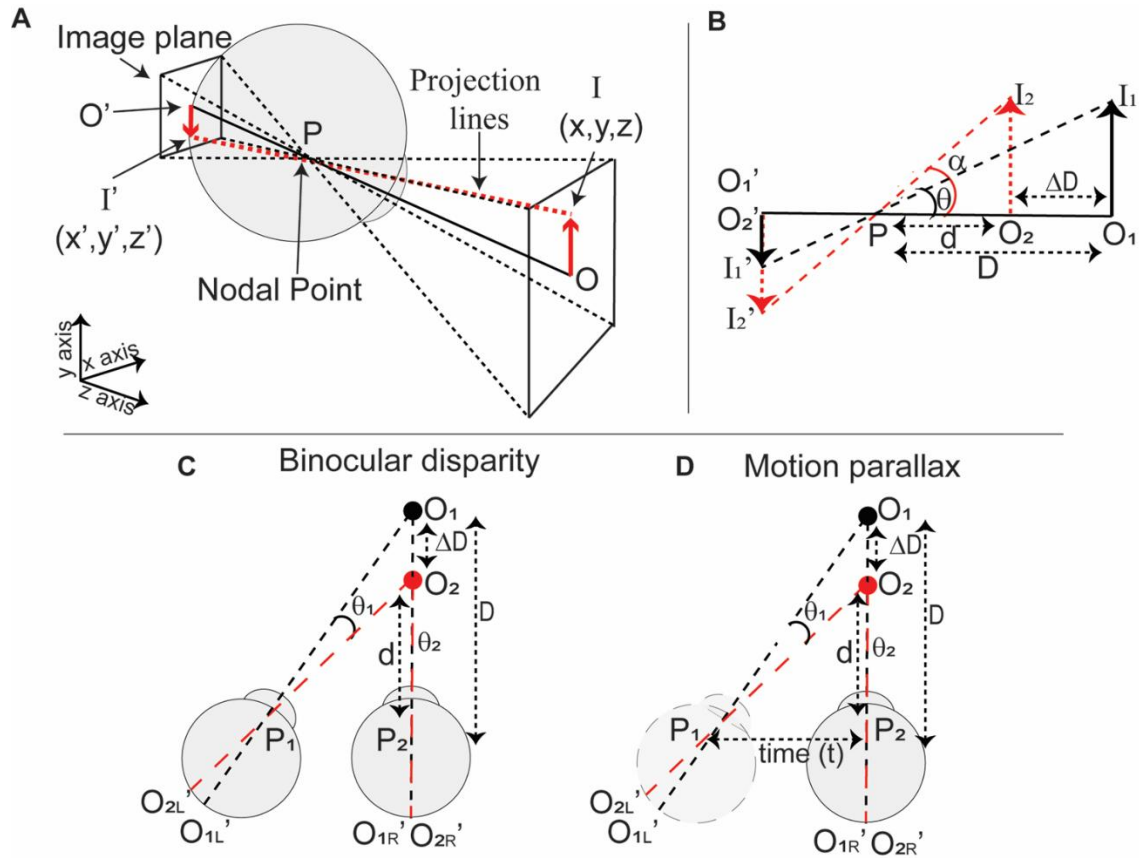


Figure 2.2 A, B, C, and D shows the schematic ray diagram for image formation on the retina. Panel A shows the basic projection geometry of an object OI on the image plane or the retina and forming the image $O'I'$. The dotted lines denote the projection lines. Panel B) Schematic of relative size depth cue. Object O_1I_1 at a farther distance (D) forms a relatively smaller image compared to object O_2I_2 placed at a closer distance of ΔD from the nodal point (P). Panel C) Schematic of binocular retinal disparity. The object O_1 and O_2 form their images on the non-corresponding points of the retina of the two eyes resulting in visual angle differences ($\theta_1 > \theta_2$). Panel D) Schematic of motion parallax. While the objects O_1 and O_2 are stationary, one eye moves from one position to the other, resulting in visual angle differences ($\theta_1 > \theta_2$).

When the same object O_1 and O_2 are viewed from two vantage points (P_1 and P_2), the objects form an image at two different locations on the image plane (Figure 2.2C). The horizontal displacement of the two eyes naturally provides two different perspectives of the world, thus forming the basis for depth from *binocular retinal disparity*. It is defined as the difference between the right and left eye's angular subtends. The same

angular disparity can be generated by moving one eye to the location of the other eye or by moving the object location from one point to the other over a period of time (Figure 2.2D). This *motion parallax* causes the object closer to cover a larger distance on the retina compared to the farther object ($\theta_1 > \theta_2$). That is, while in binocular retinal disparity, the images of an object fall on non-corresponding points of the two retinas simultaneously, in the case of motion parallax, as the image stimulates a single retina at different locations successively over time during motion (Bradshaw & Rogers, 1996; Gibson et al., 1959; Kim et al., 2016; Rogers & Graham, 1982). This similarity makes motion parallax a depth cue that can generate depth estimations similar to retinal disparity (Similarities to be discussed in section 2.1.4).

The depth from binocular retinal disparity and monocular motion parallax (ΔD) is calculated based on the following formula: (Rogers & Graham, 1982)

$$\Delta D = \frac{\eta \times D^2}{IOD} \quad \text{Eq 1}$$

To calculate depth from retinal disparity

D = Distance from the observer to the point of fixation

η = Horizontal angular disparity

IOD = Intraocular distance

To calculate depth from motion parallax

D = Distance from the observer to the point of fixation

η = Relative angular velocity of the front and back surface of the object

IOD = Head velocity

As seen in Figure 2.2D, the projection lines from object points O_1 and O_2 overlap when the eye position is aligned along the projection line. This causes the *occlusion* of object O_1 by the object O_2 . But when the eye moves to another vantage point over time, the

projection lines do not occlude anymore, in fact, as the eye starts to move towards the other vantage point, the object O_1 would start to appear from behind O_2 . This dynamic accretion and deletion in occlusion parts provides a better understanding of the depth order (Ono et al., 1988).

2.1.3 Depth from motion parallax

The optic flow field is differentiable spatially into 4 local spatial gradients of angular velocity, known as differential velocity components (Koenderink, 1986). Firstly, translational movements provide information on the object's translation in space. Secondly, expansion or compression of the optic flow indicates the movement of an object in depth, for example, a ball moving closer or farther away from the observer. The last two, rotational and shear optic flow provide information about the 3D shapes and surface orientation (Koenderink, 1986).

Researchers have investigated if the optic flow on the retina is enough for the perception of depth irrespective of the source of the optic flow, i.e. whether it originated from the observer's movement or the object's movement. Rogers and Graham (1979) used Julesz's random-dot patterns to create motion parallax to define four different corrugations (square, sinusoidal, triangular, and sawtooth corrugation). They tested the ability of their 12 participants to identify if there was depth noted in the stimulus, and if yes, they were further asked to define the shape, number and depth order of the corrugation. This was done under two conditions. In the first condition of self-produced parallax, the oscilloscope was stationary and the subject moved their head left and right while fixating the display. In the second condition of externally produced parallax, the subject's head was stationary and the oscilloscope was moved. All of their 12 subjects could perceive depth under both conditions and the number of corrugations and depth order was reliably identified.

Ono and Steinbach (1990) employed the same stimuli to investigate whether participants perceived motion in addition to depth during both self-produced and externally induced motion parallax. Participants were instructed to report the perceived depth magnitude and whether the dots appeared to undergo translational motion. If motion perception was reported, participants were further asked to identify which dots corresponded to the peaks and troughs of the corrugations. Their findings demonstrated that at an equivalent disparity of 12 arcmin, participants did not perceive dot motion when executing translational head movements (**Figure 2.3A and B**). However, when their heads remained stationary, they did report perceiving motion (**Figure 2.3A and B**). At a disparity of $1^{\circ} 53$ arcmin, motion perception occurred under both head-translational and head-stationary conditions; however, the perceived motion was attenuated during head translation compared to when the head remained stationary (**Figure 2.3A and B**). During lateral head translation along the interaural axis, while maintaining fixation on a visual scene, the eyes execute compensatory movements in the opposite direction to stabilize fixation. These compensatory eye movements ensure that the fixation point remains projected onto the fovea, while objects at varying depths produce differential retinal motion. This mechanism may explain the findings of Ono and Steinbach (1990), wherein participants making head movements failed to perceive the apparent motion of the dots due to compensatory eye movements, instead perceiving only depth cues derived from relative motion disparities. To examine whether extra-retinal signals—such as eye movements, head movements, or vestibular activation—are necessary for depth estimation, Nawrot (2003b) employed motion aftereffect and static tests to eliminate visual cues (e.g.,

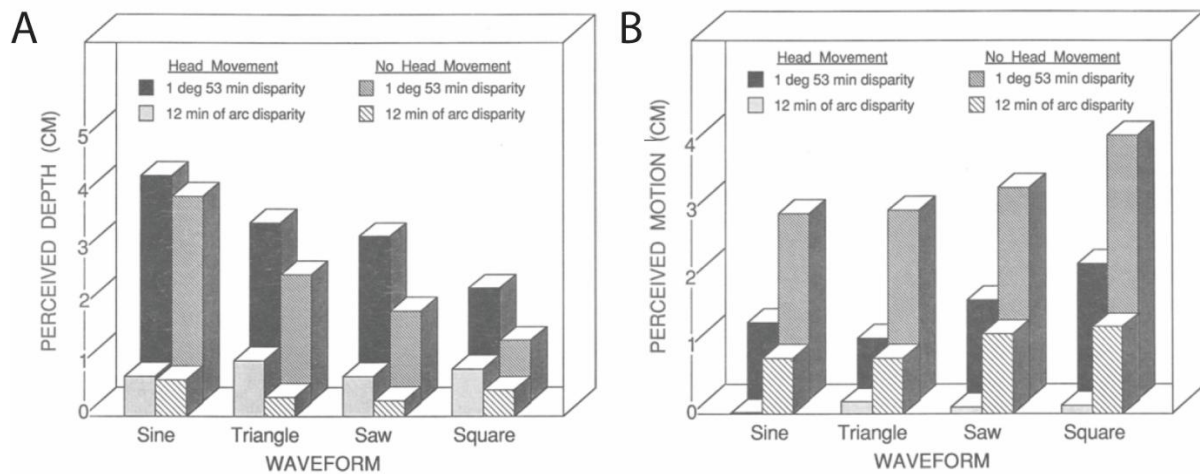


Figure 2.3 Extent of perceived depth (A) and perceived motion (B) as a function of head movement (left-side bars) versus no head movement (right-side bars), 6" disparity (front bars) versus 1°52" disparity (back bars), and profile of the gradient (sine, triangle, saw, or square waveform). Taken from Ono and Steinbach (1990).

motion perspective, relative motion, or velocity gradients) and isolate the influence of extra-retinal information on depth perception. To induce motion aftereffects, participants fixated on a stable central target while viewing a stimulus comprising four rows of vertical bars. Alternate bars moved in opposite directions, with movement directions counterbalanced by head motion along the interaural axis. This arrangement caused the alternating rows to separate in depth, such that some appeared to protrude while others receded. Following a 30-second adaptation period, participants were presented with static versions of the stimulus, in which the phase of the bars was aligned. The findings revealed that when participants moved their heads along the interaural axis, their eyes executed compensatory movements in the opposite direction, preventing the perception of motion in the static stimulus. However, the alternating rows continued to appear displaced in depth. They demonstrated that when the head moved along the interaural axis, the eyes moved towards the opposite direction and there was no apparent motion of the rows in the static rows, but

alternated rows appeared to either pop out or pop in in depth. This provides evidence that for perception of depth from motion parallax relies on extra-retinal information generated from the observer's head movements. The head movements with a central fixation generate pursuits which are independent of head motion and vestibular reflexes that originate from an attempt to keep an object on the fovea while the head moves. To isolate the pursuits from the vestibular responses, two further experiments were conducted. In the first experiment, participants' heads were stabilized using a bite bar, while both the test stimulus and the fixation target moved in the same direction. However, after a certain duration, the fixation cross shifted in the opposite direction to return to the centre. Participants reported that the strips that moved in the same direction as the eye movements were perceived to be near. In the second experiment, eye movements were synchronized with head movements. The combined results of these experiments demonstrated that smooth pursuit eye movements provide an unambiguous cue for depth perception from motion parallax. In the second experiment, the eye movement was synced with the head movement. The strips that moved along the same direction as the head movement, were noted to be farther away. The results from these two experiments demonstrated that smooth pursuit provided an unambiguous perception of depth from motion parallax.

2.1.4 Similarities between depth perceived from retinal disparity and motion parallax

The primary similarity between binocular retinal disparity and motion parallax lies in the manner in which they generate retinal images, (Figure 2.2 C and D). The second similarity lies in the shape of the depth sensitivity curve across the spatial frequencies obtained from binocular retinal disparity and motion parallax. Rogers and Graham (1982) demonstrated that the shape of the depth-sensitivity curve for both the depth cues is the same — an inverted U shape. The highest sensitivity was noted to be

around 0.2 to 0.5 cpd and the sensitivity decreased monotonically beyond this range. Of the three subjects, two of the subjects were approximately twice as sensitive to depth from binocular disparity as from a comparable amount of the threshold for motion parallax compared to binocular disparity, for all spatial frequencies (Figure 2.4A and C). For the third subject, the sensitivity for the motion parallax was indistinguishable from disparity (Figure 2.4B).

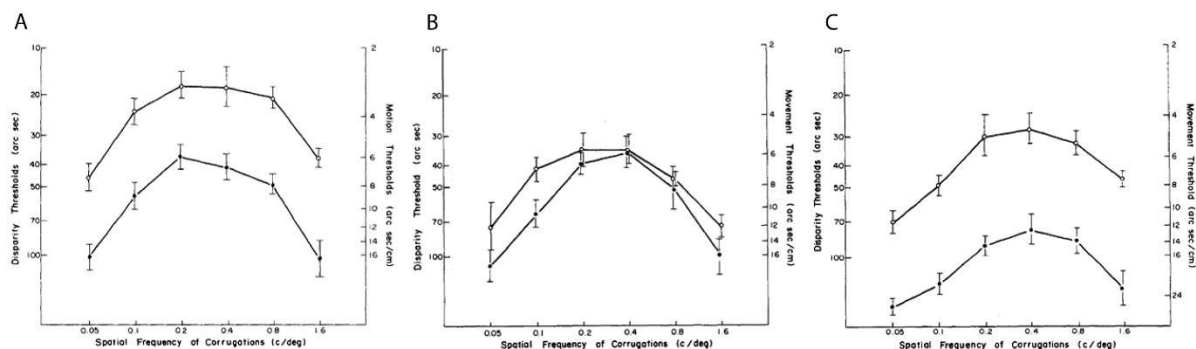


Figure 2.4 Disparity (open symbols) and motion parallax (closed symbols) threshold as a function of spatial frequency for three subjects (A, B, C) Taken from Rogers and Graham (1982).

de Vries and Werkhoven (1995) studied the slant and curvature perception with binocular disparity and motion parallax. Random-dot stimuli were used to elicit only binocular retinal disparity and motion parallax depth cues without the influence of other depth cues. The perspective projection technique was used to determine the perspective changes that a physical surface (either slanted or curved) would produce when one eye traverses through 6.5 cm. Subjects were asked to match the slant or curvature defined by the motion parallax with the slant or curvature defined by the binocular disparity. They demonstrated that the slant estimated from motion parallax is matched with a higher value (~factor of 1.33) of retinal disparity (Figure 2.5A) and curvature estimated from retinal disparity is matched with a higher value of motion

parallax (Figure 2.5B). However, due to the absence of a control experiment to test the matching ability of the 3 participants, it is not clear whether the error is a physiological error to match a slant and curvature, or purely due to the perception of slant and curvature with another depth cue.

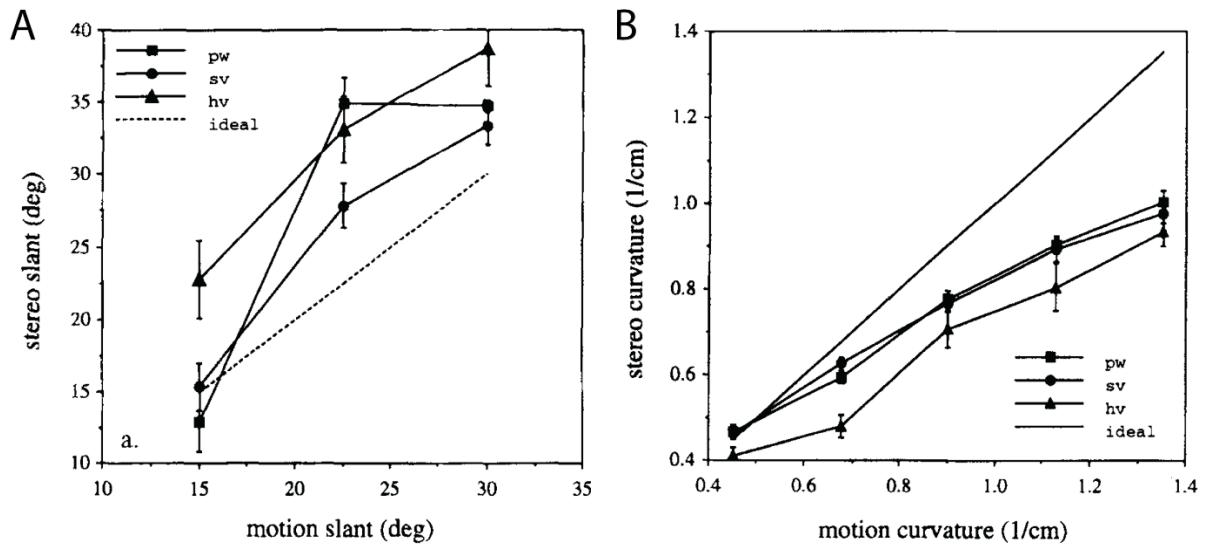


Figure 2.5 Matched stereo-specified slant (A) and curvature (B) as a function of motion-specified slant. The dashed line gives the results expected when observers judge the slants of motion- and stereo-specified surface patches equal. The three curves represent three subjects. Error bars indicate the measurement error. Taken from de Vries and Werkhoven (1995).

The similarity between the two cues is also related to the neurophysiology — both of cues are processed at a common location in the brain. Information from the two eyes passes through two visual pathways — the magnocellular and the parvocellular pathway. The information then is passed on to the two extrastriate cortical pathways — the dorsal and ventral pathways respectively. The dorsal pathway processes information related to motion and depth while the ventral pathway processes contrast, contour, and colour (Hubel, 1995). Information from both cues passes through the magnocellular pathway (Kandel et al., 2000). The magnocellular layers in the lateral

geniculate nucleus (LGN) feed to the V1 region of the visual cortex to the middle temporal (MT) to the medial superior temporal (MST) area (Figure 2.6) (Kandel et al., 2000; Nadler et al., 2013).

Nadler et al. (2009) performed single-cell recording from the MT area while the monkeys viewed motion parallax targets at various distances. They showed the MT neurons had a preference for depth signs (far or near) when extra-retinal signals (e.g. self-motion, eye movement) are present. In the absence of extra-retina signals from eye movements, the neurons fire for all depth targets without any preference for a particular distance. In the next few years, they reported that MT neurons fire for depth from motion parallax and binocular disparity, however, about 56% of MT neurons are selective for the same depth sign ("congruent" cells) but the remaining 44% of neurons are sensitive towards near depth from motion parallax but prefers far depth from binocular disparity ("opposite" cells). For targets described by a combination of motion parallax and binocular disparity, the congruent cells firing follows the trend of binocular disparity but with higher intensity, suggesting congruent cells can combine information from these two cues. For opposite cells, such a trend is not seen (Nadler et al., 2013). The MST neurons have shown sensitivity to components of optic flow like rotation (clockwise/anticlockwise) and deformation (compression/ depression) (Orban et al., 1992). A few of the MST cells sensitive to crossed and uncrossed disparity showed sensitivity towards the direction of movement (Roy et al., 1992).

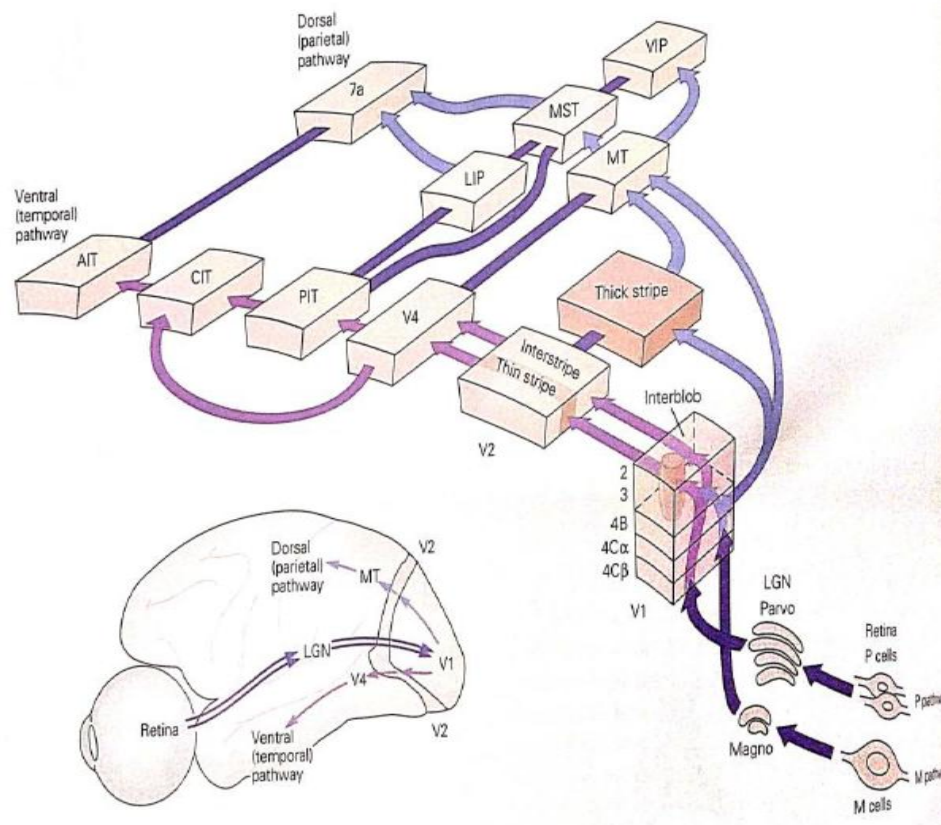


Figure 2.6 Flow of signals from retina project through LGN to V1 and higher cortical regions.
Taken from Kandel et al. (2000).

2.1.5 Bayesian framework of depth cues combination

The 3D world comprises both binocular and monocular depth cues. These cues can be consistent or in conflict with each other, or other scenes, and these cues can be sparse or dense. Perception of the depth from these cues can be explained mathematically with the Bayesian framework (Bradshaw & Rogers, 1996; Howard & Rogers, 2002; Johnston et al., 1993; Landy et al., 1995; Todorovic, 2008; Tyler, 2019b; Yuille & Bülthoff, 1996).

The external world forms a 2D image on each retina. A single retinal image may be consistent with many different 3D structures. The brain, therefore, has to process the

signals from the retina (I) using certain prior assumptions to make any meaningful inferences about the scene (S) (Yuille & Bülthoff, 1996). These assumptions can lead to bias in perception. For instance, in a natural scene, a front-parallel-oriented trapezoid can appear slanted if rectangles are assumed to be more probable (Knill, 2007). Bayesian decision theory provides a framework to model perception. This is based on the Bayes formula:(Bayes, 1991)

$$P(S|I) = \frac{P(I|S) P(S)}{P(I)} \quad \text{Eq 2}$$

where,

$P(S|I)$ = Probability of scene given retinal image (posterior distribution);

$P(I|S)$ = Probability of retinal image given scene (includes noise);

$P(S)$ = Prior probability; $P(I)$ = normalization constant

Many visual tasks require a decision about the scene. The loss function $L(S,d)$ specifies the penalty for making decision d (or inference) when the true scene is S . An optimal decision can be defined as the one that minimizes the expected loss:

$$R(d) = \int L(S,d)P(S|I)[ds] \quad \text{Eq 3}$$

The choice of the loss function is determined by the nature of the visual task that is required from the visual system i.e. does it want the decisions to be accurate or precise (Landy et al., 1995; Yuille & Bülthoff, 1996). Statistical estimators like maximum a posteriori (MAP) estimator and minimal variance (MV) estimator can be optimized with different loss functions. The MAP estimator which is mostly used in visual science is optimal with a loss function that penalizes equally every time an incorrect decision is

made i.e. it rewards only if the decision is accurate. The MV estimator, on the other hand, is optimal when the loss function penalizes decisions that are variable i.e. it rewards only if the decisions are precise, even if they are inaccurate.

2.1.5.1 Models of depth cue combinations

Using the Bayesian framework of cue combinations, two basic models are described in the literature to understand the combination of depth cues (Johnston et al., 1993; Landy et al., 1995; Yuille & Bülthoff, 1996).

Strong fusion model: In this model, the observer does not dismantle the scene into its composite depth cues or assume them to be modular. The scene that has the maximum likelihood of occurrence is multiplied by the a priori. The final interpretation is based on the scene from an accumulated set of prior scenes that has the maximum a posteriori (Figure 2.7A) (Landy et al., 1995; Yuille & Bülthoff, 1996).

Weak fusion model: This model is also known as weak coupling (Yuille & Bülthoff, 1996) where the retinal image is deconstructed separately into its constituted depth maps, thus assuming the depth cues to be modular and independent in nature. To derive the overall depth map, individual depth maps are linearly averaged after assigning a weight depending on their reliability: the higher the reliability, the higher the weight (Figure 2.7B) (Landy et al., 1995; Yuille & Bülthoff, 1996). According to the Bayes theorem, the two depth estimates from two depth cues (D_1 and D_2) are linearly combined after assigning each cue a certain weight (w_1 and w_2) depending on the to provide the final estimation of depth (D_{12}).

$$D_{12} = \frac{w_1 D_1 + w_2 D_2}{w_1 + w_2} \quad \text{Eq 4}$$

where, the weight (w_1 and w_2) is the inverse of the variability (σ_1 and σ_2),

$$w_1 = \frac{1}{\sigma_1}, \text{ and } w_2 = \frac{1}{\sigma_2} \quad \text{Eq 5}$$

However, this model applies to cues that share common retinal outputs as it is not readily possible to average cues that are qualitatively different. To average them, the cues need to be scaled and brought to the same unit and this leads to the next model (Landy et al., 1995).

The weights assigned to the cues are dynamic and vary with and within scenes. It depends on multiple factors, such as (Landy et al., 1995):

1. Availability of the cue: The variance of a cue depends on the objective availability and the quality of the cue in the scene (e.g. a scene with no or sparse texture should decrease the weight of the texture cue).
2. Ancillary information: Certain cues and information like occlusion, vestibular inputs, etc. do not estimate depth by themselves but provide information about the performance of other depth cues. Also, they provide the information about the performance of the cue only in a local region causing the reliability of a cue to change across the scene.
3. Robust estimation theory: This theory suggests that while assigning weight to individual cues, it is expected that the weights not only depend on the reliability (less variance) but also on the consistency of the weights. If all but one depth cue provides a consistent depth estimate while the other depth cue (discrepant cue) estimates a different depth magnitude, the system gets biased towards that

direction but once the discrepant cue is identified, the weights are lowered and depth is estimated correctly according to the consistent cues.

Modified weak fusion: In this model, each independent depth cue generates its depth map and provides it to other cues for depth promotion. The final depth involves a weighted average where the weights take into account both the estimated reliabilities of each cue and the discrepancies between cues (Figure 2.7C) (Landy et al., 1995). They use the word “promotion” to convey two ideas. 1) The depth cues are scaled to a common metric so that they can be averaged, and 2) the depth cues signalling for the same targets mutually help in estimating the combined depth when aligned (Johnston et al., 1993).

Tyler proposed the accelerated cue combination — a rapid mechanism of depth estimation. It finds reliable local depth information (usually structure in the region of attention and closest to the observer) to estimate the slant at that location and using this as the Bayesian prior it estimates the depth for the continuous surface until it reaches the edge. In case the local surface occludes another surface, the Bayesian “search” paradigm starts fresh again to find the local depth region for the other surface and calculates for continuous slant adjustment to it (Tyler, 2019a).

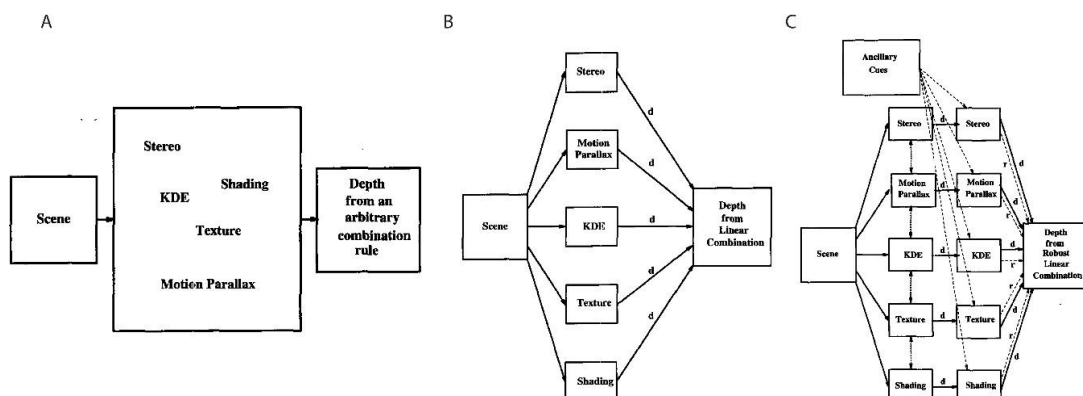


Figure 2.7 Flow diagram showing A. Strong fusion, B. Weak fusion, C. Modified weak fusion models. ‘d’ denotes depth represented by individual depth cues, and ‘r’ denotes the depth denoted by the ancillary cues. Taken from Landy et al. (1995).

Evidence for the promotion of depth cues is noted in the way binocular retinal disparity cue and kinetic depth effect (KDE) motion interact (Johnston et al., 1994). Binocular disparity distorts the shape of a 3D object when the viewing distance changes. While disparity is inversely proportional to the square of viewing distance, the size or the width of an object is inversely proportional to viewing distance. Due to these different scaling functions for the disparity and the size, changes in misinterpretation of viewing distance will distort the shape perception. Whereas, in the case of a KDE stimulus, the change in viewing distance will only lead to a linear increase in the overall size of the object without any distortion of the shape. Johnston et al. (1994) used random-dot stimuli to create a horizontally oriented elliptical 3D cylinder that was defined by binocular retinal disparity and KDE — both in isolation and combination. Subjects were asked to determine if the depth of the cylinder was more or less relative to the circular cross-section, i.e. if the cylinder was elliptical along the z-axis or the y-axis. They demonstrated that for a farther viewing distance (2m), the stereo depth was overestimated while at a nearer viewing distance of 50 cm, the depth from stereo is underestimated. However veridical depth estimates were obtained when disparity and KDE depth cues were combined. This provides evidence for the modified weak observer where adding the KDE overcomes the stereo distance scaling issues and provides veridical depth estimates. They also noted a poor estimate of depth from.

2.2 Depth cues for visuomotor task

Once the depth cues combine, the final depth estimate can be used for a perceptual task or for visuomotor actions like picking up an object, or placing the object on a surface. These two systems, perceptual and visuomotor systems, used to be thought to be serially connected, but neurophysiological studies show that this is not true. While the perception of depth from retinal disparity and motion parallax is coded by

the middle temporal (MT) neurons, the visuomotor control is mediated by the posterior parietal cortical areas (Jeannerod, 1986; Milner, 1998). Due to this, one system can be affected without affecting the other. Knill (2005) investigated the relative contributions of binocular and monocular depth cues (specifically, texture) in both visuomotor and perceptual tasks. In the visuomotor task, participants were instructed to place a physical cylinder onto a tilted surface (20° and 40°) defined by binocular disparity and texture cues. A corresponding perceptual task required participants to orient a physical cylinder such that it would be perpendicular to the tilted surface, effectively aligning their haptic response with their perceived surface slant. Additionally, in a visual matching task, participants adjusted the rotation of a rendered pin using a computer mouse to make it perpendicular to the tilted surface. The findings demonstrated that binocular depth cues were assigned a greater weight in the visuomotor task compared to both the perceptual and haptic matching tasks. This suggests that depth cues are differentially utilized depending on whether the task involves perception or visuomotor control. Thus, when the binocularity is lost upon temporary closure of one eye, the visuomotor task performance also deteriorates (Melmoth et al., 2009; Read et al., 2013).

In the case of reduced binocularity like in the case of amblyopia, or strabismus, the transport component of the prehension remains intact but the grasp is affected (Melmoth et al., 2009; Niechwiej-Szwedo et al., 2011; Niechwiej-Szwedo et al., 2012; Suttle et al., 2011). O'Connor et al. (2010b) recruited 143 subjects with varied levels of stereoacuity due to compromised binocularity arising from strabismus, refractive error, and amblyopia, and asked them to perform various tasks like putting pegs on the Purdue pegboard, inserting beads and water pouring task. The performance was noted to be poor in the group that was stereoblind compared to the reduced

stereoacuity individual. The binocular advantage was dependent on the task and the method of estimating the stereoacuity (O'Connor et al., 2010a, 2010b). Compared to the short-term absence of stereopsis caused by the temporary closure of one eye, the stereoblind, with a long-term absence of stereopsis, performed better at the pegboard and the bead task (O'Connor et al., 2010a). Piano and O'Connor (2013) further explored the impact of degraded stereopsis on the water pouring task and the bead task by degrading the monocular visual acuity by 6, 9, and 12 lines. They demonstrated that the impact of the blur on the bead task led to non-linear degradation in the performance.

The effect of the long-term absence of stereopsis has been commonly studied on stereoblind individuals (Melmoth et al., 2009; O'Connor et al., 2010a). The definition of stereoblind commonly agreed upon is clinically unmeasurable with the regular clinical tools available. This does not imply that these individuals do not have any stereopsis. In fact, with both eyes open, a stereoblind may either send a flatness signal to the brain and trigger a cue-conflict scenario with the existing monocular or binocular cues in the scene or the disparity signal can just be simply ignored, something that is still unknown. A better case of long-term deprivation of retinal disparity is the individuals with one eye, with the other eye removed surgically.

Suttle et al. (2011) investigated the eye-hand coordination skill in children with and without amblyopia and found that amblyopes took almost twice the time as normal to reach the object, with higher errors in reach direction and grip positioning. While the participants were allowed to move their heads and use motion parallax, the performance was the same as that of monocular viewing of controls, indicating if any head movements were indeed made, it was not useful. They however did not quantify the extent of head motion.

Marotta et al. (1995) studied the head movement patterns of one-eyed individuals while they performed reaching and grasping tasks. They evaluated the usage of motion parallax during a functional task of reaching out and grabbing a 2 cm thick oblong wooden block. They found that the reaching kinematics remained the same but the head movements made by the one-eyed individuals were spontaneous and also larger laterally and vertically. The head movements were also shown to increase as the time from enucleation increased. In another study, they then restricted the head movements of the normal binocular individuals and showed that under head-restricted conditions, the online velocity of the hand shows multiple corrections to reach the target compared to the head-free condition. This pattern was absent under binocular viewing. They concluded that this “retinal motion” was necessary for the task. This does not imply that the head movements made would have generated enough motion parallax. Those head movements could have been made to increase the visual field and avoid occlusion that would have been caused by the hand in front of the 3D spheres.

Watt and Bradshaw (2003) showed that the prehension behaviour is not similar to binocular retinal disparity and motion parallax. While the hand transport component of the prehension task remains the same under binocular viewing, monocular-head movement and binocular-head movement conditions, the grasp component of the prehension task was scaled with object size only under binocular viewing and binocular-head movement conditions. Monocular-head movement conditions that could generate motion parallax, did not help in scaling the grasp with the increase in the object size. Keefe et al. (2011) later argue that the binocular depth cue is not a special cue but the worsening in the visuomotor task is related to the increase in the uncertainty that arose due to the removal of a depth cue. They demonstrated this by

removing the binocular depth cue by occluding one eye and by removing the texture cue by providing random dot stimuli. In support of their hypothesis, both these conditions resulted in an increase in the grip apertures for smaller objects. Keefe and Watt (2017) went ahead to provide more evidence for the task to be more dependent on the “informative” nature of the depth cue. They demonstrated when the binocular depth cue information was dense, removing the cue made a difference whereas, in a scene with limited binocular depth cues, removing the cue by occluding one eye did not result any significant difference between binocular and monocular viewing conditions. These studies enforces that the depth perception in a visuomotor task follows the depth-cue combinations.

In this context, Gonzalez et al. (1989) measured the depth among children enucleated before the age of 2 years and compared it with age-matched controls under binocular and monocular conditions. Contradictory to their expectation, they found that both enucleated and monocular children had higher depth thresholds than binocular conditions and did not immediately use motion parallax to see the depth between the two inner edges of two plates. Once they were given verbal instructions to move their head, the threshold for enucleated and monocular conditions improved but still did not reach the level of binocular thresholds. The enucleated cohort made greater head movements with higher mean amplitude (20.69 cm) with lesser frequency (1.03 reversal/s), while the monocular cohort made them with lesser amplitude with higher frequency (16.36 cm, 1.42 reversal/s respectively) (SD or statistical information not provided by the authors).

2.3 Evidence for plasticity of visual performance

Gonzalez et al. (1989) concluded in their study that “Given the importance of the ability to resolve small depth differences in daily life, it would seem useful to instruct

monocular children on the use of parallax, and to do this at an early age". While it is tempting to believe that unocular individuals are superior in perceiving depth from monocular cues compared to the monocular view of binocular controls, the question is — to meet such an expectation, is the brain flexible enough to reorganize its neurons to fire for motion parallax in the absence of binocularity disparity?

At the lateral geniculate body and cortical V1 level, studies have shown that disruption in the binocularity from enucleation and occlusion results in shrinkage of the ocular dominance columns corresponding to the affected eye and expansion of the columns contralateral eye (Horton & Hocking, 1998; Hubel et al., 1977). Hubel et al. (1977) had enucleated one eye of two macaque monkeys at the age of 2 weeks and studied after 1.5 years. They found a single LGN layer that showed a marked increase in the widths of columns belonging to the functional eye, and a corresponding shrinkage of those belonging to the enucleated eye. They also sutured one eye at the age of 2 days for 7 weeks, 2 weeks of age for a duration of 18 months, and 3 weeks of age for 7 months. This resulted in the columns on the ipsilateral side of the closed eye reduced in size more for 2 days compared to 3 weeks; however, this decrease was less than for enucleated monkeys. One possibility is that the normal eye extends its territory and takes over the deprived/enucleated eye's columns. Interestingly they noted that monkeys at 1 week of age have very minimal segregation of the columns and segregations are noted to be more vivid and advanced by the 30th day. This might suggest that the deprivations of visual input during the segregation process or this critical period might lead to failure in normal visual development. Similar work by Crawford et al. (1975) extended the work by occluding both eyes. They demonstrated that while in the normal monkeys with uninterrupted binocularity, most of the cells respond to both eyes (Figure 2.8A). As the duration of binocular input deprivation

increased from 2 weeks to 208 weeks, the number of cells responding to binocular input decreased and a higher number of cells responded to the stimulation of the eye contralateral to the occluded eye (Figure 2.8B – D). With the closure of both eyes for a duration of 4 weeks, over 51% of the neurons did not respond, indicating the loss of sensitivity to the stimulation of either of the eyes (dotted bar in Figure 2.8E).

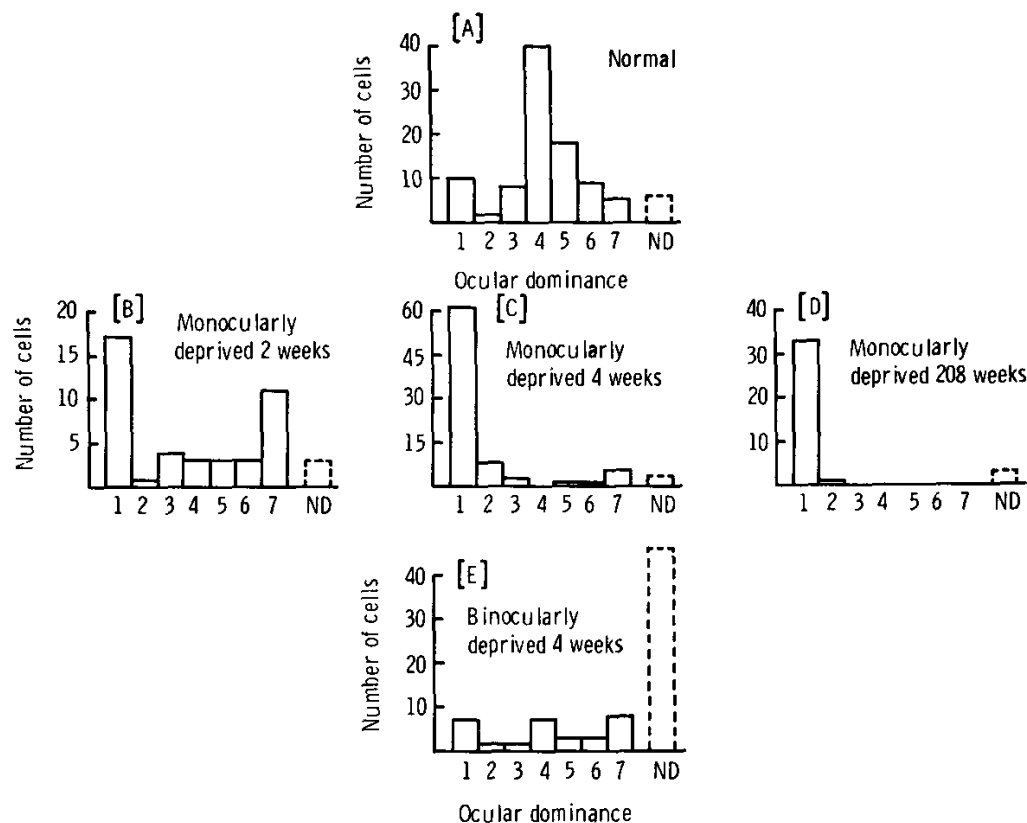


Figure 2.8 Distribution of cells based on eye dominance. Categories 1 and 7 include neurons that respond exclusively to the left or right eye, respectively and 4 are equally influenced by both eyes. Panel A) neurons from normal monkeys. Panels B–D) neurons with right eye deprived of vision through lid sutures for different durations, all starting at four weeks of age. Panel E) neurons from a monkey with binocular deprivation via lid suture between the 2nd and 8th weeks of life. The ND (non-driven) column indicates the number of cells that did not respond to visual stimulation. Taken from Crawford et al. (1975).

Horton and Hocking (1998) noted a similar pattern of changes in occipital lobe specimens of children who underwent enucleation at the age of 1 week. Enlargement of LGN input layers responsible for the contralateral side (layers 1,4 and 6) may indicate that the neurons on ipsilateral layers were reassigned to activate by the contralateral eye. This process could be an example of plasticity that the uniocular individuals might undergo that can explain better monocular visual acuity and contrast sensitivity relative to monocular viewing of controls.

From studies on the mechanism of perceptual learning, researchers found little or no evidence for changes in the neuronal sensitivities in the early or mid-level visual areas of the brain. Law and Gold (2008) trained monkeys to decide the direction of movement of random dots by making an eye movement towards the same direction. While the monkeys performed the test, the authors recorded the neuronal firing of the middle temporal (MT) neurons and the lateral intraparietal area (LIP) neurons. They expected that if the responses for weaker motion signals improve, it would have to be reflected in changes in both MT and LIP neurons. Contrary to the expectations, there were changes in the LIP neurons but not in the MT neurons. Nor were there any changes in the correlations between MT neurons. (Analogous results were obtained by (Kumano & Uka, 2013), using a depth-discrimination task.) Together, these results suggest that training somehow leads to better decoding strategies for the same incoming signals from the sensory neurons.

Some sensory neurons play a larger role in decoding strategies than others. Their relative contributions can be quantified with a set of weights. Training presumably optimises this set of weights. Indeed, there have been various attempts to infer neuronal weighting from the combination of choice probabilities (i.e. the correlations

between the activity of individual sensory neurons and a behavioural response) and the correlational structure amongst sensory neurons (e.g. Haefner et al. (2013).

Due to the joint representation of depth from binocular disparity and motion parallax, two possible outcomes arise when binocular disparity is either absent or degraded (Thompson & Nawrot, 1999). The first possibility is that motion parallax compensates for the loss of binocular disparity, effectively substituting its function in depth perception. Gonzalez et al. (1989) and Marotta et al. (1995) seemed to believe in this hypothesis. The second possibility is a joint loss in depth perception from both binocular disparity and motion parallax, indicating a breakdown in the shared neural architecture responsible for processing these cues. This has been demonstrated in individuals with amblyopia, where elevated stereoacuity thresholds correlate with higher motion parallax thresholds (Figure 2.9) (Thompson & Nawrot, 1999).

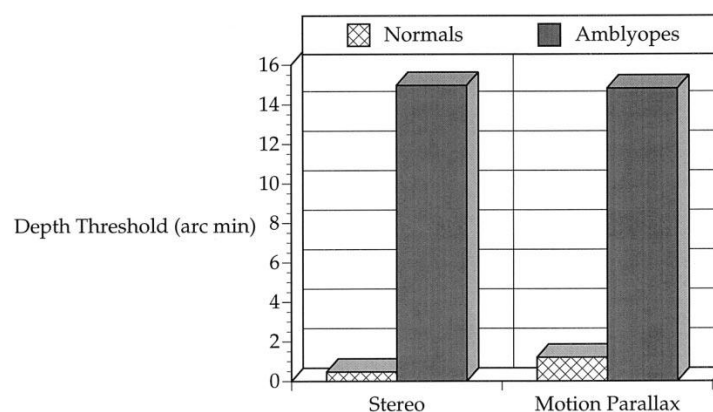


Figure 2.9 The average stereo and motion parallax depth threshold values for binocular controls (normal) and amblyopes. Taken from Thompson and Nawrot (1999).

2.4 Rationale and aim of the studies

Until now, research has primarily focused on the effects of losing a single depth cue or when multiple depth cues provide conflicting depth information. These studies have consistently demonstrated two key findings: 1) veridical depth estimates are obtained

when a scene contains multiple non-discrepant depth cues (Bradshaw & Rogers, 1996; Hillis et al., 2004; Johnston et al., 1994; Johnston et al., 1993; Knill & Saunders, 2003) and 2) the relative contribution of each cue to the final depth estimate can depend on the specific scene or task at hand (Bradshaw et al., 2000; Keefe & Watt, 2017; Knill, 2005). These findings are reported in laboratory setups by creating non-familiar viewing conditions like closing one eye or degrading the binocularity of otherwise binocular individuals. However, courtesy to certain disease conditions, individuals may naturally experience a complete absence of a single depth cue or can experience impoverished binocular and monocular depth cues. To investigate the former case—loss of a single cue—we choose uniocular individuals (i.e., those with vision in only one eye). For the second case—impoverished depth cues—we chose keratoconus, an ocular condition characterized by reduced visual acuity, diminished contrast sensitivity, and impaired stereopsis, arising from poor and aberrated retinal image quality. These cohorts of individuals provide us with an opportunity to understand the role of habituation in such viewing conditions.

Building on the findings of Keefe et al. (2011) and the potential for cue reweighting through perceptual learning literature (Kumano & Uka, 2013), we hypothesise that uniocular individuals will undergo similar weight redistribution to provide better decoding of the external depth signals from the monocular depth cues. Moreover, we propose that uniocular individuals will adopt strategies—such as increased head movements—to enhance the external depth information like motion parallax and dynamic depth information, thereby enhancing cue reliability and improving depth perception. In contrast, individuals with keratoconus, who experience overall degraded visual quality, may face additional noise in the external depth information, potentially limiting their ability to redistribute cue weights effectively.

Towards this, Gonzalez et al. (1989) represent the only study that has assessed depth vision in uniocular children. However, their investigation was confined to a controlled laboratory environment that did not replicate the complexity of natural settings where a full spectrum of monocular cues is available. Consequently, key questions remain unanswered: Can monocular depth cues adequately substitute for the absence of retinal disparity in day-to-day activities? Towards this direction, we used the buzz-wire game where subjects need to pass a loop through a convoluted wire without touching the wire. The task represents activities where the scene is continuously changing and the subject needs to be aware of the scene and also navigate objects. Activities like threading a needle, swatting flies etc. Furthermore, what roles do the age at enucleation and the duration of uniocularity play in the adaptation of depth perception? Can motion parallax be a depth cue being used?

Secondly, in cases of degraded binocularity resulting from poor and aberrated retinal image quality, keratoconus presents a multifaceted clinical profile characterized by reduced visual acuity, diminished contrast sensitivity, and impaired stereopsis. However, the functional consequences of these deficits on depth perception and visuomotor performance have not been rigorously evaluated.

Thirdly, it remains to be determined whether the deficits associated with a complete loss of binocularity can be mitigated by monocular depth cues when the task is purely perceptual, rather than visuomotor. This raises the question of whether the type of task influences the extent to which monocular cues can compensate for the absence of binocular disparity.

Lastly, there is a discrepancy in the literature regarding compensatory head movements. Gonzalez et al. (1989) reported that uniocular children do not

spontaneously exhibit significant head movements, whereas Marotta et al. (1995) observed that uniocular adults naturally display larger head movements. Irrespective of whether the head movements are made spontaneously, it remains unclear whether these head movements are sufficient to generate adequate motion parallax or whether uniocular individuals are effectively able to extract depth information from such movement.

The existing literature revealed surprisingly very little information related to the assessment of depth perception, particularly in individuals with a complete absence of binocularity. Our research aims to fill this gap by providing novel insights into real-world depth cue utilization and adaptation. While this dissertation does not explicitly investigate if weights are redistributed, it indirectly probes into such possibilities by systematically investigating the performance of individuals with absence or degraded binocularity in both perceptual and visuomotor tasks, and by examining the influence of factors such as age at enucleation, duration of uniocularity, and compensatory head movements on depth perception.

The research aims at:

1. To determine the ability of uniocular individuals to perceive depth in a functional vision task, vis-à-vis their age-matched healthy controls under both binocular and monocular viewing conditions.
2. To determine the ability of keratoconic individuals to perceive depth during functional vision tasks vis-à-vis their age-similar healthy counterparts under binocular and monocular viewing conditions.

3. To investigate whether the ability to extract depth information using monocular cues differs between visuomotor tasks and purely perceptual tasks among uniocular individuals.
4. To determine the extent to which uniocular individuals utilize motion parallax as a monocular depth cue, compared with age-matched healthy individuals under monocular conditions.

Chapter 3 Depth-related visuomotor task performance in the absence of binocularity

3.1 Introduction

Binocular retinal disparity and several monocular cues to depth like motion parallax, linear perspective, occlusion etc assist in computing depth information from two-dimensional monocular retinal images (Cutting & Millard, 1984; Landy et al., 1995; Rogers & Graham, 1979, 1982; Wheatstone, 1838). In the past, literature on visuomotor tasks like placing pegs on a pegboard or placing beads on a needle, (O'Connor et al., 2010b; Piano & O'Connor, 2013; Suttle et al., 2011) has noted that individuals with degraded binocularity, like in amblyopia and strabismus, have reduced depth perception from disparity (Levi et al., 2015; O'Connor et al., 2010a, 2010b; Read, 2015). In these scenarios, the integration of the rudimentary binocular disparity cue and the monocular depth cues might impoverish the cumulative depth estimations during the visuomotor task (Landy et al., 1995). Therefore, ascertaining the influence of monocular depth cues independent of binocular disparity's influence on the visuomotor task performance, may not be possible for these individuals. Uniocular individuals are completely devoid of binocular cues and the aforementioned judgments become entirely dependent on monocular cues. These individuals also have the advantage of estimating and interacting with depth exclusively from monocular cues over a long period of time. There might be a possibility of development of strategies to overcome the difficulties posed by the absence of retinal disparity. Gonzalez et al. (1989) tested the relative depth between two rods and found that compared to binocular viewing, uniocular children and those with one eye occluded temporarily were equally poor at the task. While the result suggests sub-optimal depth

perception following loss of vision in one eye, the results may be limited to the impoverished cues of the experimental apparatus and may not generalize to more complex real-world visuomotor activities of daily living where multiple monocular depth cues are available. While Marotta et al. (1995) conducted a few studies on uniocular individuals, it was mainly to understand the head movement used while performing the task and did not provide any information regarding the accuracy or speed at which their subjects were able to grasp objects. Considering there are no studies regarding the ability of uniocular individuals to perform depth-related visuomotor tasks, for the present study we asked two fundamental questions related to the functional depth vision of uniocular individuals. Firstly, is the performance of uniocular individuals in a depth-related visuomotor task equivalent to fully binocular individuals under monocular viewing conditions? Secondly, is the performance of uniocular individuals dependent on the person's age, duration of uniocularity and/or the use of head movements that could have provided monocular depth cues such as motion parallax or occlusion?

The answers to these questions may be task-dependent (Bradshaw et al., 2000). Tasks that are “easy” to perform may not be able to differentiate the performance between uniocular/monocular from binocular performance owing to a ceiling effect. On the other hand, tasks that are too “tough” to perform may again result in indistinguishable outcomes owing to a floor effect. Hence, it is critical to choose a task that can reliably differentiate the performance change between loss of binocularity and intact binocularity. The functional depth-related visuomotor task used in this study was the buzz-wire task, inspired by Read et al. (2013). They showed a significant difference (~5 times) in task performance for binocular and monocular viewing conditions, compared to the Morrisby Fine Dexterity Test, which is similar to the pegboard test.

The buzz-wire task requires the participants to pass a loop around a convoluted wire track set in depth, without coming in contact with the wire (Figure 3.1A). An error in the task is marked by a contact between the loop and the wire, which results in an auditory “buzz”. The goal of the participant is to navigate the length of the wire while making as few errors/buzzes as possible. Read et al. (2013) noted that the number of contacts and the total time taken to complete the task were lower under binocular viewing conditions compared to their monocular viewing conditions. This advantage potentially arises from the need for estimates of the wire’s slant, curvature, and diastereopsis using the several depth cues that are consistent with each other and combined in a statistically optimal fashion during natural viewing (Landy et al., 1995). Similar tasks involving the buzz-wire apparatus have also been employed by Joy et al. (2001) and Murdoch et al. (1991) for investigating the impact of degraded binocularity on visuomotor task performance, albeit more qualitatively than Read et al. (2013).

The following four hypotheses were framed to address the questions raised earlier. First, with an absence of binocularity, the variability of depth estimates may increase resulting in a greater number of errors in the buzz-wire task in uniocular individuals and controls under monocular viewing. The speed of task performance also may decrease in these individuals/viewing conditions, reflecting an increase in caution being exercised to avoid errors. Second, the uniocular participants may be superior to monocular viewing of controls in their performance owing to such tasks being performed habitually by the uniocular group using monocular depth cues while it is an unnatural and forced behaviour for the controls under monocular viewing. Third, the performance might be superior in individuals who are chronically uniocular from young ages, compared to acute and older cases, as the visual system is overall more mouldable (Barry & Bridgeman, 2017; Hubel et al., 1977) and has greater habituation

time in the former than latter cohorts (Nemanich & Earhart, 2015; Ruitenberg et al., 2023). Fourth, the uniocular individuals may also move their heads more than controls, as observed by Marotta et al. (1995) facilitating the use of motion depth cues as a means of optimizing task performance and restricting these head movements will consequently affect the performance negatively.

3.2 Methods

3.2.1 Participants

The study was carried out at the L V Prasad Eye Institute (LVPEI), Hyderabad, India between September 2022, and April 2023. The study was approved by the Institutional Review Board of LVPEI and the Optometry Proportionate Review Committee of City, University of London, UK and adhered to the tenets of the Declaration of Helsinki. Written informed consent was obtained from all the adult participants. Verbal consent was obtained from children <18 years of age, and a written informed consent form was signed by their parents/legal guardians. The cases were recruited from the patient pool of LVPEI, diagnosed with either congenital uniocularity or who underwent enucleation/evisceration due to retinoblastoma, or suffered unilateral vision loss following trauma (Table 3-1). Cases with an ambiguous history of vision loss, progressive loss of vision leading up to blindness in one eye, visual field loss, anomalous eye movements, any ophthalmic dysfunction in their functional eye, any systemic condition that restricted body movement, visibly shaking hands, or an inability to follow instructions were all excluded from this study. Age-similar, binocular controls

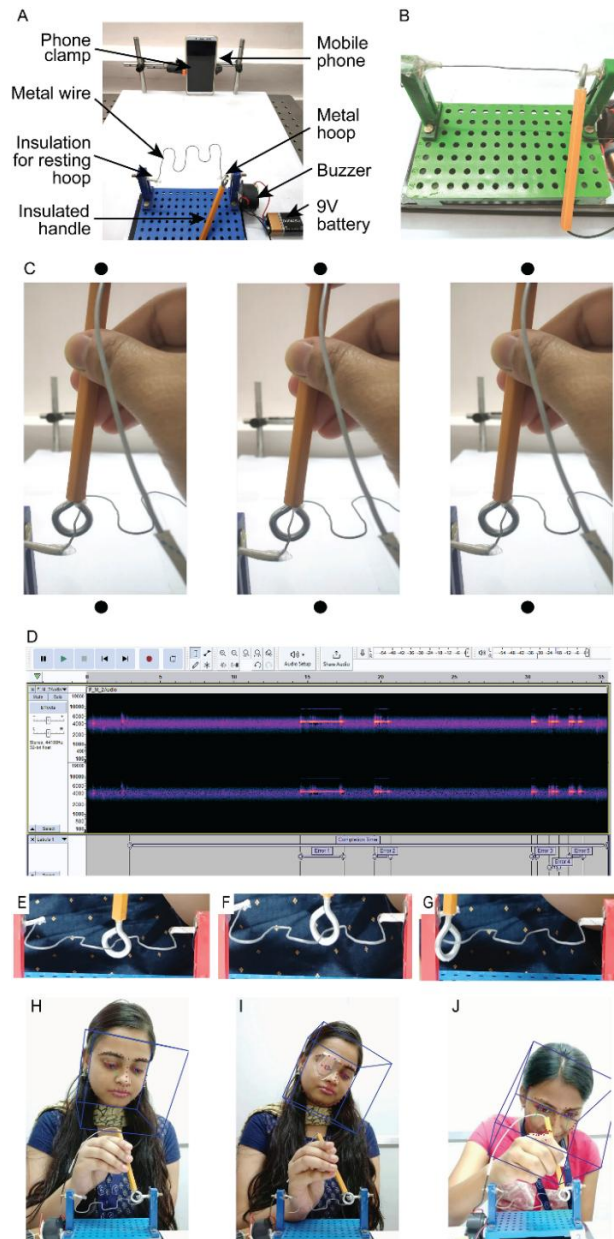


Figure 3.1 A) Buzz-wire experimental setup from the participant's view with key elements highlighted. B) The unbent buzz-wire used in this study. C) Representative stereoscopic image depicting the position of the metal loop and the wire track in depth. To view the stereogram in-depth, either fuse the left and middle panels by converging the eyes or fuse the middle and right panels by diverging the eyes. D) Representative screenshot of a spectrogram obtained using the Audacity software, with markings for completion time and the epochs of error time (high contrast tracks in the spectrogram). E – G) Representative images of the loop position during the straight (E), transition (F), and curved (G) portions of the wire track. H – J) Representative frames of head tracking performed by the OpenFace software: successful tracking in binocular (H) and monocular (I) views, and failed tracking (J). Consent was obtained from the participants shown above to use their pictures in this figure.

Table 3-1 Demographic details of controls and cases and the cause of uniocularly in cases that participated in the study. Chronological age and the age and duration of uniocularly are reported as median (25th – 75th quartiles).

		Age (years)	Gender (M : F)	Age at uniocularly (yrs)	Duration of uniocularly (yrs)	Reasons
Cases (n = 45)	Children (n = 16)	12 (9.8 – 15.3)	7 : 9	3.3 (1.2 – 4.1)	10.0 (6.4 – 11.3)	Retinoblastoma (n = 11); Trauma (n = 4); Anophthalmus (n = 1)
	Adult (n = 29)	29 (23 – 31)	22 : 7	6.40 (3.4 – 16.8)	17.8 (9.7 – 25.9)	Retinoblastoma (n = 8); Trauma (n = 18); Microphthalmos (n = 1); Contracted socket (n = 1); Rhino-cerebral mucormycosis (n = 1)
Controls (n = 45)	Children (n = 15)	10 (8.5 – 12)	11 : 4	NA	NA	NA
	Adult (n = 30)	26.5 (24.5 – 30)	11 : 19	NA	NA	NA

were recruited from the institute's student and staff and their associates, and from amongst the acquaintances of patients visiting the institute. All the participants had best-corrected, high contrast, distance acuity of 20/20 and near acuity of N6 or better at 40 cm viewing distance in both eyes (for binocular controls) or in their functional eye (for uniocular cases). Binocular stereoacuity of 50 arcsec or better at 40 cm viewing distance on the Titmus-fly test was an added criterion for the controls.

An a priori power analysis was conducted using G*Power version 3.1.9.4 for sample size estimation (Faul et al., 2007), based on data from Gonzalez et al. (1989) which compared depth precision in 10 uniocular children with depth precision in 13 binocular children. The effect size in that study was 1.1, considered to be large using conventional criteria (Cohen, 1988). With a significance criterion of $\alpha = 0.05$ and power $(1 - \beta) = 0.95$, the minimum sample sizes needed with this effect size is $N = 24$ for a t-test between cases and controls, supporting the adequacy of our sample size of 45 cases and 45 controls.

3.2.2 The buzz-wire apparatus

Four buzz-wire setups were constructed from wires of 0.10 cm in diameter. Three of those wires were 33.5 cm long and were curved multiple times to provide for modulation in depth along the anterior-posterior direction (Figure 3.1A). The fourth wire remained straight and 10 cm long (Figure 3.1B). Unlike Read et al. (2013), the buzz wires used in the present study did not have any vertical modulation; the bending was parallel to the tabletop. The insulated portions at the edges were clamped onto vertical posts separated by 11 cm distance. The vertical posts were secured to a horizontal base, which was then positioned on a larger horizontal surface that was wrapped with white matte-finished paper. The wire pattern was fixed parallel to the horizontal base, resulting in depth modulation from one end of the vertical post to the other end (Figure 3.1C, free-fuse the stereo pair to experience the depth). A 1 cm diameter and 0.3 cm thick metal loop passed around the wire and was connected to a buzzer to deliver an audible sound each time the loop contacted the wire (Figure 3.1A). The 9 cm long stalk of the loop was moved by hand along the length of the wire during each trial. The start and end of the convoluted wire were insulated so the loop could be rested silently before and after the task. The buzz-wire apparatus and the participant's face were video recorded using the front-camera setting of an Android-operated cellular phone (Redmi Note 5 Pro®, Xiaomi, Beijing, China). The phone was fixed 30 cm distance from the buzz wire using a custom-built clamp to ensure the stability of the video recording. At this distance, the video recording subtended a viewing angle of $42^\circ \times 55^\circ$ at the camera aperture of the mobile phone.

3.2.3 The buzz-wire task

Participants were seated 30 cm away from the buzz-wire and at a mean elevation angle (minimum to maximum range) of 45° ($36 - 53^\circ$, depending on the seating height

relative to the buzz-wire apparatus) (Figure 3.1A). For enhanced participant engagement, the buzz-wire task was described as a “game” to make fewer errors. Pre-set instructions, either in English or in the participant’s local language were provided to every participant at the start of the game.

This is a game in which the idea is to move this loop along to the end of the wire without touching it. 1) Look at the camera without moving for 5 sec, during which I will give a verbal countdown and say “start”, upon which you will start the game. 2) Your task is to pass the loop from one end to the other without touching the wire. 3) In case the loop touches the wire, you will hear the buzzer ring. When you hear the buzzer, stop your movement, and make the buzzing stop by centring the wire within the circular loop. 4) Once the buzzing stops, proceed forward until you reach the other end. 5) Make sure the loop is held upright throughout the game.

No specific instructions were provided regarding the speed with which the participant needed to perform the task or whether the participants could move their heads while performing the task. The instructions were accompanied by the examiner demonstrating each step to ensure the participants understood what should and should not be done. However, no prior practice trials were given to the participants to retain the difference in the viewing conditions (O'Connor et al., 2010b).

In random order, all participants participated in the four versions of the wire pattern. Controls performed the buzz-wire tasks under both binocular and monocular viewing conditions, in random order, while cases performed the tasks only under uniocular viewing conditions. For controls under monocular viewing, one eye was randomly selected to be occluded using a pirate patch. Upon applying or removing the pirate

patch, participants were asked to report if they could see any dark spots in the vision (none reported seeing anything abnormal). Additionally, the buzz-wire tasks were conducted with the participant either having their head free to move or with their head stabilized using a chin and forehead rest. These too were performed in random order. The direction of movement of the loop through the wire pattern – i.e., from the left end to the right end of the wire or vice versa – was determined randomly at the beginning of each session. In total, controls repeated the task 16 times (4 wire patterns x 2 viewing conditions x 2 head movement conditions = 16 repetitions) while cases repeated the task 8 times (4 wire patterns x 1 viewing condition x 2 head movement conditions = 8 repetitions). It took approximately 40 sec to complete each buzz-wire task, following which 1 min of break was given prior to the start of the next task to avoid fatigue and boredom. Once it was ensured that the participant was looking straight at the camera clamped in front of the buzz-wire (Figure 3.1A), the examiner pressed the recording button on the phone. The participant's performance on each buzz-wire was recorded separately for offline analysis. Every video was inspected by the examiner to pick up instances of invalid task performance where the participant would drag the loop along the wire without stopping to correct their error. This resulted in the removal of 9 trials from the binocular controls and 3 trials from the uniocular cases.

3.2.4 Determination of the key outcome variables in the buzz-wire task

The video recordings were cropped to include only the duration from the start of the task to when the loop reached the insulated section at the opposite end of the wire. These videos were then converted to waveform audio files (.wav format) using custom-written Python code (3.10 Version, Centrum voor Wiskundeen Informatica Amsterdam, The Netherlands). These audio files were then analysed for buzzes using the open-

source Audacity® software (3.2.1 version, Audio.com, Boston, MA). Each file was visualized as a spectrogram, showing signal strength across frequency bands over time (Figure 3.1D). A bandpass filter (4.0–4.1 kHz) was applied and audio intensities were cut off at -30 db to differentiate buzzes from the background noise (Figure 3.1D). The key information obtained from Audacity was firstly, the task-completion time (i.e., the time between the examiner's verbal "Start" command to the end of the audio file), and secondly, the number of buzzes and its time stamps corresponding to the onset and termination of each buzz. From these, the outcome parameters were 1) the error rate, calculated by dividing the number of buzzes by the task completion time (errors/sec) and 2) speed, calculated by dividing the total length of the wire (33.5 cm) by the difference between task completion time and total error duration (cm/sec).

3.2.5 Determination of the error location in the buzz-wire task

The buzz-wire apparatus had regions of a straight portion (anterio-posterior orientation) that transitioned into a curved region, thus containing locations of various degrees of difficulty that may contribute unequally to the errors made during the task. For instance, the curved wire locations would pose a greater navigational challenge relative to the other regions, as the participants need to veridically estimate the slant, curvature and diastereopsis to avoid contact with the loop (Figure 3.1E – G). The hypothesis was that the curved locations would result in an increase in the number of errors, compared to the other regions and would be also greater for monocular and unocular viewing than for binocular viewing. To test this hypothesis, a total of 390 frames (130 frames for each viewing condition) were randomly selected where an error occurred. Three examiners who were naïve to the experiment objectives, viewed each of these frames in random order and were asked to make a forced-choice psychophysical judgement and assign the loop positions to either of one of these

locations, 1) straight portion of the wire or 2) at a transition zone from straight to the curved portion of the wire, or vice versa, or 3) at a curved portion of the wire (Figure 3.1E – G). The identity of the study participant and the viewing condition were masked to the 3 examiners by placing a black box occluding the participant's face, to avoid examiner bias. No time limit was imposed on the examiners to decide on each presentation. The mode of the response choices from the three examiners was taken as the final location of the loop along the wire. The decision of a fourth naïve examiner was sought in instances where the response choices of the three examiners disagreed with each other.

3.2.6 Analysis of head movements

Videos recorded under the free head condition with depth-modulated buzz-wires were analyzed using the open-source software OpenFace (Amos et al., 2016). This software identified and tracked facial landmarks, allowing for the measurement of translational head movements (horizontal, vertical, and anteroposterior directions) and rotational head movements (yaw, pitch, and roll axes) (Figure 3.1H–J). 37% of the videos failed in localization of facial landmarks due to face obstruction caused by participants' hands (43% of total failed videos) (see Figure 3.1J) or due to sudden change in focus to the buzz-wire causing decreasing the brightness of the face (33% of total failed videos), dark skin tone of the participants (24% of total failed videos), and were excluded from the analysis. Finally, binocular trials from 40 cases (children: 14; male: 19) and monocular trials from 31 cases (children: 12; male: 21) of the 46 controls, and 32 trials from 45 unocular cases (children: 12; male: 21) were used for the head analysis. During the task, the range of translational and rotational head movement was calculated as the difference between the maximum and minimum head position and frontal orientation along the horizontal (x), vertical (y), and antero-

posterior (z) axes. A few of the participants were noted to adopt a preferential head tilt to get comfortable before starting the task as soon as they were instructed to start the task. In such instances, the translational and rotational head movements were calculated once the preferential head position was reached. The head movement velocity was calculated by dividing the total magnitude of horizontal head translation by the task completion time.

Representative videos of head movements made by a control participant under binocular ([Video - Binocular](#)) and monocular ([Video - Monocular](#)) viewing conditions and by a uniocular participant ([Video - Uniocular](#)). The high-pitched audio buzz arising from the contact between the hoop and the wire was analyzed with the Audacity software to generate the primary outcome variables of this study (Figure 3.1D). The associated graphs show changes in the translational (horizontal, vertical and anteroposterior) and the rotational (pitch, yaw, and roll) head movements for each frame of the video, normalized to the head position during the first 5 seconds where the subjects looked directly at the camera. A positive horizontal, vertical and anteroposterior head movement indicates the head to move towards the left, down and farther respectively. A positive Pitch, Yaw and Roll head movement indicate downward, right head turn and right head tilt movements respectively. The negative values indicate the opposite direction of head movements.

The equivalent disparity generated from motion parallax during the buzz-wire task to view the depth between one side of the loop edge to the wire was calculated using Equation 1. The equivalent disparity was calculated only for the monocular viewing of controls and for uniocular participants as motion parallax becomes a primary depth cue in the absence of binocular disparity. Since the head velocity of the participants was quite slow, it was assumed that the motion parallax signal was derived primarily

from the relative retinal image velocities between the wire and the loop edge, without any influence of head velocity (Hell, 1978; Ujike & Ono, 2001). Equivalent retinal disparities for binocular viewing of controls were determined using Equation 2 (Rogers & Graham, 1982). For both equations, the distance between one side of the loop edge and the wire was constant ($\Delta D = 4$ mm). The antero-posterior distance between the participant and the buzz-wire apparatus (D) and the magnitude of horizontal head translation (ΔH) were obtained from the head motion analysis data. The interocular distance (IOD) was based on age-appropriate values reported by MacLachlan and Howland (2002) (MacLachlan & Howland, 2002).

$$\delta_{ed} = \frac{\Delta H \times \Delta D}{D^2} \times \frac{60 \times 180}{\pi} \dots\dots\dots \text{Equation 1}$$

$$\delta_{rd} = \frac{IOD \times \Delta D}{D^2} \times \frac{60 \times 180}{\pi} \dots\dots\dots \text{Equation 2}$$

where, δ_{ed} = Equivalent disparity from head movements (arcmin); δ_{rd} = Binocular retinal disparity (arcmin); ΔH = Magnitude of horizontal head translation (mm); ΔD = Distance between the edge of the loop (mm); D = Antero-posterior distance between the participant and the buzz-wire apparatus (mm); IOD = Interocular distance (mm).

3.2.7 Statistical analysis

Statistical analysis was performed using IBM SPSS Statistics® (Version 21; Armonk, NY) and Matlab (R2016a). The three repetitions of the buzz-wire task demonstrated strong test-retest reliability and showed no short-term practice effects (Figure 3.2). Consequently, data from the three repetitions were averaged for further analysis. The Shapiro-Wilk test indicated that the dependent variables — error rate, speed, and the magnitude of translational and rotational head motion were not normally distributed. Since parametric tests are more effective in detecting data trends when the data follow a normal distribution, all dependent variables were transformed using a square root transformation to improve normality, ensuring appropriate conditions for parametric

statistical analyses. However, for visualization purposes, all figures (except Figure 3.4) display raw, untransformed data. The square root of the error rate was regressed against age using a bilinear model. The kink point in the bilinear fit occurred at 16.6, 17.5 and 20.0 years for binocular, monocular and uniocular conditions, respectively (data not shown). Thus, for consistency, age was categorised into two groups according to the formal 18-year age point for the transition to adulthood. To analyze the control group, a five-factor repeated measures multivariate analysis of variance (RM-MANOVA) was conducted. This examined the between-subject factors of age (children vs. adults) and gender (male vs. female), along with the within-subject factors of viewing condition (binocular vs. monocular), buzz-wire pattern (curved vs. straight), and head position (free vs. fixed) on the dependent variables of error rate and speed. Additionally, a separate four-factor MANOVA was performed for the uniocular participants' data to evaluate the effects of the between-subject factors age and gender, as well as the within-subject factors buzz-wire pattern and head position, on the same dependent variables. A forward stepwise linear regression analysis was conducted to identify the potential predictors of the square root-transformed error rate in children and adults from the candidate variables of age and the duration of uniocularity (Wani, 2018). Variables were added at each step of the regression analysis based on their p-values, with a threshold of $p \leq 0.05$ to determine the total number of variables to be included in the final model. This analysis was not conducted for speed, as age had no significant effect on this dependent variable. Also, the age of uniocularity was excluded from the analysis since it was simply the difference between the participant's age and their duration of uniocularity. To examine the effect of head movement magnitude across three viewing conditions and two age groups, a two-factor MANOVA was performed. The dependent variables were the six degrees of head movements - 3 translations and 3 rotations and the between-subject factors were

the viewing condition (binocular vs. monocular vs. uniocular) and the age groups (children vs adults) P-value <0.05 was considered statistically significant in all analyses.

3.3 Results

Table 3-1 provides the demographic details of all the participants along with the reason for uniocularity among the cases. The participants' age ($p = 0.76$) and gender ($p = 0.49$) were not significantly different between cohorts.

3.3.1 Repeatability of error rate and speed across the three buzz-wire trials

Every study participant performed three variants of the buzz-wire task. This allowed a determination of the test-retest variability of the task performance. Figure 3.2 shows Bland-Altman plots for the error rate (Figure 3.2A) and speed (Figure 3.2B) for the binocular and monocular viewing of controls and the uniocular participants. These data showed no bias across the three repetitions of the task (mean unsigned difference for error rate: <0.05 errors/sec; mean unsigned difference for speed: <0.15 cm/sec). The difference in error rate and speed across any two repetitions showed no systematic trend with the mean value across these repetitions. The 95% limits of agreement of the error rates and speed were in the same range among the three viewing conditions tested. Also, intraclass correlation coefficients revealed good reliability of error rate (binocular = 77.7%; monocular = 79.5%, uniocular = 77.8%) and speed (binocular = 82.7%; monocular = 81.8%; uniocular = 79.1%) across the three repetitions. These results indicate no systematic difference in task performance across the three repetitions. Therefore, the outcome measures obtained from these three repetitions were averaged for further analyses.

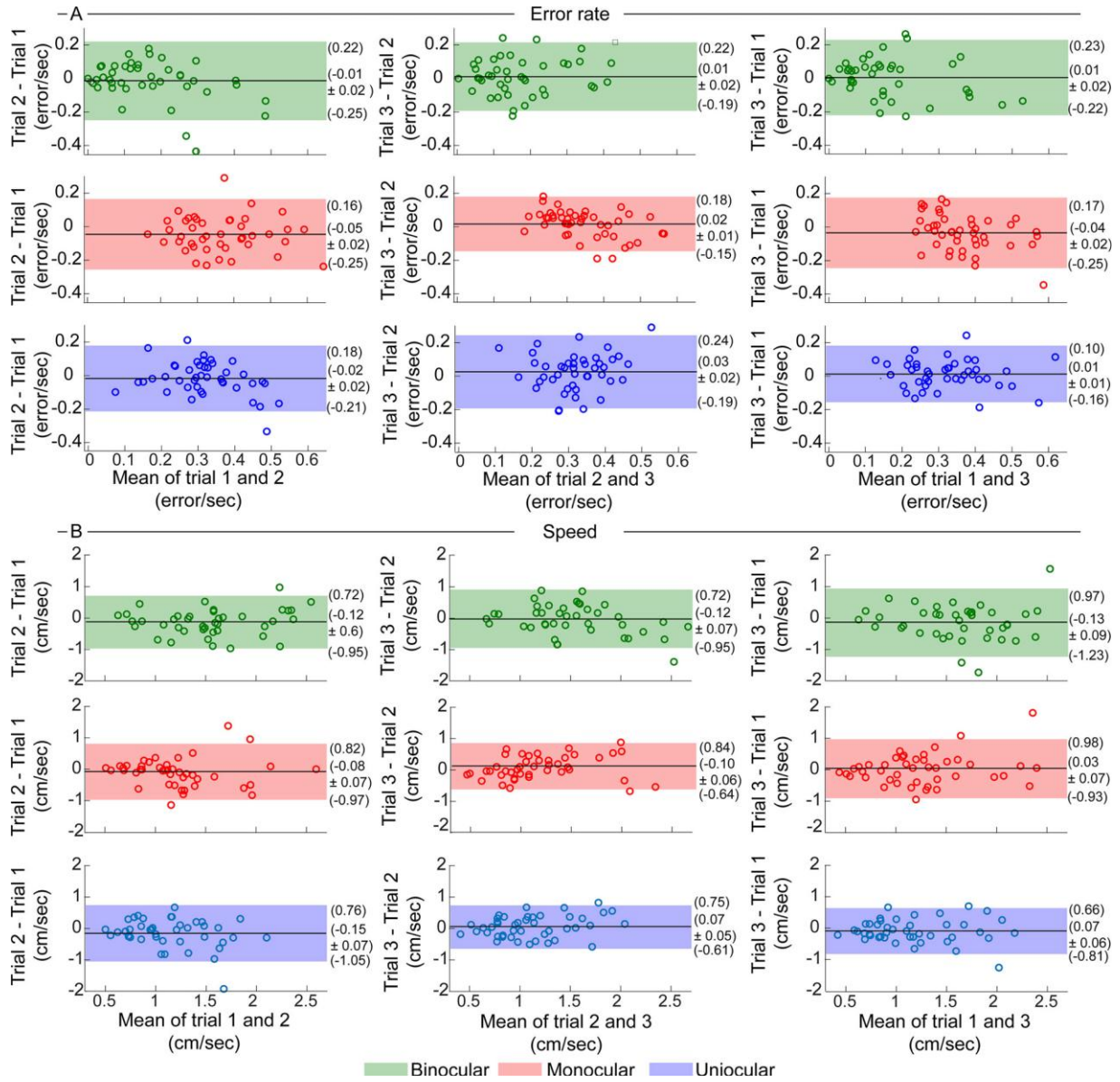


Figure 3.2 Bland-Altman plots for error rate (A) and speed (B) observed across the three trials of the buzz-wire task with depth modulation under head-free viewing for individual controls under binocular (green) and monocular (red) viewing conditions (top panel) and for the uniocular participants (bottom panel). The left columns compare data obtained from trials 1 and 2, the middle columns compare data obtained from trials 2 and 3 and the right columns compare data obtained from trials 1 and 3. In each panel, the solid black line represents the mean difference, with the value $\text{mean} \pm 1\text{SD}$ of the mean mentioned on the right side of the line. The upper and lower edge of the coloured box indicates the upper and lower limits of agreement, respectively, with the specific value specified on the right of the edges.

3.3.2 Cohort-level task performance

Figure 3.3 plots a combination of violin and box-and-whisker plots for the two outcome measures obtained from all controls and cases, who performed the buzz-wire task with depth modulation under head-free conditions. The median (25th – 75th quartiles) error rate under binocular viewing condition of controls [0.15 errors/sec (0.09 – 0.22 errors/sec); i.e., an error every 6.67 seconds] was smaller than their monocular viewing [0.33 errors/sec (0.28 – 0.41 errors/sec); i.e., an error every 3.03 seconds] and that of the uniocular subjects [0.31 errors/sec (0.25 – 0.38 errors/sec); i.e., an error every 3.23 seconds] (Figure 3.3A). Additionally, the controls moved significantly faster under binocular conditions [1.55 cm/sec (1.31 – 1.87 cm/sec)], compared to their monocular viewing [1.16 cm/sec (0.97 – 1.44 cm/sec)] and the uniocular cohort [1.05 cm/sec (0.81 – 1.46 cm/sec)] (Figure 3.3B).

3.3.3 Multivariate analysis of task performance in controls

The five-factor RM-MANOVA comparing binocular and monocular viewing in controls revealed significant main effects of age, viewing condition and buzz-wire pattern on the combined dependent variables (Table 3-2). The results of five-way RM-MANOVA comparing the binocular and monocular task performance of controls. Multivariate test results are shown for the main effects and interaction between relevant independent variable pairs). Amongst these factors, the age group was statistically significant for the error rate but not for the speed (Table 3-2; Section 1). The relationship between the square root of the error rate and the square root of age for binocular and monocular viewing conditions is shown in Figure 3.4A and B, respectively. The data of children showed a decrease in error rate at the rate of 0.03 errors/sec and 0.002 errors/sec per unit increase in age under binocular and monocular viewing conditions, respectively. The equivalent data for adults showed no significant change with age, but the y-

intercept showed an overall lower error rate under binocular (0.35 errors/sec) than monocular (0.50 errors/sec) viewing conditions (Figure 3.4A and B). The interaction between the viewing condition and buzz-wire pattern was also significant (Figure 3.5, Table 3-2; Section 1).

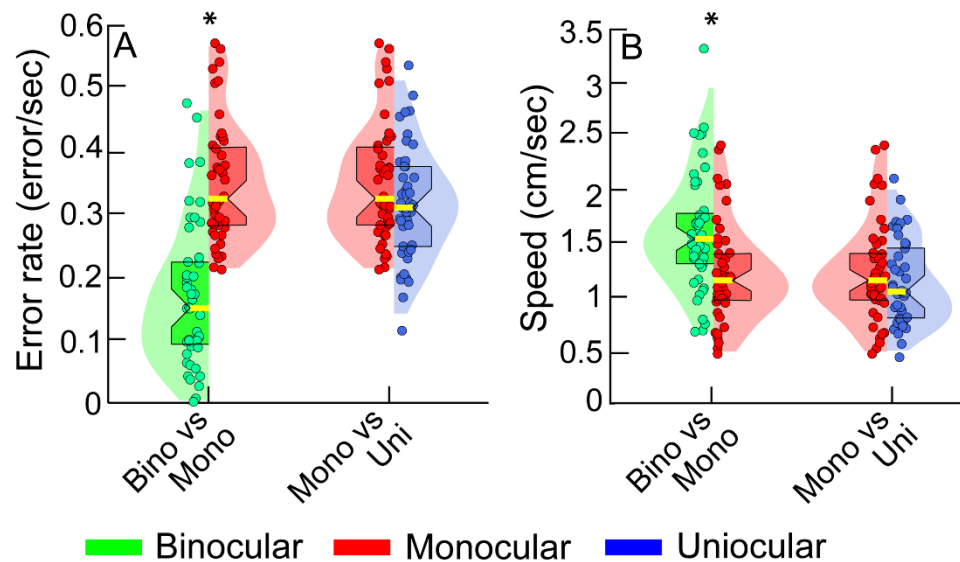


Figure 3.3 Violin plot pairs showing the distribution of the error rate (panel A) and speed (panel B) for the binocular and monocular viewing of controls and uniocular cases while they performed the buzz-wire tasks with depth modulation under head-free viewing conditions. Each violin plot is constructed with a kernel density that was calculated by taking the maximum and minimum data range for each outcome variable in a given cohort and dividing it into ten equal bins. Superimposed within the violin plots are box and whisker plots, with the central yellow solid line within each plot, indicating the median value, the notch of the box indicating the 95% confidence interval of the median and the edges of the box indicating the 25th and 75th percentile. The violin plot is truncated at the 1st and 99th percentile. The circles, with random jittering along the abscissa, indicate the individual subjects' error rate, averaged over the three trials with the depth-modulated buzz-wire and under head-free conditions. The asterisk symbol indicates statistical significance at $p \leq 0.05$.

Table 3-2 The results of five-way RM-MANOVA comparing the binocular and monocular task performance of controls. Multivariate test results are shown for the main effects and interaction between relevant independent variable pairs.

Section 1 – Five-factor mixed model RM–MANOVA Analysis (for controls)							
Effect of age, gender, viewing condition (Bino vs Mono), buzz-wire pattern (depth modulated, straight), head position (free, restricted)on error rate and speed	1a. Multivariate tests						
			F	p-value	Partial η²		
		Age group	13.7	<0.001	0.45		
		Gender	2.3	0.12	0.12		
		Viewing condition	49.3	<0.001	0.74		
		Buzz-wire pattern	35.6	<0.001	0.68		
		Head position	1.00	0.37	0.06		
		Viewing condition x Age group	3.1	0.06	0.16		
		Viewing condition x Buzz-wire pattern	7.1	0.003	0.29		
		Viewing condition x Head position	2.2	0.13	0.11		
		Buzz-wire pattern x Age group	0.4	0.69	0.02		
		Head position x Age group	0.1	0.95	0.00		
		1b. Univariate tests					
			Error rate		Speed		
		(errors/sec)		(cm/sec)			
		Mean ± SE	p-value	Mean ± SE	p-value		
	Age group	Children	0.50 ± 0.02	<0.001	1.27 ± 0.05	0.56	
		Adults	0.37 ± 0.02		1.23 ± 0.04		
	Viewing condition	Binocular	0.36 ± 0.02	<0.001	1.31 ± 0.04	<0.001	
		Monocular	0.51 ± 0.01		1.19 ± 0.04		
	Buzz-wire pattern	With modulation	0.51 ± 0.01	<0.001	1.18 ± 0.03	<0.001	
		W/o modulation	0.37 ± 0.02		1.33 ± 0.04		
Section 2– Five-factor mixed model RM–MANOVA Analysis (Monocular vs Uniocular)							
Effect of age, gender, viewing condition (Mono vs Uni), buzz-wire pattern (depth modulated, straight), head position (free, restricted)on error rate and speed	2a. Multivariate tests						
			F	p-value	Partial η²		
		Gender	0.08	0.92	0.01		
		Age group	10.17	0.001	0.43		
		Buzz-wire pattern	73.51	<0.001	0.85		
		Head position	3.16	0.06	0.19		
		Buzz-wire pattern x Age group	7.35	0.003	0.35		
		Head position x Age group	0.23	0.8	0.02		
		2b. Univariate tests					
			Error rate		Speed		
			(errors/sec)		(cm/sec)		
			Mean ± SE	p-value	Mean ± SE	p-value	
		Age group	Children	0.56 ± 0.02	<0.001	1.15 ± 0.05	0.08
			Adults	0.47 ± 0.01		1.03 ± 0.04	
	Buzz-wire pattern	With modulation	0.58 ± 0.01	<0.001	1.04 ± 0.04	<0.001	
		W/o modulation	0.45 ± 0.02		1.15± 0.03		

Relationships with $p < 0.05$ appear in bold.

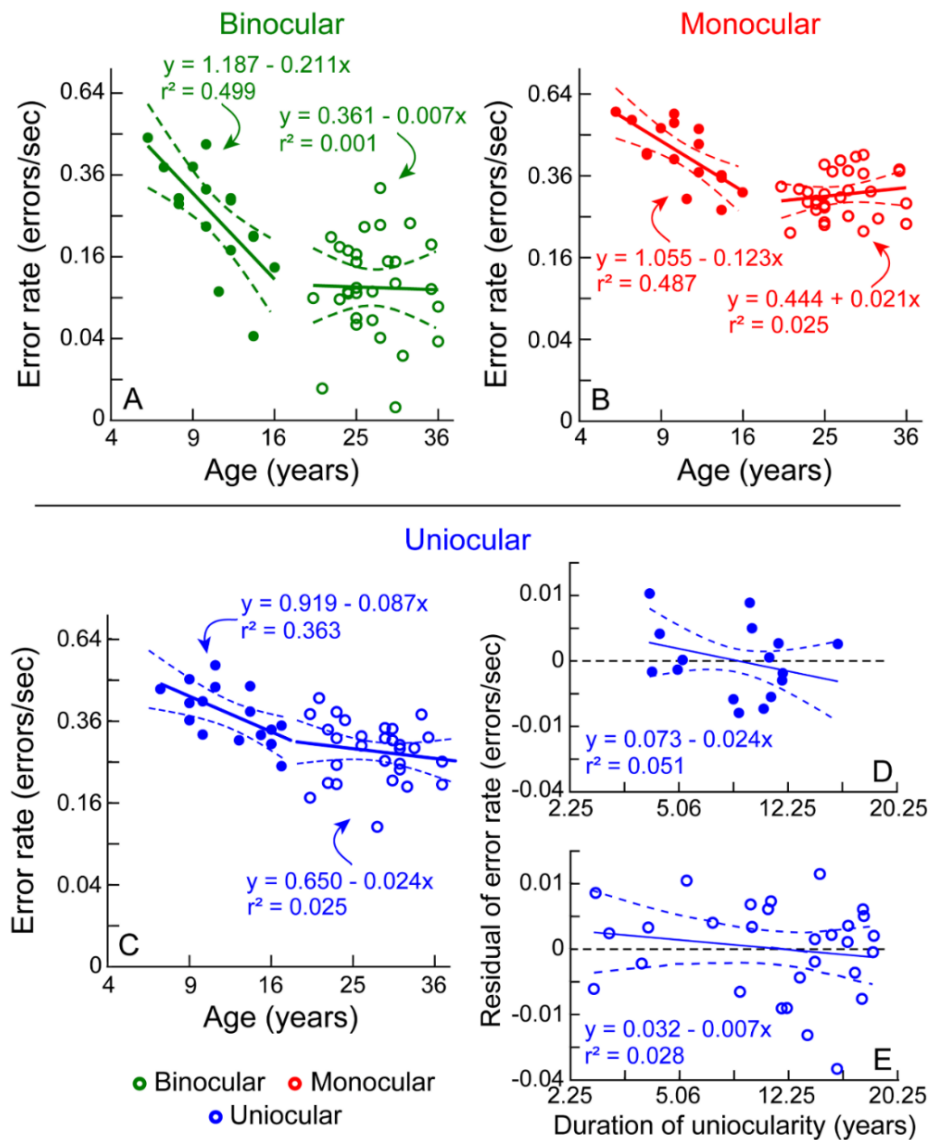


Figure 3.4 Panels A-C) Scatter diagrams of the square root of the error rate plotted as a function of the square root of the participant's age under binocular (panel A), monocular (panel B) and uniocular (panel C) viewing conditions. Panels D and E) Partial residual plots for children (panel D) and adults (panel E) demonstrating the impact of the duration of uniocularity on the error rate after adjusting for the effect of the participant's age, as shown in panel C. The solid and curved lines in each panel indicate the best-fit linear regression equation and its $\pm 95\%$ confidence interval obtained for the data of children (closed symbols) and adults (open symbols), separately. The abscissa and ordinate of Panels A-C are relabelled for the untransformed age and duration of uniocularity for ease of interpretation. Similarly, the abscissa and ordinate of Panels D and E are relabelled for the untransformed duration of uniocularity and residuals of the error rate for ease of interpretation.

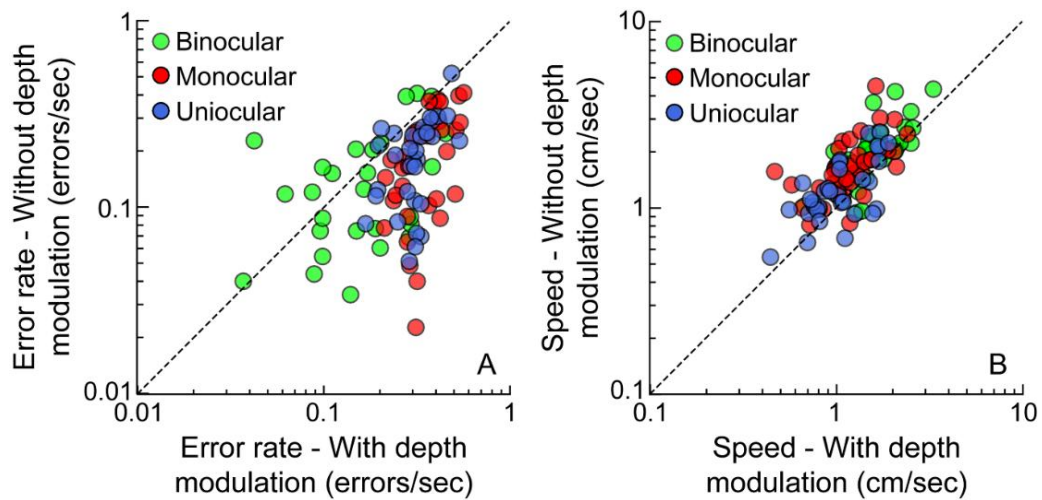


Figure 3.5 The error rate (panel A) and speed (panel B) obtained for buzz wires with depth modulation plotted against those without depth modulation in controls and cases in the free head condition. The diagonal line in each panel represents the line of equal performance.

The error rate was higher, and the speed was lower for the buzz-wire with depth modulation relative to without-depth modulation, with this effect being more pronounced under monocular than binocular viewing conditions (Figure 3.5), reflecting a significant interaction between the viewing condition and buzz-wire pattern in Table 3-2; Section 1. In contrast to the buzz-wire pattern, the head-free and head-restricted conditions did not have any impact on the error rates or speed among controls viewing under binocular and monocular conditions (Table 3-2; Section 1 and Figure 3.6). Also, the violin plot pattern in Figure 3.6 for the head-restricted viewing was very similar to that of the head-free viewing condition in Figure 3.3.

3.3.4 Multivariate analysis of task performance in the uniocular cases

The four-factor MANOVA revealed a significant effect of age on the error rate but not on the speed (Table 3-2; Section 2, Figure 3.4C). As was the case in controls, Figure 3.4C shows that there was a reduction in the error rate at the rate of 0.013 errors/sec per unit increase in age for children but no change in the error rate with age for adults. The forward stepwise regression analysis revealed that only age was a statistically

significant predictor of the error rate in children (Table 3-3, Figure 3.4D). The addition of the duration of uniocularity increased the r^2 estimate of the regression model by 9% in the data of children, but this increase was not statistically significant (Table 3-3, Figure 3.4D). Neither age nor the duration of uniocularity were found to be statistically significant predictors of error rate in adults (Table 3-3, Figure 3.4E). The MANOVA analysis also revealed a significant main effect of the buzz-wire pattern on the error rate and speed (Table 3-2; Section 2, Figure 3.4).

The uniocular cases performing the buzz-wire task with depth modulation resulted in higher error rates and lower speeds than those without depth modulation (Table 3-2; Section 2, Figure 3.5). As for the controls, the head position did not have any impact on the error rate and speed for the uniocular cases (Table 3-2; Section 1, Figure 3.6).

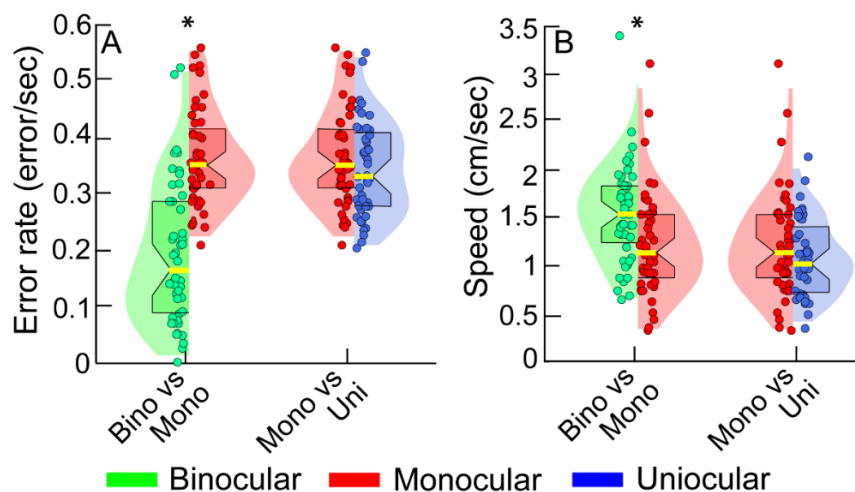


Figure 3.6 Similar to Figure 3.3 but buzz-wire performance for the head-restricted viewing condition.

Table 3-3 The results of step-wise multiple regression investigating the relationship between the error rate with uniocular participant's age alone and upon adding the duration of uniocularity into the regression model

		Change Statistics			
	Model	r^2	r^2 Change	F Change	Sig. F Change
Children	Age only	0.36	0.36	7.93	0.01
	Age + Duration of uniocularity	0.46	0.09	2.27	0.16
Adult	Age only	0.03	0.03	0.69	0.41
	Age + Duration of uniocularity	0.05	0.03	0.74	0.40

Relationships with significance $p < 0.05$ appear in bold.

3.3.5 Analysis of the location of the error in the buzz-wire task

Figure 3.7 shows the histogram of the proportion of errors made by controls under binocular and monocular viewing and by uniocular participants in the straight, curved, and transition portions of the buzz-wire. Of the 390 video frames with errors that were analysed, close to half the frames showed errors being made in the transition portion of the wire track [Binocular: 45.4% (95% CI of proportion: 36.8 – 53.9%); Monocular: 50.0% (41.4 – 58.6%); Uniocular: 43.1% (34.6 – 51.6%)]. The remaining errors were approximately equally distributed between the straight [Binocular: 25.4% (17.9 – 32.9%); Monocular: 20.8% (13.8 – 27.7%); Uniocular: 33.1% (25.0 – 41.2%)] and curved [Binocular: 29.2% (21.4 – 37.1%); Monocular: 29.2% (21.4 – 37.1%); Uniocular: 23.9% (16.5 – 31.2%)] portions of the wire track. A chi-square test did not reveal any association between the location of errors and the viewing condition [$\chi^2(4) = 5.42$; $p = 0.25$]. Unlike the error proportions, the duration of the errors did not show any significant difference across the three regions of the buzz-wire [$\chi^2(2) \geq 2.20$, $p \geq 0.33$] (Figure 3.7B). As expected, the transition zone in the wire-track resulted in the maximum number of errors during the task, relative to the other two locations.

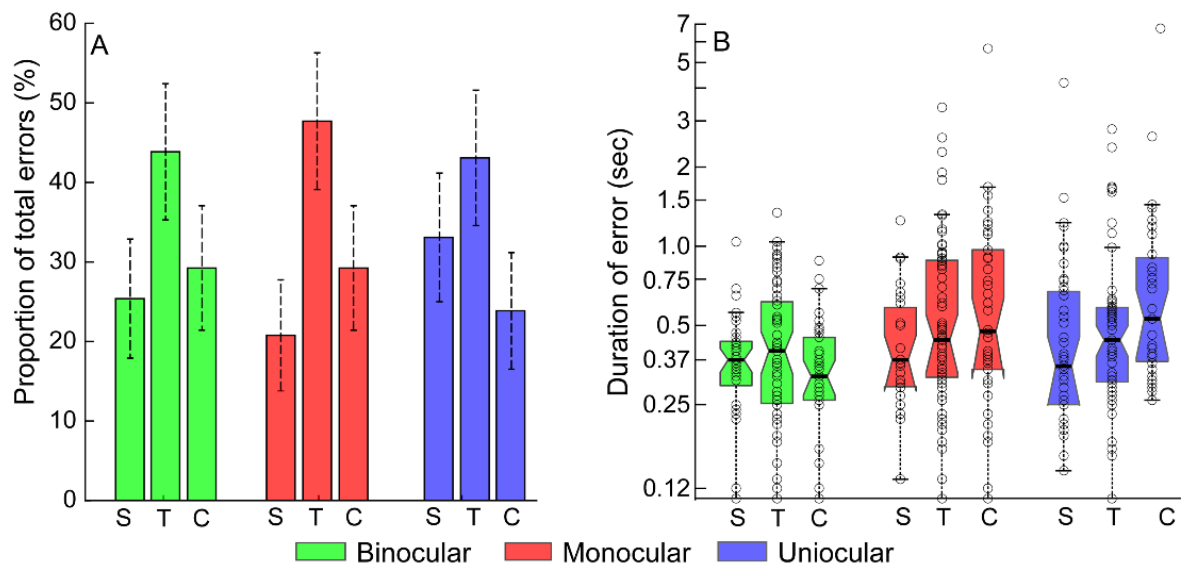


Figure 3.7 Panel A shows histograms of the proportion of errors made at the straight (S), transition (T), and curved (C) regions of the buzz-wire across the randomly selected error frames analysed under binocular (green) and monocular (red) viewing conditions of controls and unocular viewing condition of cases (blue). Error bars indicate the upper and lower (95%) confidence interval of each proportion shown in this panel. Panel B shows box and whisker plots of the duration of errors made by controls under binocular and monocular viewing conditions and by unocular participants in each of the locations of the wire. The middle black horizontal line in each box and whisker plot indicates the median value, the lower and upper horizontal lines indicate the 25th and 75th quartiles and the dotted vertical lines indicate the 1st and 99th percentile of the data distribution. The open circles represent the data of individual participants.

3.3.6 Analysis of head movements

Figure 3.8A-F shows the magnitude of head movements made by the participants from their preferred position under binocular, monocular and unocular conditions. The multivariate analysis performed on this data revealed a significant impact of viewing condition ($p = 0.003$) and age ($p = 0.04$) on the magnitude of head movements but with no interaction between these factors ($p = 0.12$) (Table 5-1). Univariate comparison showed significantly larger translational movements and head rotations (except roll head movement) in the unocular conditions, compared to the binocular viewing ($p \leq$

0.01, for all). Compared to the monocular viewing condition, the uniocular participants made larger vertical, antero-posterior and yaw head movements ($p \leq 0.03$, for all). No difference in these head movements was noted between binocular Vs. monocular ($p \geq 0.24$, for all). The univariate comparison revealed children made statistically significantly larger translational and rotational head movements (except pitch head movement), compared to adults ($p \leq 0.02$, for all). While the median head speed of the uniocular cases was 0.16 cm/sec (0.10 – 0.28 cm/sec) ($p=0.7$; Figure 3.8G), the head movement speed for monocular controls was 0.15 cm/sec (0.08 – 0.21 cm/sec) (Figure 3.8A). The monocular median (25th – 75th quartile) equivalent disparity obtained from horizontal translational head movements was 4.08 arcmin (2.89 – 7.83 arcmin) (Figure 3.8G) and 5.63 arcmin (3.97 – 11.82 arcmin) for the uniocular cases (Figure 3.8H). The median retinal disparity for binocular controls was 10.18 arcmin (7.60 – 11.91 arcmin) (Figure 3.8G-H). These values exceeded the thresholds for detecting depth from motion parallax (~ 1 -1.3 arcmin (Rogers & Graham, 1979, 1982; Ujike & Ono, 2001) and retinal disparity (clinically accepted stereo threshold = 0.67 arcmin, or 40 arcsec (Read, 2015) reported in the literature. Thus, even while suprathreshold levels of disparity from motion parallax were available to the participants in the absence of binocularity, these disparities did not influence buzz-wire task performance, as indicated by the comparable outcomes between head-free and head-restricted viewing conditions (Table 3-2; Section 2 and Figure 3.6 and Figure 3.8). As expected, the disparity variations derived from head motion were also not significantly correlated to the error rate ($p \leq 0.2$, $p > 0.11$, for all).

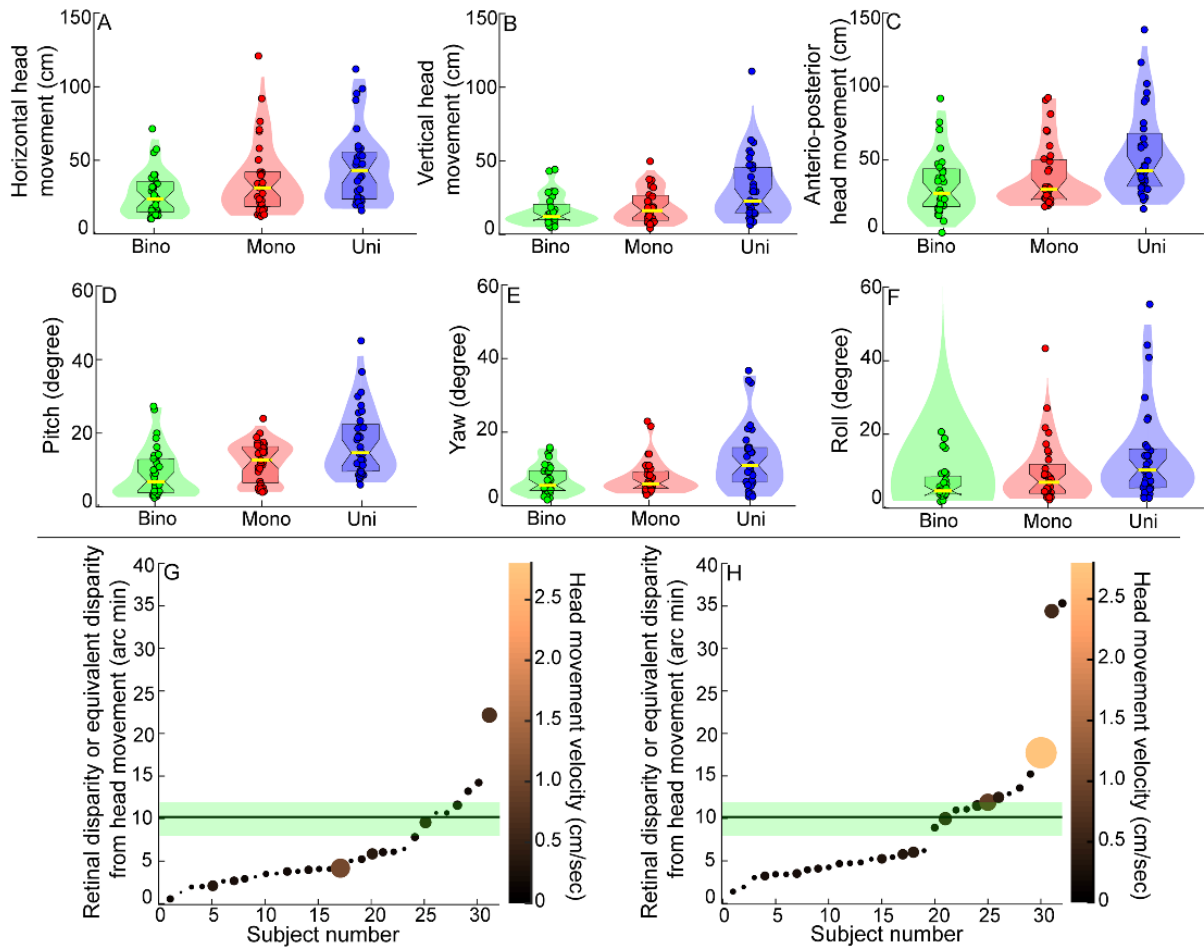


Figure 3.8 Violin plot pairs showing the distribution of the translational [horizontal (panel A), vertical (panel B) and antero-posterior (panel C)] and rotational [pitch (panel D), yaw (panel E) and roll (panel F)] head movements for the binocular and monocular viewing of controls and unocular cases while they performed the buzz-wire tasks with depth modulation under head-free viewing conditions. All other details are similar to Figure 3.3. Bubble plots showing the disparity available for depth computations in the buzz-wire task with depth modulations from horizontal head translation in the monocular viewing of controls (Panel G) and unocular cases (Panel H). In both panels, the participants are arranged in ascending order of the disparity available to each participant in the cohort. Lighter-coloured and larger-sized bubbles indicate a larger velocity of head motion. The horizontal line with the green shaded area in each panel denotes the median with 25th and 75th quartile of binocular retinal disparity available for depth calculations under binocular viewing conditions.

Table 3-4 Results of the two-way MANOVA comparing the head movements made by controls under binocular and monocular conditions, and by uniocular participants.

<i>Multivariate test</i>					
			F	p-value	Partial η^2
Viewing			2.6	0.003	0.95
Age group			2.38	0.04	0.13
Viewing x Age group			1.53	0.12	0.09
<i>Univariate test</i>					
Head movements	Viewing condition			Age	
	Bino	Mono	Uni	Children	Adult
Horizontal	5.38 ± 0.27	6.00 ± 0.32	6.66 ± 0.31*	6.44 ± 0.28§	5.59 ± 0.21
Vertical	3.96 ± 0.22	4.27 ± 0.26	5.50 ± 0.24*#	4.96 ± 0.22§	4.20 ± 0.16
Anterio-posterior	5.72 ± 0.28	6.05 ± 0.33	7.26 ± 0.31*#	6.81 ± 0.29§	5.88 ± 0.21
Pitch	0.40 ± 0.02	0.46 ± 0.03	0.54 ± 0.03*	0.49 ± 0.02	0.45 ± 0.02
Yaw	0.35 ± 0.02	0.35 ± 0.02	0.46 ± 0.02*#	0.43 ± 0.02§	0.36 ± 0.02
Roll	0.37 ± 0.03	0.40 ± 0.04	0.48 ± 0.04	0.46 ± 0.03	0.38 ± 0.02

The * and # symbols indicate statistically significant differences in head movements between binocular and uniocular conditions and between monocular and uniocular conditions, respectively. The § symbol indicates a significant difference between children and adults. The mean ± standard error (SE) shown here are the square-root-transformed values, as described in the Methods section. Mean values need to be squared for comparison with the data shown in the figures.

3.4 Discussion

3.4.1 Summary of the results

1. Binocular error rates were significantly lower than monocular error rates of controls and uniocular participants (Figure 3.3A; Table 3-2; Sections 1 and 2). Binocular speed was faster compared to the monocular and uniocular speed (Figure 3.3B;

Table 3-2; Sections 1 and 2). Most of the errors were made in the transition and curved locations of the wire (Figure 3.7)

2. Error rate decreased with age until the late teen years, while speed revealed no such trend (Figure 3.4A – C; Table 3-3).
3. There was no significant additional reduction in error rates with duration of uniocularity (Figure 3.4D – E; Table 3-3).
4. Uniocular participants made larger head movements (Figure 3.8; Table 3-4), however, it did not provide any added advantage (Figure 3.6 and Figure 3.8 Table 3-2).

3.4.2 Is the buzz-wire task sensitive enough to pick the differences in task performance with and without binocular disparity?

As the functional vision of an individual is heavily task-dependent (Bradshaw et al., 2000), it was crucial to select a task that would provide unbiased answers to the questions raised in the present study. For the study, it was imperative that the functional depth task chosen for evaluation could demonstrate the expected worsening of task performance under monocular viewing, relative to binocular viewing (Grant et al., 2007; Jones & Lee, 1981; Joy et al., 2001; Melmoth & Grant, 2006; Piano & O'Connor, 2013; Read et al., 2013). The present results confirmed this trend for the buzz-wire task by showing a 2.2-fold increase in the error rate and a 1.3-fold reduction in speed under monocular conditions, relative to binocular viewing by controls (Table 3-2, Figure 3.3). These findings are similar to Read et al. (2013) who reported a 3.5-fold increase in the number of errors and a 1.3-fold increase in the task duration under monocular viewing, relative to binocular viewing. Joy et al. (2001) and Piano and O'Connor (2013), observed longer task-completion times in monocular viewing for buzz-wire and bead-threading tasks, respectively, though they did not report error

rates. Additionally, the data are consistent with the findings of Joy et al. (2001) and Piano and O'Connor (2013), who observed longer task-completion times in monocular viewing for buzz-wire and bead-threading tasks, respectively, though they did not report error rates. Also, the reduction of speed under monocular viewing was not accompanied by any reduction in error rate indicating that there was no significant speed-accuracy trade-off in the buzz-wire performance.

Better performance in the binocular viewing condition can also be due to the mere presence of two eyes and not due to binocular retinal disparity. Jones and Lee (1981) demonstrated that the participants demonstrated binocular advantage in a bead threading task even in the absence of binocular retinal disparity. However, the binocular advantage was 1.17, less than the ratio (1.41) expected from binocular summation. Bradshaw et al. (2004) on the other hand, provided evidence that the improvement of performance under the binocular condition compared to monocular view during the prehension task is due to disparity and not because of having two eyes. They found the performances were similar between the bi-ocular and monocular view and poorer than the binocular view which had additional disparity information in addition to the bi-ocular view.

3.4.3 The effect of age on performance

The primary effect of age on performance (Table 3-2 and **Figure 3.4 A-C** revealed that error rates decreased with increasing age among the younger participants, reaching adult levels around 16 years of age (Figure 3.4A – C). This observed trajectory of visuomotor maturation and cue integration aligns with previous developmental trends reported in manual dexterity tasks and cue combination studies. Typically developing children aged 5–6 years tend to exhibit ballistic hand movements under monocular viewing conditions, with minimal advantage from binocular vision (Suttle et al., 2011).

Children around 7-11 years demonstrate binocular advantage similar to adults (>20 years) (Suttle et al., 2011) and show adult-like movement kinematics (Watt et al., 2003). However, when binocularity is disrupted during early childhood—as seen in amblyopic children aged 4-8 years, performance remains suboptimal under both binocular and monocular viewing conditions, and movements tend to be slower (Grant et al., 2014; Suttle et al., 2011). These findings are consistent with the conclusions drawn in the scoping review by Rao et al. (2025).

This pattern aligns well with evidence from multisensory integration research, which shows that children typically begin integrating visual and haptic information between the ages of 8 - 10 years (Gori et al., 2008) and integrate egocentric cues for navigation at a similar developmental stage (Nardini et al., 2008). Ernst (2008) suggests a potential explanation for the delay in multisensory integration. For an effective integration of the visual and haptic information, it might require reliable correspondence between sensory signals, a process that is challenging at a young age when the sensory systems are still developing.

The present maturation curve corresponds much better with the age at which flicker sensitivity reaches adult levels (14 – 18 years), suggesting that the maturation of accuracy in visuomotor performance might be influenced by the contrast processing capabilities of the developing visual system (Tyler, 1989). A causal relationship between the two, however, needs to be established in the future. Whatever the reason for the maturation trends, the results clearly showed that the binocular task accuracy improved at nearly twice the rate of the monocular and unocular viewing (Figure 3.4A – C). This observation is in line with previous reports of binocular cues being weighted more than monocular cues for depth-related visuomotor tasks, relative to tasks involving the perception of depth (Knill, 2005) and with the reports of binocular vision

contributing to the training and maturation of the visuomotor system via the disparity processing in “action control” areas of the posterior parietal cortex (Castiello, 2005; Sakata et al., 1997).

In **Figure 3.4**, the slope for error rates against age was flatter for uniocular individuals (Panel C) compared to monocular and binocular viewing (Panel B) conditions followed by the binocular viewing of controls (Panel A). This could be due to deficiencies in Manual Dexterity tasks (aiming, catching, and balance-related tasks) due to a loss of stereopsis as noted among amblyopes (Kelly et al., 2020).

Having established task relevance and the age effect, the present study outcomes may be used to answer the questions raised in the introduction section about the functional-depth related task performance of individuals who have undergone uniocular enucleation over extended periods of time.

3.4.4 Is the task performance of uniocular individuals better than expectations from chronological maturity?

The present study did not provide any evidence for an impact of the duration of uniocularity on task performance, beyond the age effect (**Table 3-3**, Figure 3.4C and D). As observed in Figure 3.4B and C, there was no significant difference in the developmental trend of error rates between uniocular children compared to binocular children who were temporarily made monocular. Children constituted only 35.5% (16 out of 45) of the total uniocular cohort but their durations of uniocularity were also long in relation to their age (5 – 15.5 years) (Table 3-1). The acute effects of uniocularity (within the first few months) may have revealed the maximum impact on the error rates, and thus could not be captured in the present dataset. Adults in this study did have a large range in the duration of uniocularity (2.4 months to 31.2 years) and even

in this cohort, the duration of uniocularity failed to reveal any statistically significant impact on the error rates (**Table 3-3**, Figure 3.8E). Despite these limitations, the forward stepwise linear regression on the children's data did show an approximately 6.7% improvement in the error rate with the duration of uniocularity after accounting for the age effect, however, it was not statistically significant (**Table 3-3**). Overall, while this study does not support the notion that the duration of uniocularity significantly influences depth-related visuomotor performance, further investigation focusing on individuals with more acute durations of uniocularity may still be warranted.

3.4.5 Larger head movements but limited utility to dynamic visuomotor task performance

The uniocular individuals made sizeable head movements during the buzz-wire task that generated suprathreshold level of disparity signals from motion parallax (Table 3-4, Figure 3.8). The head movements made by uniocular individuals were also larger than those made by binocular controls (Table 3-4). Despite this, the results revealed no additional benefit of head movements in improving the buzz-wire task performance relative to the head-restricted condition (**Table 3-2**). This finding aligns with Marotta et al. (1995) who observed that larger head movements did not offer any additional benefit to hand-reaching actions amongst uniocular individuals. Four reasons may be considered for this result. First, the need to continuously move the loop around the wire in the task requires a dynamic estimation of distance, depth, and curvature information, and modifying the visuomotor actions accordingly to avoid errors in the task. Perhaps the monocular cues to depth are not employed for such complex dynamic computations and may function better for static depth estimates (Bradshaw et al., 2000). Introducing motion parallax in the mix may further complicate the viewing scenario, for this cue derived from one form of motion action (head movements) should

be updated dynamically and temporally synchronized to drive another form of motor action (hand movements). Second, the task requires precise hand movements to manoeuvre the loop around the wire. The advantage that is obtained from larger head movements could be negated by the hand instability arising from the head/body movement. Thirdly, extra-retinal cues from head position (Rogers & Graham, 1979) and eye movements (Kim et al., 2016; Nawrot, 2003a, 2003b) are critical for disambiguating the sign of depth derived from motion parallax. Unlike the binocular viewing condition where the binocular disparity signal was present throughout the task, the motion parallax was not. Also, the estimation of the extent of head movement might be noisier compared to intraocular distance. Stabilizing the head position during a depth-from-motion task or creating a conflict with head velocity might result in a significant weakening of the depth information derived from the motion parallax cue (Nadler et al., 2013; Nawrot, 2003a). Since participants had to pay keen attention to the location of the loop relative to the wire, they may have limited their eye or head movements during the buzz-wire task, leading to ambiguous depth information from motion parallax. Fourth, unlike a typical motion parallax task where the object of interest is stationary in space, both the object of interest i.e. the loop and the head are in constant motion in the buzz-wire task. Therefore, the visual system has to disambiguate retinal image motion arising from head velocity from that arising from the velocity of object motion. This ambiguity, while possible to resolve (Rogers & Collett, 1989; Rushton et al., 2007) may be challenging enough to impair the depth calculations in a dynamic visuomotor task like the buzz-wire employed here.

Taken together, while the perception of depth may be benefitted by the motion parallax cue derived from head movements, it may not benefit complex and dynamic visuomotor tasks engaged by humans as a part of their daily living activities.

Alternatively, the head movements made by participants during such visuomotor tasks may very well be a strategy to expand the field of view of objects in space in the absence of binocularity.

3.4.6 Role of proprioceptive feedback in the buzz-wire task performance

In addition to the visual cues, the proprioceptive pull/pressure of the loop's contact with the wire may provide useful feedback to the brain about whether an error is made or not. In fact, several participants in the monocular/uniocular viewing conditions of the present study described this sensation as a “magnetic force” that seemed to prevent them from breaking contact between the loop and the wire, despite their attempt to disengage this contact. The complexity of the motor navigational operation and the associated proprioceptive feedback perhaps also explains why the proportion of contact between the loop and the wire was significantly higher in the curved regions of the buzz-wire track, relative to the straight regions (Figure 3.7). While proprioceptive information is inherent to the buzz-wire task, this cue is unlikely to have dominated performance in this study. If this was indeed true, the binocular and monocular task performance of controls would have been identical, making the task unfit for investigating the questions raised in the present study.

Chapter 4 Depth-related visuomotor performance

in degraded binocularity

4.1 Introduction

Consider the acts of inserting a key into a keyhole, placing a light bulb in its socket, or threading a needle. These seemingly straightforward activities of daily living are complex visuomotor tasks that require precise estimation of the spatial configurations for the planning and execution of appropriate hand movements and grasp actions (Fielder & Moseley, 1996; Knill, 2005; Read et al., 2013). The visual system's ability to estimate 3D information, particularly for motor actions as opposed to perception (Knill, 2005), is largely governed by the processing of retinal disparity arising from the triangulation of both eyes onto the object of interest (Wheatstone, 1838). The loss of binocularity arising from temporary occlusion or from the permanent loss of vision in one eye significantly impairs visuomotor performance (Read et al., 2013). Similar results are observed with the deterioration of binocularity from optical blurring (Piano & O'Connor, 2013), pathologies like amblyopia (O'Connor et al., 2010a, 2010b), and macular degeneration (Verghese et al., 2016). In general, task accuracy worsens and the speed of task performance decreases with degraded/absent depth vision, relative to viewing with intact binocularity.

This background led us to investigate the status of visuomotor task performance in the optical condition of keratoconus. This progressive ophthalmic disease, typically affecting individuals in their 2nd to 3rd decades of life, (Santodomingo-Rubido et al., 2022) is characterized by spatial and depth vision losses arising from degraded retinal image quality caused by an abnormally shaped cornea of one or both eyes (Devi et al., 2023; Devi et al., 2022; Kumar et al., 2023). The keratoconic eye's optical quality,

when described using the Zernike polynomial series, shows elevated levels of coma, trefoil and spherical aberrations (Nilagiri et al., 2020; Pantanelli et al., 2007). The resultant radially asymmetric blur produces significant contrast demodulation and “doubling” or “ghosting” of local image features due to optical phase shifts (Marella et al., 2024; Metlapally et al., 2019). Usually, even in bilateral keratoconus, the grade of disease and the topography are different between the two eyes, resulting in dissimilar blur patterns (Ferdin et al., 2019). The combination of the radial and bilateral asymmetry in blur significantly impacts the formation of the cyclopean image needed for processing binocularity (Marella et al., 2024; Metlapally et al., 2019). All grades of binocularity appear to be degraded in keratoconus, relative to age-similar controls: retinal disparity processing is impaired due to correspondence mismatches in the aberrated retinal images (Metlapally et al., 2019); the worse of the two eyes may be suppressed (Marella et al., 2021), and stereo thresholds maybe 3–7 fold worse, independent of keratoconus severity (Nilagiri et al., 2018). Motor fusion and ocular accommodation may also be impaired in keratoconus, thereby preventing clear and single binocular vision at near viewing distances (Dandapani et al., 2020).

Three specific objectives surrounding the impact of the optical limitations on the depth-related visuomotor task performance in keratoconus were investigated in the present study. The primary objective was to compare the monocular and binocular visuomotor task performance in keratoconic participants and similarly aged controls on the stereoscopic buzz-wire task. We hypothesised that the degraded/absent binocularity in keratoconus would result in the error rate and speed of task performance becoming similar under monocular and binocular viewing conditions. The losses in spatial and depth vision arising from the degraded retinal image quality in keratoconus are typically managed using rigid contact lenses that replace the distorted cornea with a

smoother refracting surface (Deshmukh et al., 2023). Therefore, the second study objective tested the hypothesis that an improvement in retinal image quality using rigid contact lenses would result in a commensurate improvement in the buzz-wire task performance in keratoconus.

While the status of binocularity may be investigated using several psychophysical paradigms, stereo thresholds obtained using dichoptic stereograms remain the most widely used measure in the clinic and research investigations (Scheiman & Wick, 2008). Interestingly, the depth-related visuomotor task performance of individuals with amblyopia, strabismus and those with purposely induced degradations in binocularity have all revealed a negative correlation with their stereo threshold (O'Connor et al., 2010a, 2010b; Piano & O'Connor, 2013). Given this, the third study objective tested the hypothesis that binocular advantages would be smaller with high stereo thresholds in keratoconus.

4.2 Methods

4.2.1 Participants

Thirty participants with keratoconus (henceforth called “cases” in this chapter) and 26 similarly aged participants without keratoconus (henceforth called “controls”) were recruited from the patient base and staff/student pool of the L V Prasad Eye Institute (LVPEI), Hyderabad, India. With a minimum sample size of 24 subjects as calculated for our previous experiment, we enrolled 30 cases and 26 controls.

The study adhered to the tenets of the Declaration of Helsinki and was approved by the Institutional Review Board of LVPEI. All participants signed a written informed consent form before study induction. Diagnosis of keratoconus was based on a comprehensive eye examination that showed evidence of keratoconus with objective,

non-cycloplegic refraction, slit-lamp examination, and corneal tomography. Standard clinical management was followed for all cases, with no influence of the study protocol on their clinical care. If necessary, keratoconus was managed with rigid contact lenses as per standard operating protocols (Downie & Lindsay, 2015). Disease severity was determined using the D-index, a multimetric measure of the corneal structural deformation, obtained using Scheimpflug imaging tomography (Pentacam HR®, Oculus Optikgeräte; Wetzlar, Germany) (Hashemi et al., 2016). The D-index was derived for both eyes of all participants using the Belin-Ambrósio enhanced ectasia display map and included deviations of front and back surface elevations of the cornea, pachymetric progression, thinnest corneal point, and deviation of Ambrósio relational thickness maximum (Hashemi et al., 2016). This metric has been shown to have good reliability in the diagnosis and progression of keratoconus, with higher D-index values indicating greater disease severity (Muftuoglu et al., 2015).

The best spectacle-corrected, high contrast, monocular distance visual acuity in each eye, as estimated using the routine clinical protocol, ranged from 0.00 to 1.60 logMAR in cases and 0.00 to 0.2 logMAR for controls. All cases and controls had monocular near acuities between 0.00 and 0.40 logMAR (N8) at 40 cm. Unaided visual acuity was not recorded in this study. Again, participants with any other ophthalmic dysfunction, or any systemic condition that resulted in restricted body movement, visible shaking of hands, inability to follow instructions, or inability to fuse the stereogram for stereopsis measurements, were excluded.

Seventeen cases were habitual rigid contact lens users [one case wore a Rose K2® lens (Menicon Co. Ltd., Nagoya, Japan), while the rest wore conventional rigid gas permeable lenses (Purecon McAsfeer, Silver line laboratory Pvt. Ltd, India)] (Appendix 1). Based on the severity and requirement for contact lenses, 11 participants wore

contact lenses in both eyes and the rest wore these lenses only in one eye (Appendix 1). The lenses were fitted by experienced contact lens practitioners at LVPEI, using the manufacturer's recommended protocols, and the final lenses were ordered and dispensed to the participants as a part of the regular clinical protocol. The visual acuity, stereo thresholds and buzz-wire performance were tested both before and after contact lens fitting. The visual acuities ranged from 0.00 to 0.40 logMAR with their contact correction.

4.2.2 The buzz-wire apparatus and task performance

The buzz-wire task was performed following the previously mentioned paradigms. The instruction set and outcome parameter calculation remain the same (Sections: 3.2.2, 3.2.3, and 3.2.4). All participants performed the buzz-wire task under binocular and monocular viewing conditions. They performed the task thrice for each viewing condition with different patterns of wire formation, all in random order. For monocular viewing of controls, one eye was randomly occluded, while the worst eye (based on visual acuity) of cases was occluded to minimize the impact of resolution loss on task performance. In cases with equal acuity in both eyes, one eye was randomly occluded. Their heads remained free to move during the task. Each run took approximately 40 sec to complete, following which participants were given 1-min of break prior to the next trial.

4.2.3 Measurement of stereo threshold

The stereo threshold was measured at a 50 cm viewing distance using random-dot stimuli presented on a gamma calibrated LCD monitor (1680 × 1050 pixel resolution, 59 Hz refresh rate) and controlled using the Psychtoolbox-3 interface of MATLAB (R2016a; The MathWorks, Natick, USA, Brainard (1997)). The random-dot stimuli incorporated a rectangular disparity-defined bar oriented either with a leftward or a

rightward tilt in crossed retinal disparity (Figure 1D). The dichoptic stimuli were fused using a handheld stereo viewer with built-in periscopic mirrors to adjust for the participant's horizontal phoria and interpupillary distance (Screen-Vu Stereoscope, Portland, USA). Vertical phoria, if any, was corrected with minor adjustments in head orientation. Data collection began once the participant reported stable fusion of the bounding box that presented the random-dot stimuli (Figure 4.1). Participants identified the direction of the bar tilt for every stimulus presentation while the retinal disparity varied in a 2 down and 1 up adaptive staircase manner with each presentation. For better visibility of the stereoscopic rectangular bar, the initial disparity value was set anywhere between 2000 and 4000 arcsec. Until the first reversal, the disparity was changed by 50% of the previous disparity value. At the subsequent reversals, the disparity changed with a 5% step size. The staircase was terminated after 11 reversals. Response frequencies were fit with Weibull functions to obtain maximum-likelihood estimates and credible intervals for the 70.7% correct threshold level (Watson, 1979).

4.2.4 Protocol

The buzz-wire and stereo tasks were performed by all participants with natural pupils and accommodative states. Among the cases, the first measurements were always made with their habitual spherocylindrical spectacles and then with their habitual rigid contact lenses, if any. The measurements were made in this order to not deform the cornea with the rigid contact lens wear, which, in turn, would alter the pattern of retinal image blur experienced by the participant (Jinabhai et al., 2012). Change in the monocular task performance with contact lens wear was not determined in this study.

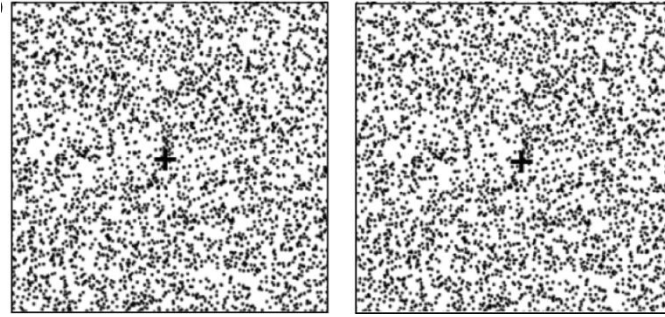


Figure 4.1 A representative, cross-fusible, example of the random-dot stereogram used for estimating the stereo threshold. The fused stereogram shows a leftward tilted rectangular bar in crossed retinal disparity.

4.2.5 Schematic framework for data interpretation

To enable ease of interpretation of the buzz-wire performance, the data clouds obtained for error rate and speed in controls and cases were fit with bivariate contour ellipses using `plot_ellipse.m` code in Matlab (Gillay, 25 Aug 2022). The x- and y-coordinates of the centroid and the major axes of the ellipses were determined from the fits. These outcomes were interpreted in the context of a schematic framework described below (Figure 4.2A). In this schematic, the binocular and monocular error rates are plotted against each other. Whereas the 45° line of equality indicates no binocular advantage and thus dominance of the task by monocular factors (purple cloud in Figure 4.2A), data below this line would indicate a performance advantage derived from binocular depth cues (e.g. retinal disparity) and/or from the integration of monocular cues (e.g., occlusion, perspective cues) from the two eyes. The data could be uniformly distributed below the line of equality, indicating a uniform binocular advantage across the range of monocular error rates (blue cloud in Figure 4.2A). The orientation of the data could also be steeper than 45°, indicating that the binocular and monocular error rates are becoming more and more similar, with an increase in the monocular error rates (turquoise cloud in Figure 4.2A). That is, the binocular

advantage in error rate reduces with an increase in the monocular error. This could indicate that the binocular advantage in error rates may be determined by factors that limit the monocular performance in this task (e.g., retinal image quality, in this case) or simply that the error rates have reached the maximum that could be measured by the apparatus.

A range of possible comparisons between controls and cases is further illustrated in Figure 4.2B - I. The data of cases and controls may overlap along the line of equality, indicating no impact of viewing condition or cohort on task performance (Figure 4.2B). The data clouds may remain overlapped but with both shifted below the line of equality, indicating a significant impact of only viewing condition but not cohort on task performance (Figure 4.2C). The data clouds may also appear translated along the equality line, indicating a significant impact of the cohort (cases producing more errors than controls in this schematic) but not of viewing condition on task performance (Figure 4.2D). The data clouds may be shifted below the line of equality and appear horizontally translated relative to each other, indicating a significant impact of both viewing condition and cohort but with no interaction between the factors (Figure 4.2E). Figure 4.2F–I show data clouds wherein the main effect of both factors and the interaction between them is significant. In Figure 4.2F, the binocular advantage is present only for controls and not for cases. In Figure 4.2G and H, the binocular advantage is present for both cohorts, but only one cohort shows a monocular dependence of the binocular advantage - cases in Figure 4.2G and controls in Figure 4.2H. Finally, in Figure 4.2I the binocular advantage in error rates shows monocular dependence, but to varying extents, in both cohorts. This data schematics can also be extrapolated to the speed of task performance wherein faster movement under

binocular viewing is indicated by the data lying above the line of equality (schematic not shown here).

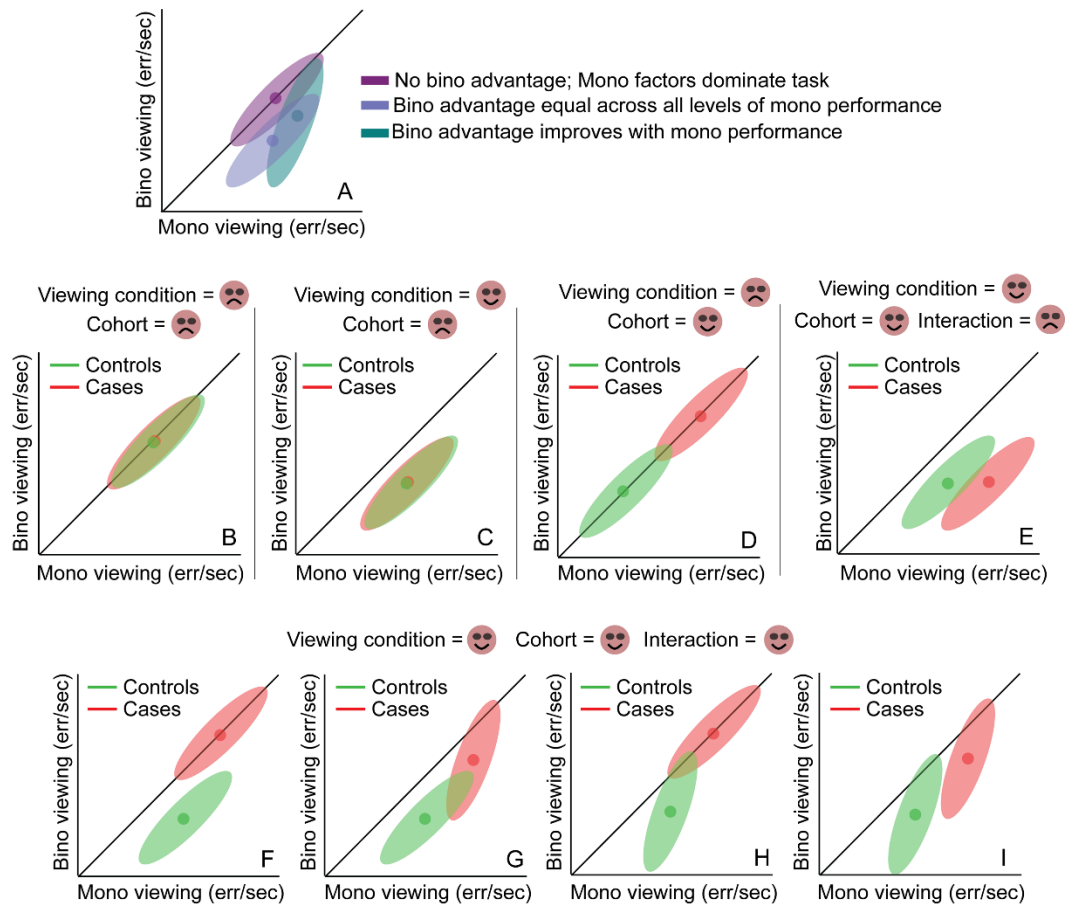


Figure 4.2 Schematics for the different patterns of results that may be obtained across controls and cases for the error rates in the buzz-wire task used in this study. Data clouds are assumed to have elliptical distributions. The solid circle is the centroid of the elliptical data cloud. The “smiley” face indicates statistically significant impact of the independent variable (i.e., viewing condition) on the dependent variable (i.e., error rate, in this case) while the “gloomy” face indicates no evidence of such a statistical significance. Panels B–I are described in the text

4.2.6 Data analyses

Statistical analyses were performed using IBM SPSS Statistics® (Version 21; Armonk, NY), Matlab (R2016a) and Wolfram Mathematica (Version 14.1.0, Wolfram Research, Inc., Champaign, IL). Similar to the earlier method of analysing, the error rate and

speed across the three repetitions of the buzz-wire task were averaged for further analyses. The Shapiro-Wilk test revealed that error rate, speed and the binocular advantage of error rate and speed were non-normally distributed. Hence, the datasets of error rate and speed were Box-Cox transformed using a λ value of 0.15 and the datasets of binocular advantage of error rate and speed were log-transformed to achieve normality, thereby making them amenable to parametric statistics. Note, however, that Figure 4.3 - 6 containing the study results are all constructed on the raw untransformed data for visualization purposes. Two-factor repeated measures multiple analysis of variance (RM-MANOVA) was performed to investigate the between-subject factor of cohort type (controls vs. cases) and the within-subject factor of viewing condition (binocular vs. monocular) on the dependent variables of error rate and speed. A separate one-factor, between-subjects MANOVA was performed to compare the binocular advantage in error rate and speed between controls and cases. Similarly, a separate one-factor, within-subjects MANOVA was performed to compare the impact of optical correction modality (rigid contact lens vs. spectacles) on the stereo threshold, error rate, and speed.

4.2.7 Comparison of buzz-wire performance in cases with those of uncorrected myopes

The results from the main experiment revealed that the monocular and binocular buzz-wire task performance was worse in cases than in controls. An additional experiment was performed to determine whether this deterioration was unique to keratoconus or generic to any form of optical blur experienced by the individual – for instance, optical blur from uncorrected axial myopia, but with a regularly shaped cornea. This experiment tested the hypothesis that the error rate and speed in the buzz-wire task will be similar in cases and uncorrected myopic cohorts with comparable levels of

visual acuity and stereo thresholds. Ten participants with -6.00D to -13.00D of uncorrected myopia (21 - 34 years) repeated the monocular and binocular versions of the buzz-wire task. All other details were identical to the main experiment.

4.3 Results

Table 4-1 describe the demographic and clinical details of the study participants (see Appendix 1 *for individual cases*). Ten of the 30 cases had bilateral keratoconus with similar severity in both eyes. The remaining were either bilateral keratoconus with different disease severities in the two eyes or those with clinically manifest keratoconus in only one eye (Appendix 1).

4.3.1 Buzz-wire task performance in controls and cases

Figure 4.3A shows scatter diagrams of the binocular and monocular error rates for controls and cases with their habitual spectacles. The error rate patterns in both cohorts resembled the schematic in Figure 4.2G. The orientation and the centroid locations of the bivariate contour ellipse for controls indicated a uniform shift in the data below the line of equality (Figure 3A). In contrast, the bivariate contour ellipse for cases was steeper than 45° , with its y-axis centroid remaining significantly lower than its x-axis centroid (Figure 4.3A). Additionally, the rightward and upward shift in the x and y-axis centroids, respectively, of cases, relative to controls, indicated an overall higher error rate in cases than in controls (Figure 4.3A).

The bivariate contour ellipses for speed were oriented close to the 45° line of equality in controls and cases (Figure 4.3B). For controls, the x-axis centroid of the ellipse was lower than the y-axis centroid, indicating a slowing down under monocular viewing

Table 4-1 Demographic and clinical details of study participants

Cases (n = 30)	Age (years)	20 (17 to 34)	
	Sex (M : F)	20 : 10	
		Right eye	Left eye
	D-index (unitless)	8.09 (2.13 to 27.13)	7.28 (0.53 to 22.05)
	SER (D)	-3.50 (-12.00 to 0.00)	-3.50 (-24.00 to -0.38)
	J ₀ (D)	0.00 (-2.59 to 2.82)	0.09 (-2.35 to 4.59)
	J ₄₅ (D)	0.77 (-0.94 to 2.95)	-0.99 (-3.87 to 2.38)
	BSCVA (logMAR)	0.30 (0.00 to 1.60)	0.30 (0.00 to 1.40)
	Stereo threshold (arcsec)	547.13 (52.66 to 1906.00)	
Controls (n = 26)	Age (yrs)	24 (17 to 29)	
	Sex (M : F)	10 : 17	
		Right eye	Left eye
	D-index (unitless)	0.72 (-0.37 to 2.45)	0.76 (-1.16 to 2.61)
	SER (D)	0.00 (-5.00 to 0.88)	0.00 (-5.00 to 0.88)
	J ₀ (D)	0.00 (0.00 to 1.25)	0.00 (0.00 to 1.25)
	J ₄₅ (D)	0.00 (0.00 to 0.00)	0.00 (0.00 to 0.32)
	BSCVA (logMAR)	0.00 (0.00 to 0.00)	0.00 (0.00 to 0.00)
	Stereo threshold (arcsec)	29.99 (3.18 to 77.70)	

The values indicate the median (minimum to maximum) for each parameter described in the study. The SER, J₀ and J₄₅ power vector terms represent the spherical equivalent of refraction and the regular and oblique astigmatic components of refraction, respectively (Thibos et al., 1997). BSCVA = best spectacle-corrected visual acuity.

condition (Figure 4.3B) while in cases, the x- and y-axes centroids for cases were not different to each other (Figure 4.3B), indicating that the cases did not slow down as much as the controls under monocular viewing. Additionally, the speed ellipse of cases was shifted rightwards, relative to controls, suggesting that under monocular viewing,

the former cohort performed the task faster than the latter cohort under monocular viewing conditions (Figure 4.3B).

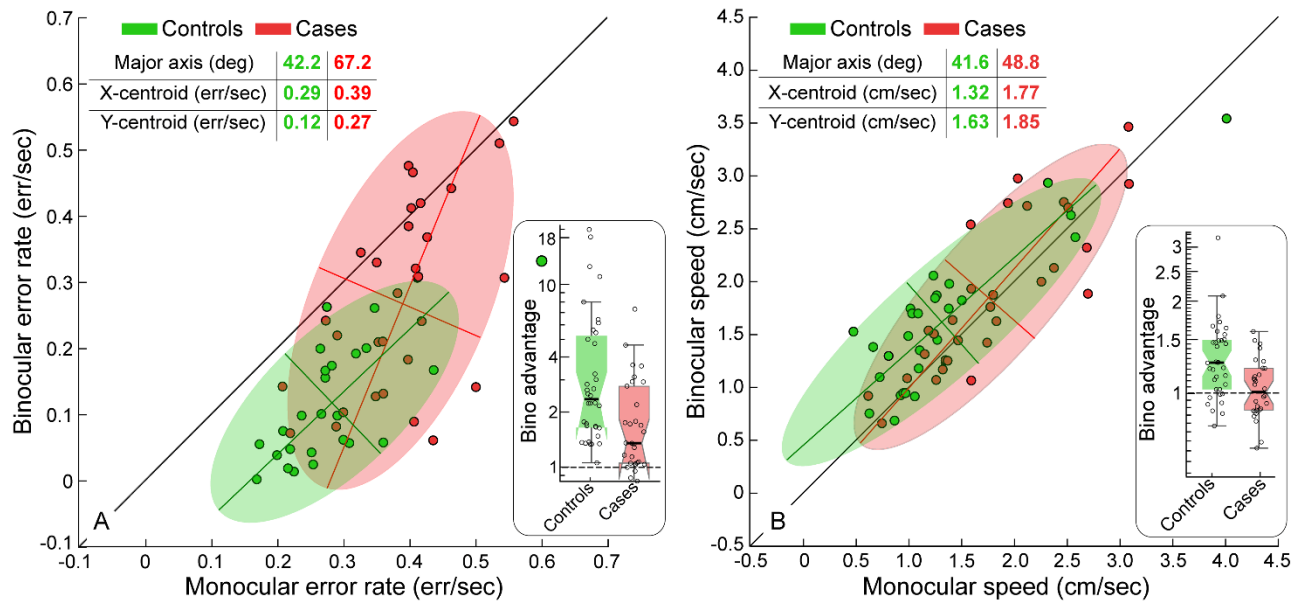


Figure 4.3 Scatter diagrams of the error rate (panel A) and speed (panel B) obtained from controls (green symbols) and cases (red symbols) while performing the buzz-wire task in this study. The coloured patches represent the best-fit bivariate contour ellipse for the controls and cases datasets. The major and minor axes are shown for each ellipse, the intersection of which represents its centroid (see text inset for details). The diagonal line in each panel represents the line of equality for monocular and binocular performance. The gestalt obtained from these contours may be readily compared with the schematics described in Figure 4.2. The insets show Box and Whisker plots of the binocular advantage in error rate and speed obtained for controls and cases in this study (see figure insets in each panel). For each box and whisker plot, the horizontal line is the median, the edges are the 25th and 75th quartiles and the whiskers are the 1st and 99th quartiles. The black dots are the individual data points, jittered randomly along the X-axis for ease of visualization.

Table 4-2 Results of the main statistical analyses conducted in this study.

Section 1: T-Tests								
Comparison of error rate and speed among controls and cases	1a. Paired t-tests							
			Error rate			Speed		
			Mean diff ± SEM	t value	p-value	Mean diff ± SEM	t value	p-value
	Control	Bino vs Mono	-1.00 ± 0.19	-5.23	<0.001	0.26 ± 0.06	4.26	<0.001
	KC	Bino vs Mono	-0.44 ± 0.09	-4.92	<0.001	0.03 ± 0.05	0.5	0.62
	KC below threshold	Bino vs Mono	0.71 ± 0.10	-7.11	<0.001	—		
KC above threshold	Bino vs Mono	0.08 ± 0.04	-1.93	0.07				
Section 2: Two-factor RM-MANOVA Analysis								
Effect of viewing condition (Bino vs Mono) and cohort type (control vs cases) on error rate and speed	2a. Multivariate tests							
			F			p-value		Partial η²
	Viewing condition		41.8			<0.001		0.61
	Cohort type		9.33			<0.001		0.26
	Viewing condition x Cohort type		11.72			<0.001		0.31
	2b. Univariate tests							
			Error rate			Speed		
			Mean ± SEM	p-value	Partial η²	Mean ± SEM	p-value	Partial η²
	Viewing condition	Binocular	-1.73 ± 0.11	<0.001	0.48	0.50 ± 0.06	<0.001	0.24
		Monocular	-1.03 ± 0.03			0.36 ± 0.06		
Cohort type	Controls	-1.66 ± 0.10	<0.001	0.26	0.31 ± 0.08	0.03	0.08	
	KC	-1.10 ± 0.10			0.55 ± 0.08			
Viewing condition x Cohort type	—	—	0.004	0.15	—	0.004	0.14	
Section 3: One-factor RM-MANOVA Analysis								
Binocular advantage in error rate and speed among control and cases	3a. Multivariate tests							
			F			p-value		Partial η²
	Cohort type		13.06			< 0.001		0.33
	3b. Univariate tests							
			Error rate			Speed		
			Mean ± SEM	p-value	Partial η²	Mean ± SEM	p-value	Partial η²
	Cohort type	Controls	0.53 ± 0.06	< 0.001	0.21	0.14 ± 0.03	0.003	0.13
		KC	0.22 ± 0.06			0.02 ± 0.03		
Section 4: One-factor MANOVA Analysis								
Effect of spectacle and contact lenses on stereo, error rate and speed	4a. Multivariate tests							
			F			p-value		Partial η²
	Correction modality		163.89			<0.001		0.97
	4b. Univariate tests							
			Stereo threshold		Error rate		Speed	
	Correction modality		Mean ± SEM	p-value	Mean ± SEM	p-value	Mean ± SEM	p-value
		Spectacle	2.71 ± 0.12	0.001	-1.23 ± 0.12	<0.001	0.69 ± 0.12	0.001
		Contact lens	2.34 ± 0.12		0.76 ± 0.02		1.10 ± 0.01	
Section 5: One-factor RM-MANOVA Analysis								
Effect of viewing on error rate and speed among uncorrected myopes	5a. Multivariate tests							
			F			p-value		Partial η²
	Viewing condition		23.06			0.001		0.72
	5b. Univariate tests							
			Error rate			Speed		
	Viewing condition		Mean ± SEM	p-value	Partial η²	Mean ± SEM	p-value	Partial η²
		Binocular	-1.56 ± 0.12	0.001	0.72	0.16 ± .15	0.003	0.64
		Monocular	-0.99 ± 0.05			0.08 ± 0.19		
Section 6: Mann-Whitney test								
Bino advantage myopes Vs. cases with comparable stereo loss			Error rate			Speed		
			Median (IQR)	Z	p-value	Median (IQR)	Z	p-value
	Cohort type	Myopes	1.98 (1.37 – 2.32)	-2.26	0.02	1.27 (1.09 – 1.53)	-2.72	0.005
		Cases	1.16 (0.99 – 1.81)			1.03 (0.87 – 1.12)		

Relationships with $p < 0.05$ (uncorrected for multiple comparisons) appear in bold.

The Box-Cox transformed monocular error rates of controls and cases were higher than the binocular values (Table 4-2, Section 1a). The multivariate test in the two-factor RM-MANOVA revealed significant main effects of viewing condition and cohort and significant interaction between the two main effects on the combined dependent variables of error rate and speed (Table 4-2, Section 2a). These effects were retained in the univariate tests, with the effect size being stronger for the former than the latter outcome variable (Table 4-2, Section 2b). To further investigate the pattern of error rates obtained in cases, their monocular and binocular error rates were divided into two subgroups about the y-axis centroid i.e., participants with binocular error rates lower and higher than the y-axis centroid. The mean difference in the Box-Cox transformed monocular and binocular error rates was found to be significant only for the latter subgroup and not the former subgroup (Table 4-2, Section 1a).

The one-factor MANOVA performed on the log-transformed binocular advantage scores showed a significant difference between controls and cases for the combined dependent variables (Figure 4.3 insets, Table 4-2, Section 3a). The univariate tests showed that the binocular advantages in error rate and speed were higher in controls than in cases, with the effect size being higher for error rate than speed (Table 4-2, Section 3b). These trends were expected from the binocular and monocular data of these outcome variables reported in Table 4-2, Sections 1 and 2.

4.3.2 Relationship between stereo threshold and binocular advantage in error rate

Unlike controls, the addition of binocularity had a differential impact on the error rates of cases (Figure 4.3A). To determine if this pattern was related to the participants' stereo thresholds, the binocular advantages in error rates of cases were plotted against their stereo thresholds (Figure 4.4). The same relationship for controls is also shown in this figure for comparison. All controls had stereo thresholds lower than the

buzz-wire task's diastereopsis threshold (vertical line in Figure 4), making the task a suprathreshold activity. While all the controls showed a distinct binocular advantage in error rate, this advantage was poorly correlated with stereo threshold (Pearson's $r = -0.25$, $p = 0.22$). Only 10 cases had stereo thresholds lower than the diastereopsis threshold, all of whom also showed a binocular advantage in the error rate (Figure 4.4). Amongst the remaining 20 cases with stereo thresholds poorer than the diastereopsis disparity threshold, 10 exhibited near unity binocular advantage, 3 had binocular advantage comparable to that of controls and the binocular advantage of the rest was somewhere in between (Figure 4.4). Overall, like controls, there was a non-

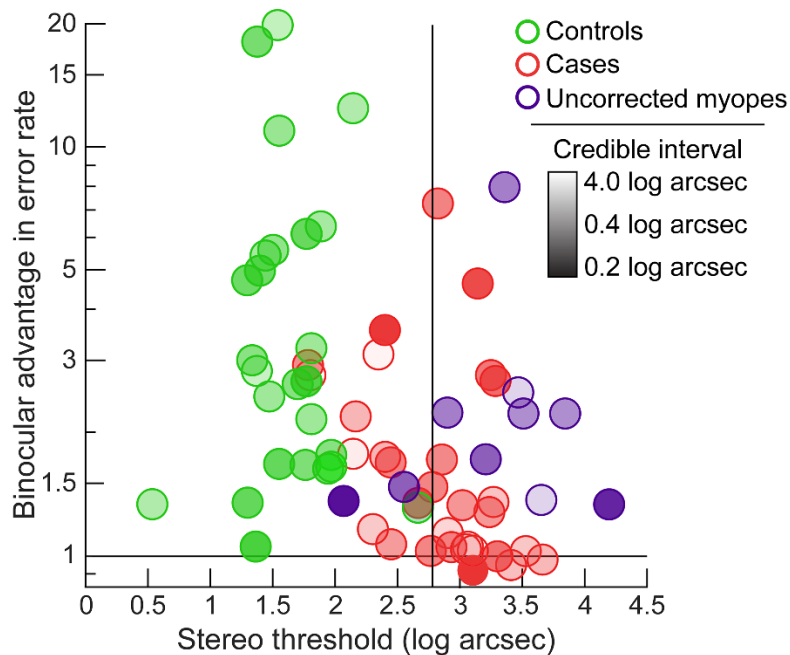


Figure 4.4 Binocular advantage in error rate plotted against the random-dot stereo threshold for controls (green), cases (red), and uncorrected myopes (blue). The transparency of the dots represents the 68% credible interval for the stereo thresholds. The vertical line indicates the disparity threshold (611 arcsec or 2.79 log arcsec) for diastereopsis. The horizontal line denotes the level where there was no binocular advantage.

significant correlation between binocular advantage in error rate and stereo threshold in the cases (Pearson's $r = -0.32$, $p = 0.08$).

Amongst cases, the binocular advantage in error rate poorly correlated with the two eyes' maximum D-index, the difference between the two eyes' D-indices, and the maximum, mean, and the difference between the two eyes' best-corrected visual acuity ($r \leq -0.32$, $p \geq 0.08$, for all).

4.3.3 Impact of rigid contact lenses on the error rates of the cases

With rigid contact lens in place, the stereo thresholds and error rate of cases were below the 1:1 line, indicating an improvement in these variables relative to spectacles (Figure 4.5A and B, Table 4-2, Section 4b). The one-factor MANOVA showed a statistically significant impact of the correction modality for the combined dependent variables (Table 4-2, Section 4a). The univariate tests confirmed this effect for both stereo threshold and error rate, with the effect size being larger for the latter than the former variable (Table 4-2, Section 4b). However, the proportional improvements in stereo threshold and error rate, obtained by dividing the value obtained with spectacles by the value obtained with contact lenses, proved to be uncorrelated (Pearson's $r = 0.02$, $p = 0.94$; Figure 4.5C).

4.3.4 Buzz-wire task performance of uncorrected myopes

Visual acuities amongst the uncorrected myopes (0.91 ± 0.07 logMAR) were significantly poorer than amongst those cases that were above the diastereopsis threshold (0.50 ± 0.07 logMAR; $t = 4.01$, $p = 0.001$). Stereo thresholds, on the other hand, were comparable between the two cohorts (uncorrected myopes: 3.28 ± 0.20 log arcsec; cases: 3.20 ± 0.06 log arcsec, $t = 0.43$, $p = 0.67$) (blue vs red bubbles in Figure 4.4)].

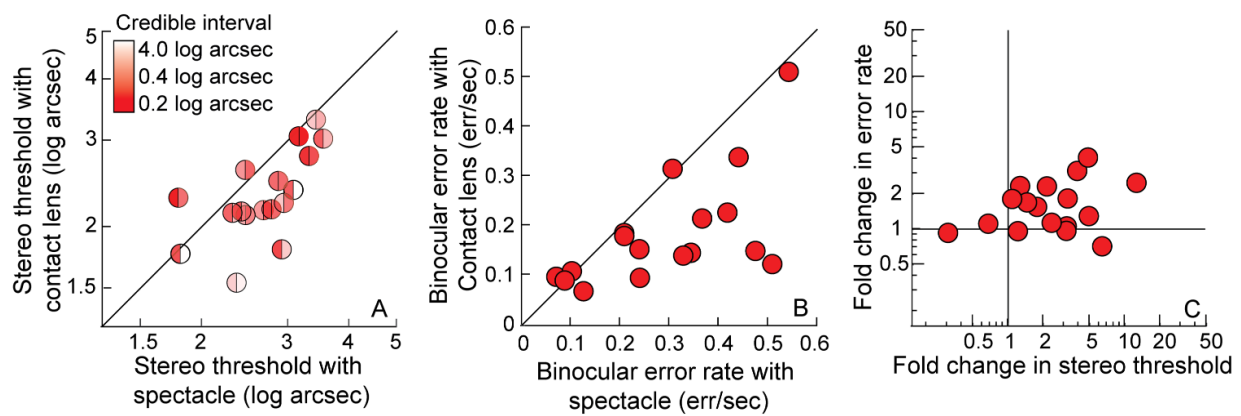


Figure 4.5 Panels A and B show the stereo threshold and error rate, respectively, obtained with the spectacle and contact lens corrections in cases. The transparency on the right and left hemispheres in Panel A, represents the 68% credible interval for the spectacle and contact lens, respectively. Panel C shows the fold-change in stereo threshold from spectacles to contact lens wear plotted against the corresponding fold-change in error rates of the buzz-wire task. The region above the intersection of the vertical and horizontal lines indicates an improvement in both parameters with contact lens wear in this panel. The region diagonally opposite this indicates worsening of performance in both parameters with contact lens wear.

Scatter diagrams of error rate and speed for the participants with uncorrected myopia have been fit with bivariate contour ellipses and superimposed on the corresponding ellipses for controls and cases in Figure 4.6. The bivariate contour ellipse for error rates in the uncorrected myopes was oriented at 57.9° , with its x-axis centroid remaining higher than its y-centroid (Figure 4.6A). The one-factor RM-MANOVA analysis showed a significant impact of viewing condition on the combined dependent variable (Table 4-2, Section 5a) and the univariate tests confirmed a significant impact of viewing condition for both error rates and speed (Table 4-2, Section 5b). The log-transformed binocular advantage in error rate (mean \pm SEM: 0.22 ± 0.04) was well correlated with logMAR visual acuity (Pearson's $r = -0.73$; $p = 0.02$) (data not shown) but poorly correlated with stereo threshold (Pearson's $r = -0.09$; $p = 0.80$) (Figure 4.4). The binocular advantages in error rate and speed were also significantly higher amongst

uncorrected myopes than amongst cases with comparable levels of stereo threshold (Figure 4.4; Table 4-2, Section 6).

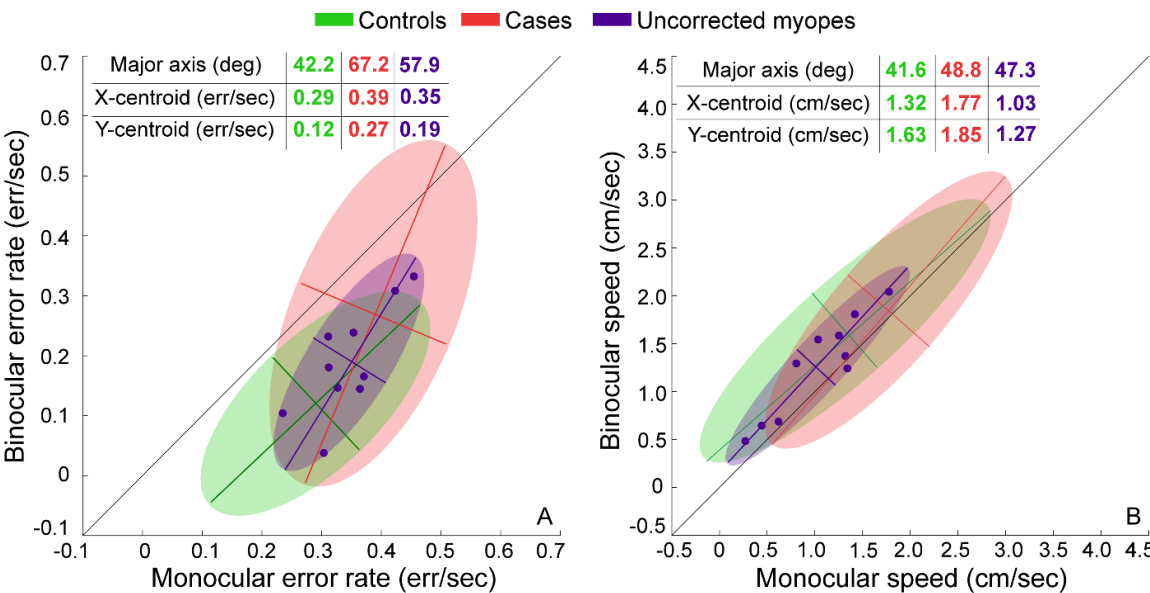


Figure 4.6 Scatter diagrams of the error rate (panel A) and speed (panel B) in uncorrected myopes (blue symbols) while performing the buzz-wire task plotted along the corresponding bivariate contour ellipses. The ellipses of the controls (green) and cases (red), identical to those in Figure 4.3, are also reproduced here for comparison purposes. All other details are the same as Figure 4.3

4.4 Discussion

4.4.1 Summary of results

1. Controls made fewer errors when viewing the buzz wire binocularly (Figure 4.3A). However, only those cases with relatively low monocular error rates showed a similar advantage from binocular viewing (Figure 3A). Cases with high monocular error rates also had higher error rates when viewing the buzz wire binocularly (Figure 4.3A).

2. An improvement in the retinal image quality of cases with rigid contact lens wear reduced the binocular error rates in the buzz-wire task, vis-à-vis, spectacles (Figure 4.5B).
3. Two observations indicate that psychophysical estimates of stereo thresholds may not be a good predictor of error rates in visuomotor activities like the buzz-wire task. First, the stereo threshold proved to be poorly correlated with the binocular advantage in error rate amongst the participants within each cohort. Second, stereo threshold proved to be poorly correlated with the reduction in error rate enjoyed by cases, when they switched from their best-corrected spectacles to contact lenses (Figure 4.5C).
4. Controls, uncorrected myopes and cases executed the buzz-wire task faster under binocular than monocular conditions (Figure 4.3B and Figure 4.6B). However, the magnitude of speed reduction from binocular to monocular viewing was smaller in cases than in the controls and uncorrected myopes (Figure 4.3B and Figure 4.6B, Table 4-2).

These results compare well with previous findings of deficient visuomotor task performance in other forms of ophthalmic disease such as amblyopia and strabismus (O'Connor et al., 2010a, 2010b), and indicate that functional depth vision may be severely compromised with degraded binocularity, irrespective of the cause of this dysfunction.

4.4.2 Stereo threshold as a poor predictor of visuomotor task performance

There are at least two reasons why the psychophysical stereo threshold may correlate poorly with the error rate in the buzz-wire task. First, the executive requirements of the

random-dot stereogram task and the buzz-wire task may be quite different (Stevenson et al., 1989). The former is a hyperacuity task, requiring good quality correspondence matching of the monocular images for fusion, computation of retinal disparity from the fused percept, and inference about the geometric shape of the 3D object in an otherwise two-dimensional field of random dots (Julesz, 1960). The buzz-wire task, on the other hand, relies on the accurate and continuous judgment of the diastereopsis of a physical 3D structure that guides hand movements to avoid contact between the loop and the wire in the task. These two measures may respond very differently to the degraded retinal image quality experienced in the present study. Random-dot stereo targets may be more vulnerable to contrast loss and phase distortions in the blurred retinal image (Marella et al., 2024; Marella et al., 2023), reaching stereo-blindness levels when thresholds exceed 1300 arc sec (Chopin et al., 2019), while useful information regarding diastereopsis may still be available in the buzz-wire task for comparable levels of blur. Evidence for this possibility arises from the uncorrected myopes continuing to show a binocular advantage in the buzz-wire task, even while they were all nearly stereo-blind (Figure 4.4 and Figure 4.6A). This binocular advantage may be derived from non-stereoscopic cues that may aid the identification of the gap between the loop and the wire in this task, unlike random-dot stereograms that are entirely reliant on the retinal disparity cue for stereo processing. However, the prominent monocular cue of motion parallax derived from head movements may not be useful for depth judgments in the buzz-wire task, as reported in the earlier chapter (section 3.3.6). The complexity of integrating retinal image motion arising from head velocity with the velocity of object motion arising from passing the loop through the buzz wire may make this cue less beneficial to the present task performance.

The second reason is that the stereoscopic information in a random-dot target is to be inferred from a two-dimensional field of random dots might make this task more unnatural and, thus, more vulnerable to retinal image quality degradation. On the contrary, the buzz-wire task is similar to routine depth-related activities of daily living wherein the stereoscopic information is derived from objects that are physically separated in space. Perhaps a top-down knowledge of the buzz-wire configuration, and/or the depth information derived from convergence eye movements while tracking the depth convoluted buzz-wire makes this task less vulnerable to retinal image quality degradation (Rogers, 2023). After all, our ability to generate accurate vergence eye movements remains largely unaffected in the presence of either iso-ametropic or anisometropic retinal image blur (Bharadwaj & Candy, 2009). Future studies could employ depth judgments between physically separated objects to determine the relationship between stereo thresholds and errors in the buzz-wire task.

4.4.3 Retinal image quality and its impact on visuomotor task performance

The nature of the blur experienced by the participant and its bilateral asymmetry could have a determining impact on the buzz-wire task investigated in this study. Deeper insights into this issue may be obtained through simulation of how the buzz-wire apparatus may appear from the blur in cases, uncorrected myopia, and controls (Figure 4.7). All the following simulations were performed for 555 nm light and 5 mm pupil diameter, using standard Fourier optics techniques (Jaskulski M, 2019). The point spread function (PSF) of the eye with clear vision was generated using only population average higher-order Zernike wavefront aberrations obtained from Cheng et al. (2004) (Figure 4.7A). The PSFs of uncorrected myopes were generated by adding 1 D, 3 D, and 10 D worth of defocus to the population average higher-order Zernike aberrations

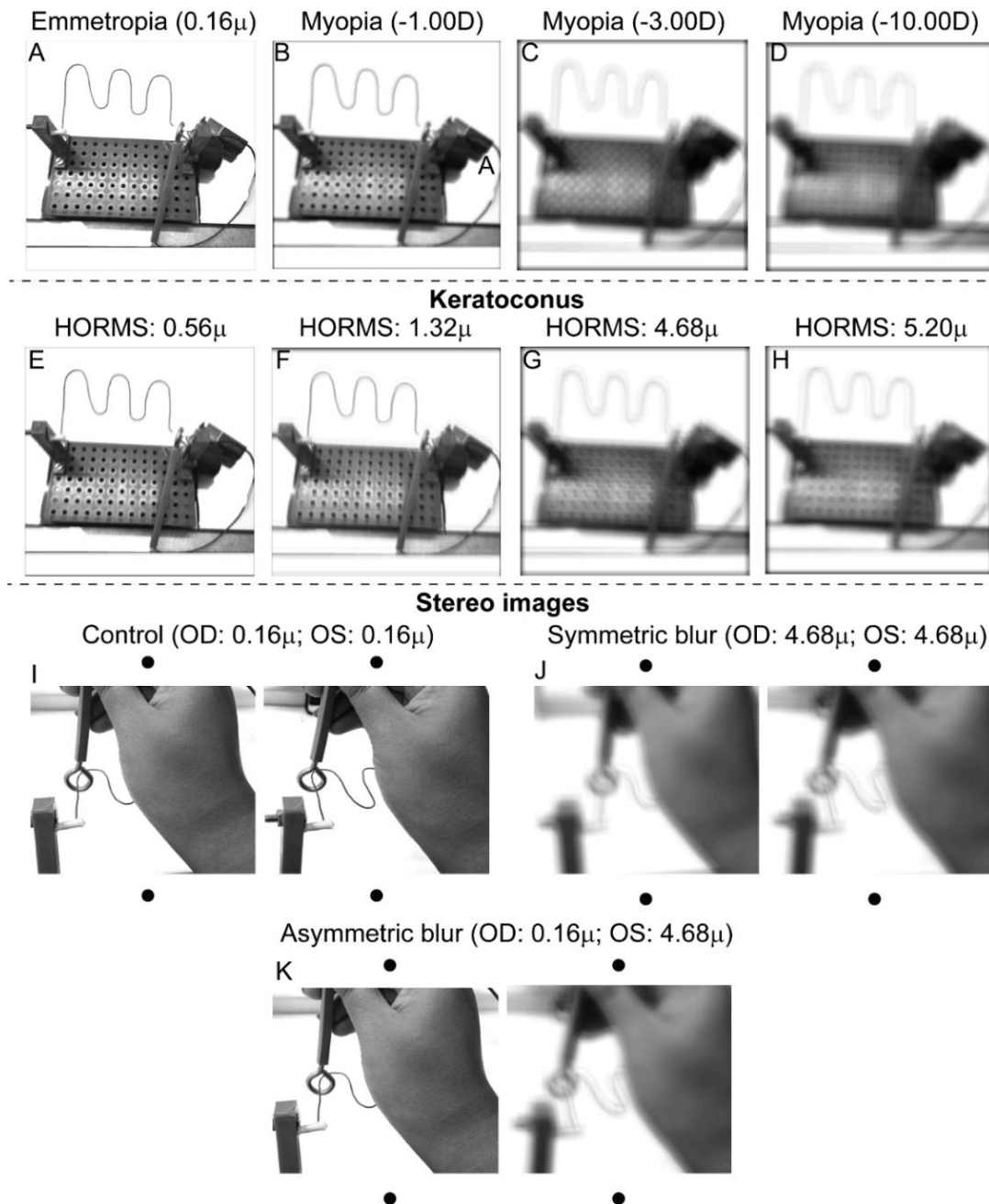


Figure 4.7 Panels A–H) Point-of-view optical simulations of the buzz-wire apparatus with clear vision (panel A), blurred vision from uncorrected myopia (panels B – D) and blurred vision from cases, whose severity is indicated on top of each panel by the root-mean-squared values of the higher-order aberrations (HORMS) (panels E–H). Panels I–K show cross-fusible zoomed-in stereoscopic image pairs of the buzz-wire apparatus illustrating the location of the loop relative to the wire when vision is clear in both eyes (panel I) and when vision is bilaterally (panel J) or unilaterally (panel K) blurred from keratoconus. The wavefront aberration values used to blur the right and left eye of the stereogram pair are indicated on top of each figure panel.

(Figure 4.7B - D, respectively). Case PSFs are obtained from higher-order Zernike aberrations, corresponding to early, mild, moderate and severe keratoconus already available in the laboratory (Figure 4.7E–H) (Nilagiri et al., 2020). Lower-order aberrations are assumed to be fully corrected in keratoconus, while in reality, some may remain owing to variability in estimating the subjective refraction endpoint (Davis et al., 1998; Raasch et al., 2001).

The uncorrected myopes in the present study were all iso-ametropic, resulting in similar magnitudes of radially symmetric blur in the two eyes. This radial symmetric blur is characterized largely by contrast demodulations while retaining the spatial relationship between the loop and the wire (Figure 4.7B–D). The bilateral symmetry of blur continues to support the fusion of the monocular percept (Figure 4.7J). Both features may help retain the diastereopsis information under binocular viewing in uncorrected myopia (Figure 4.7J). In contrast, the cases experience radially *asymmetric* blur that may be of bilaterally dissimilar owing to interocular differences in disease severity (Appendix 1). The radially asymmetric blur introduces significant phase distortions that disrupt the spatial relationship between the loop and the wire under monocular viewing (manifesting as “ghosting” or “doubling” of the wire in Figure 4.7E–H) (Marella et al., 2024). Binocularly, the phase distortions may disrupt the correspondence matching between the monocular precepts (Metlapally et al., 2019) and the bilaterally asymmetric blur may induce interocular suppression of the more blurred percept, (Marella et al., 2021) both of which may lead to poor quality diastereopsis (Figure 4.7K). These effects may explain the absence of binocular advantage in the buzz-wire task for the cases, even while it was retained in the uncorrected myopes (Figure 4.6). Relative to spectacles, rigid contact lenses may have improved buzz-wire task performance in cases by reducing the contrast demodulation and phase disruption in the monocular retinal images and by improving the symmetry in the retinal image quality of the two eyes (Marella et al., 2021; Marella et al., 2024; Marella et

al., 2023). A future study could compare the buzz-wire task performance in uncorrected anisometropia and bilaterally asymmetric keratoconus to gain deeper insights into this issue.

4.4.4 Clinical implications

The present results suggest that keratoconus may increase the difficulty in executing activities of daily living that involve 3D depth judgments (e.g., driving, navigating obstacles and climbing stairs) (Figure 4.3). These factors, combined with their sub-optimal spatial vision,(Kumar et al., 2023) may contribute towards an overall deterioration in their quality of life and general well-being (Gothwal et al., 2022). Rigid contact lenses that improve retinal image quality may be one way to minimize this deterioration (Figure 4.5B). Interestingly, neither the disease severity nor the routinely evaluated clinical measures of visual acuity or stereoacuity were good predictors of such visuomotor activity limitations (Figure 4.4). This observation, on one hand, reveals the limitation of the clinical measures in reflecting the real-world visual experience of the patient, and, on the other hand, underlines the need for expanding the visual assessment battery to include measures that emulate the complexities of daily tasks.

The lack of a prominent speed reduction in the buzz-wire task in keratoconus is contrary to the expectation of how this parameter may decline in the presence of uncertain sensory inputs (arising from blurred vision and poor stereopsis(Kumar et al., 2023; Nilagiri et al., 2018)). This may be so for two reasons. First, the binocular and monocular viewing experience in keratoconus in such tasks may be similar, given their habitually sub-optimal vision. Thus, there may be no overt reason to decrease the speed under monocular viewing, relative to binocular viewing. Second, keratoconics may harbour false beliefs that they can see well in depth despite their degraded

binocularity. This may reflect the general personality trait of keratoconics and the difficulties they may experience coping with vision loss (Aiello et al., 2024; Mannis et al., 2018). These hypotheses need further investigation.

Chapter 5 Exploration of usage of monocular cues for perception of depth

General introduction

Our previous work on uniocular individuals (described in Chapter 3) found limited evidence that monocular depth cues can support depth perception to the extent that the addition of binocular disparity can offer. This suggests that even after years of adaptation, monocular cues are not sufficient to compensate for the loss of binocular disparity. However, this finding might be specific to the visuomotor task used in the study. To investigate this possibility, we conducted two additional pilot studies, maintaining the hypothesis that prolonged exposure to monocular cues could enhance depth estimation precision with them. Since the visuomotor task's dynamic nature may have prevented monocular cues from contributing effectively, we modified it by removing both its dynamic and motor components, transforming it into a purely visual (perceptual) task. Part 1 of this chapter describes the experiment and its findings. Part 2 of the chapter exclusively studies the ability of motion parallax to trigger the perception of a 3D structure. This experiment is in its infancy and describes only pilot results.

5.1 Part 1

5.1.1 Introduction

In a standard prehension task, “reaching” is studied as the hand extending towards the point of interest guided by extrinsic properties like the location and the orientation of the object. The “grasp” component corresponds to the grip aperture in the prehension task, reflecting perceived intrinsic properties like object size. Although the

buzz-wire does not resemble a typical prehension task involving “reach” and “grasp” components, the visual system does need to process the extrinsic and intrinsic information. In the buzz-wire task, the hand extends along the straight portion of the wire, moving either from front to back or back to front, akin to the reaching movement in a prehension task. The loop movement at the transition and curved location, where the loop needs to be rotated to match the perceived curvature, draws its similarity to the grasping component. However, there are a few key distinctions between the two tasks. Firstly, the visual demands differ between the prehension task and the buzz-wire task. In the prehension task, accurately estimating absolute distance is crucial to determine how far the hand needs to move to reach the target object. In contrast, the buzz-wire task requires not only absolute distance estimation to guide movement along the anteroposterior axis of the wire but also precise assessment of absolute disparity to identify the planes of the loop and the wire, to prevent or correct contact between the loop and the wire. Secondly, the accuracy or precision of reach and grasp actions in the prehension task is quantified using the metric system, whereas, in the buzz-wire task, performance is measured by the number of buzzes.

Theoretically, to perform the above-mentioned tasks, both binocular disparity and motion parallax could provide comparable depth estimation due to the similarities between the two depth cues (Rogers & Graham, 1982). Watt and Bradshaw (2003) demonstrated that motion parallax can aid in scaling the reach component relative to object distance in a prehension task, although the grasp action was compromised. In our previous experiment, the uniocular individuals were noted to make sizeable head movements during the buzz-wire task that generated suprathreshold disparity signals from motion parallax. Nonetheless, neither were those uniocular individuals better than the controls performing the task monocularly (Figure 3.3A) nor did they have any

lesser errors at the straight portion of the buzz-wire (Figure 3.7A). This might indicate that the uniocular individuals were not able to use motion parallax for the absolute disparity estimations.

This raises the question: if the task was less demanding like ordinal depth estimation, would the uniocular individuals be better than the binocular controls with transient occlusion of one eye?

5.1.2 Method

The study adhered to the tenets of the Declaration of Helsinki and was approved by the Institutional Review Board of LVPEI, India and the Optometry Proportionate Review Committee of City, University of London, United Kingdom. All subjects participated after signing a consent form. Similar to the previous study 1, the inclusion and exclusion criterion and the sample size were the same.

5.1.2.1 *The static buzz-wire apparatus*

A perceptual version of the buzz-wire task was conceptualised to secure the loop at fixed positions along the wire. To achieve this, the experimental setup featured a U-shaped structure (here called a 'wire' for lack of better terminology) of 0.4cm thickness, representing a small segment of the wiring pattern of the buzz-wire apparatus (see Fig. 5.1). The wire consisted of an anteroposterior straight, section that smoothly transitioned into a curved portion. The wire was threaded through a 1.2 cm wide loop and fixed to two vertical beams, ensuring that it was oriented parallel to the tabletop. These beams were further anchored to both a horizontal base and a roof for stability. Twelve such models were made.

The loop was held by a shaft that ended with a magnet, that would attach itself with the opposite pole of one of the five magnets present on the roof. The five magnets

were strategically placed on the roof to ensure that loop 1) would be positioned correctly at one of three predefined locations along the wire, i.e. the straight, transition and curved portion (Figure 5.1C D and E), and 2) would remain suspended with a gap or contact with the wire (Figure 5.1A). The 12 buzz-wires with 5 presentations consisted of a total of 60 trials. These trials were equally divided across six conditions based on both location and contact criterion: 10 trials each for the straight section with a gap, the straight section with contact, the transition section with a gap, the transition section with contact, the curved section with a gap, and the curved section with contact. These twelve models were placed on a round turntable with a single viewing port, allowing the participant to view only one static buzz-wire model at a time (Figure 5.1A and B). A mobile stand was incorporated into the setup to record the head movement of the participant (Figure 5.1A and B).

The experiment was conducted in a dark room, where only one model was illuminated using a Wi-Fi-controlled LED strip, fixed at the border of the viewing slot.

5.1.2.2 Procedure

The uniocular participants and control group completed both the visuomotor buzz-wire task and the perceptual static buzz-wire task, with the order of tasks randomized. The controls also performed both tasks under binocular and monocular viewing conditions, randomly. The procedure and instructions for the visuomotor task remained the same as mentioned earlier. The head movement from both these two tasks was analysed using the same OpenFace software.

For the static buzz-wire task, the participants were seated 30 cm from the setup. The participants were instructed as follows:

The lights will be on for a specific time. During this time observe the model and respond verbally “Yes” if you see a gap between the loop and the wire, and “No” if you don’t see any gap. You will be awarded 1 mark for every correct identification of a gap, but 2 marks will be deducted for every incorrect “Yes”. Therefore, say “Yes” only if you are certain you see a gap.

No explicit instruction was given regarding head movements. But in certain instances, when the participant enquired if they could move their head during the experiment, the generic answer “whatever you are comfortable with” was provided. Each setting was tested 3 times, leading to $60 \times 3 = 180$ trials.

To ensure that the model was directly in front of the participant, the red vertical line in front of every model was ensured to be aligned with the red line on the viewing slot (Figure 5.1A). Once aligned, the examiner would switch on the LED light, which automatically turned off after 2 sec. The participant then provided a response, which the examiner recorded in an Excel sheet as 1 for “Yes” and 2 for “No”. Although the Excel sheet contained stimulus characteristics and indicated whether responses were correct, these columns were hidden with a black background. This prevented examiner bias and accidental cues to the participant. Throughout the task, participants were periodically reminded of the scoring system.

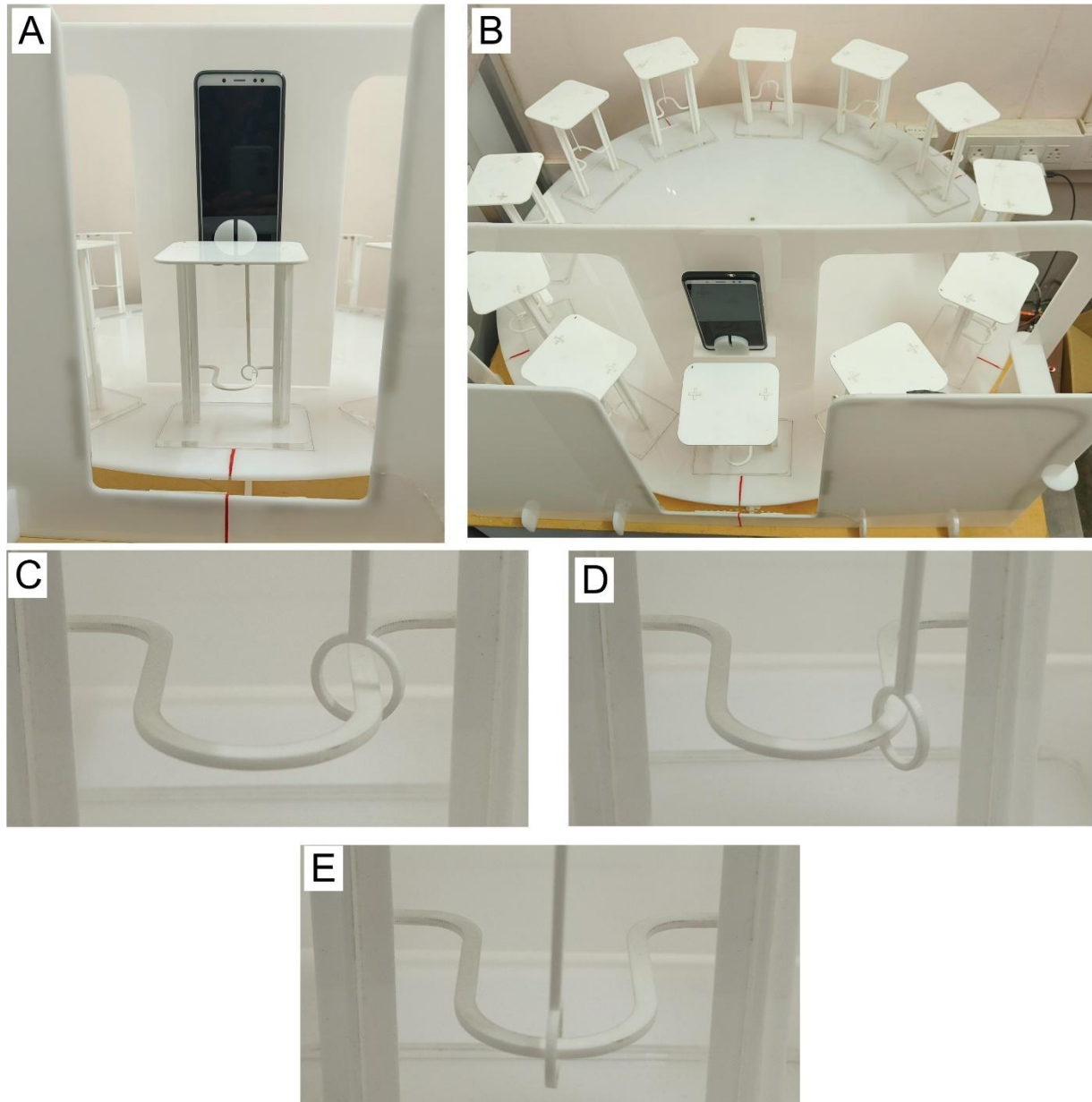


Figure 5.1 The static buzz-wire apparatus. A) One model from the participant's point of view. B) Top view of the 12 models on the turntable. C, D and E) Straight (S), transition (T) and curve (C) sections.

5.1.2.3 Outcomes of the static buzz-wire task

The gap detection sensitivity (d') was calculated as:

$$d' = z(\text{Hit rate}) - z(\text{False alarm rate})$$

Since there are chances of getting all the all the responses correct or incorrect, where the Hit rate or the False alarm rate will be 1 or 0 respectively, making the z score

“undetermined”. To overcome this, a loglinear approach was taken (Stanislaw & Todorov, 1999), where,

$$\text{Hit rate} = \frac{\text{Number of hits} + 0.5}{\text{Total number of trials with gap present} + 1}$$

$$\text{False alarm rate} = \frac{\text{Number of false alarm} + 0.5}{\text{Total number of trials with gap absent} + 1}$$

The chance level performance would result in $d'=0$, and a higher value would indicate better sensitivity.

The head movements from the OpenFace software were exported to Excel and the variability of the head movements was calculated. The higher the variability, the larger their head movements.

5.1.2.4 Similarities between the visuomotor and the perceptual task

The perceptual buzz-wire setup was built to mimic the visuomotor buzz-wire apparatus. To do so, firstly the loop and the wire setup were replicated. Secondly, the perceptual buzz-wire setup should pick up the difference in performance between the binocular and monocular viewing of the controls. To pick up this difference, the viewing duration had to be constant among all participants. If the viewing duration was too short, the participants would not have time to move their heads. To find the minimum viewing duration that could generate consistent and different d' prime values, we first titrated the viewing duration time. Five binocular participants were asked to perform the perceptual buzz-wire task while the viewing duration (duration for which LED was switched on) varied randomly between 0.5, 1, 2, and 3 sec.

Figure 5.2 shows the averaged d' for the binocular and monocular performance across the viewing duration in seconds. Under binocular viewing conditions, the detection

sensitivity increased as the viewing duration increased. While the monocular detection sensitivity remained similar between the 1 and 2 sec, the difference between the two viewing conditions was noted to be a maximum of 2 sec of viewing duration. For the main study, the viewing duration was kept constant at 2 sec.

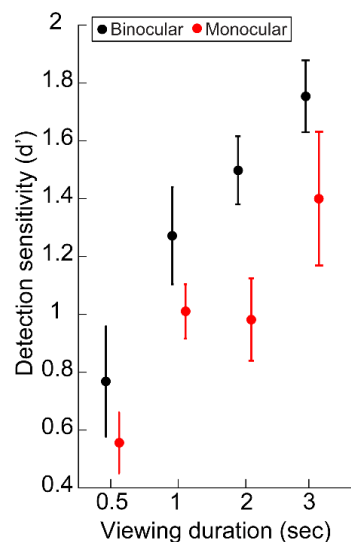


Figure 5.2 Scatter plot showing the average detection sensitivity (d') across different viewing durations (0.5, 1, 2, and 3 sec) for control participants under both binocular and monocular viewing conditions. Error bars denote the SEM.

5.1.2.5 Statistical Analysis

The statistical analysis was performed using SPSS. Shapiro-Wilk test showed that the error rates in the visuomotor task and the detection sensitivity in the straight, transition and curve portion of the perceptual buzz-wire task were normally distributed. Thus, parametric analysis was used.

For the error rates, paired t-tests were used for the binocular and monocular viewing comparison and independent t-tests were used to compare the uniocular error rates with binocular and monocular viewing. A 2-factor RM-ANOVA was performed on the data of controls, to investigate the effect of within-subject factors of viewing condition (binocular vs monocular) and location of the loop (straight, transition and curve portion)

on the detection sensitivity. Two separated 2-factor mixed model RM-ANOVA were performed on the data of the uniocular and controls to investigate the effect of within-subject factor of location of the loop (straight, transition and curve portion) and between-subject factor (uniocular vs binocular or uniocular vs monocular) on the detection sensitivity.

5.1.3 Result

A total of 14 uniocular participants were recruited for the study. However, one was excluded due to difficulty following instructions in the perceptual buzz-wire task. This participant repeatedly alternated their “Yes” responses between detecting a gap and detecting contact. Despite clarifications and repeated sessions, the participant continued to respond inconsistently, likely due to confusion (Stanislaw & Todorov, 1999). This was confirmed by negative d' values, indicating a higher false alarm rate than a hit rate. Ultimately, the study included 13 uniocular participants (mean \pm SD: 24.29 ± 4.21 years) and 11 age-matched binocular controls (26.82 ± 2.28 years; $t = 1.93$, $p = 0.07$).

Figure 5.3A shows the results obtained from the visuomotor buzz-wire task. The result remains the same as reported in the earlier experiments (Figure 3.3). The uniocular error rates (0.26 ± 0.03 error/sec) were not significantly different from the monocular viewing of controls (0.28 ± 0.03 error/sec, unpaired $t=0.59$, $p=0.56$). The binocular error rates (0.09 ± 0.01 error/sec) were significantly lower than the monocular (paired $t=-8.30$, $p<0.001$) and uniocular error rates (unpaired $t=-5.25$, $p<0.001$).

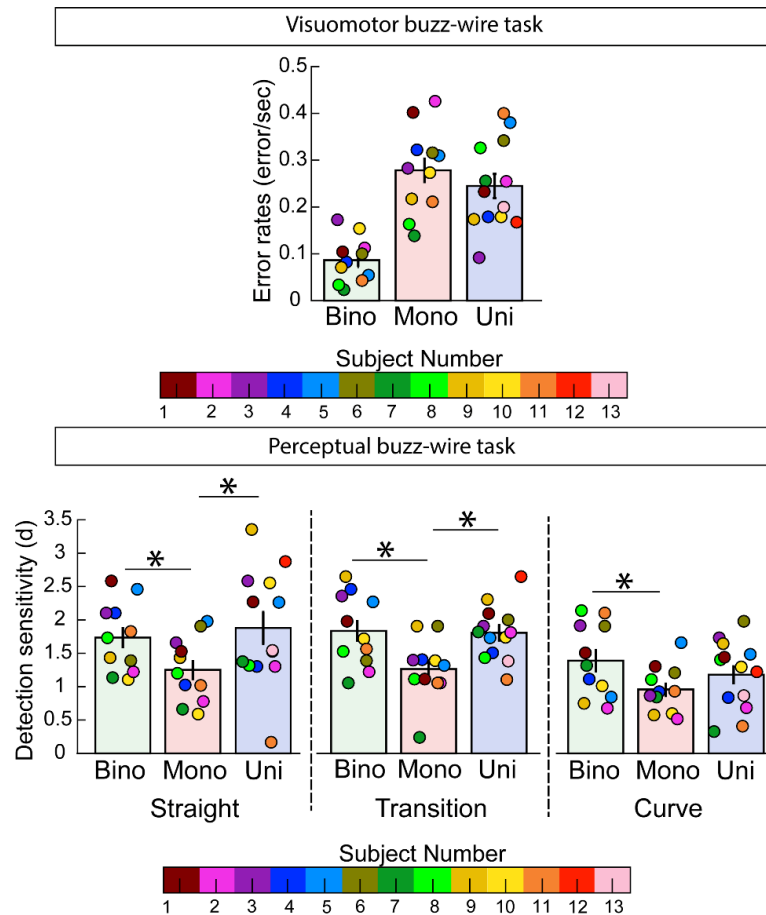


Figure 5.3 A) Bar graph for the mean error rates obtained from the visuomotor task for the binocular and monocular viewing of controls and uniocular cases. B) Bar graph for the mean detection sensitivity for the binocular and monocular viewing of controls and uniocular cases obtained at the straight, transition and curve sections of the perceptual buzz-wire task. The error bars represent the SEM. The circles represent the data of individual participants. The colour of the circle indicates the subject number. The circles with the same colours under the binocular and monocular viewing conditions represent the same subject, while the same colour under uniocular bars indicates a different participant. The circles are jittered for better visibility of individual data points. The horizontal bar with the asterisk marks the group that showed significant differences ($p < 0.05$).

Table 5-1 Results of the main statistical analyses conducted for the perceptual buzz-wire task.

Section 1 – Two-factor RM-ANOVA Analysis				
Effect of viewing and location on dependent variable of binocular and monocular data of controls	1a. Multivariate tests			
		F	p-value	Partial η^2
	Viewing	15.3	0.001	0.77
	Location	1.77	0.16	0.16
	Viewing X Location	1.44	0.24	0.13
	1b. Univariate tests			
			Detection sensitivity (d')	
			Mean \pm SE	p-value
	View	Binocular	1.65 \pm 0.11	<0.001
		Monocular	1.16 \pm 0.10	
Location	Straight	1.50 \pm 0.14	0.07	
	Transition	1.55 \pm 0.13	0.20	
	Curve	1.17 \pm 0.11	-	
Section 2 – Two-factor mixed model RM-ANOVA Analysis				
Effect of viewing and location on the dependent variable of monocular and uniocular data	2a. Multivariate tests			
		F	p-value	Partial η^2
	Viewing	3.24	0.04	0.3
	Location	5.78	0.003	0.55
	Viewing X Location	2.21	0.11	0.32
	2b. Univariate tests			
			Detection sensitivity (d')	
			Mean \pm SE	p-value
	View	Monocular	1.16 \pm 0.14	0.02
		Uniocular	1.62 \pm 0.13	
Location	Straight	1.57 \pm 0.15	0.00	
	Transition	1.54 \pm 0.09	0.00	
	Curve	1.07 \pm 0.09	-	
Section 3 – Two-factor mixed model RM-ANOVA Analysis				
Effect of viewing and location on the dependent variable of binocular and Uniocular data	3a. Multivariate tests			
		F	p-value	Partial η^2
	Viewing	1.95	0.17	0.16
	Location	5.04	0.006	0.52
	Viewing X Location	0.92	0.47	0.162
	3b. Univariate tests			
			Detection sensitivity (d')	
			Mean \pm SE	p-value
	View	Binocular	1.65 \pm 0.14	0.86
		Uniocular	1.62 \pm 0.13	
Location	Straight	1.81 \pm 0.15	0.00	
	Transition	1.82 \pm 0.10	0.00	
	Curve	1.28 \pm 0.11	-	

Sections 1a and b show the results of the multivariate and univariate two-factor RM-ANOVA comparing the binocular and monocular detection sensitivity. Sections 2a and b show the results of the multivariate and univariate two-factor mixed model RM-ANOVA comparing the monocular and uniocular data. Sections 3a and b show the results of the multivariate and univariate two-factor mixed model RM-ANOVA comparing the binocular and uniocular data. The p-value along the location rows under univariate test shows the significance level compared to the curved section. Straight and transition sections did not show any significant difference (data is not shown in the table).

Figure 5.3B shows the detection sensitivity under the binocular and monocular viewing conditions of controls and uniocular individuals. The two-factor RM-ANOVA performed on the control's binocular and monocular viewing data revealed a significant main effect of viewing conditions on the detection sensitivity. There was neither a main effect of the location of the loop nor any significant interaction between the viewing condition and the location of the loop on the detection sensitivity (Table 5-1, Section 1a). Univariate test (Table 5-1, Section 1b) revealed detection sensitivity under binocular viewing to be significantly higher than the monocular viewing. Two-factor mixed model RM-ANOVA performed on the monocular viewing of controls and uniocular participants, found a main effect of both viewing and the location of the loop on the detection sensitivity in the multivariate testing (Table 5-1, Section 2a). Again, no significant interaction between the two independent variables was found. Univariate tests revealed the detection sensitivity of the uniocular subjects to be higher than the monocular viewing condition of controls (Table 5-1, Section 2b). The detection sensitivity was significantly lower when the loop was at the curved location relative to the straight and transition sections (Table 5-1, Section 2b). Two-factor mixed model RM-ANOVA performed on the binocular viewing of controls and uniocular participants, found a significant main effect of only the loop location and not of the viewing condition on the detection sensitivity (Table 5-1, Section 3a). Univariate tests revealed the detection sensitivity was lower at the curved section compared to the straight and transition sections (Table 5-1, Section 3b).

5.1.3.1 Head movement analysis

The video recorded for the perceptual depth-related task was noisy due to the reduced brightness. The OpenFace software would fail to track the head and provided spurious head locations. In future, we need to measure the head movement with some other

method or change the setup with a better resolution camera. For convincing evidence for larger head movements of the uniocular participants relative to the control's binocular and monocular viewing, the reader can view the following videos [Head movement - Bino](#), [Head movement - Mono](#) and [Head movement - Uni](#), showing the 4 controls under binocular and monocularly and the 7 uniocular participants, respectively performing the task.

5.1.4 Discussion

5.1.4.1 *Summary of results*

The uniocular individuals did not show significant improvement compared to monocular viewing of controls in a visuomotor task that required them to move the loop along a wire convoluted wire without making contact. However, in a perceptual version of the same task involving the participant to determine if a stationary loop is in contact with the wire, they were better compared to the controls with transient occlusion of one eye. The result suggests that long-term uniocular individuals may adapt to monocular depth cues for perceptual tasks but not for visuomotor tasks.

5.1.4.2 *Usage of monocular depth cues for depth-related visuomotor and perceptual task*

The visuomotor task in this study required the use of absolute and relative depth judgment to successfully manoeuvre the loop along the convoluted wire without making contact. Tyler (1975) demonstrated that a line stimulus could generate depth from binocular disparity and given the optical similarity between binocular disparity and motion parallax, theoretically, the buzz-wire task can be achieved by just two depth cues, binocular disparity or motion parallax. However, the use of motion parallax was impractical for the buzz-wire task.

A key feature of motion parallax is that it is time-dependent. To take advantage of this cue, a participant would need to make head movements to generate relative motion between the loop and the wire. However, this extra movement requires time. In the visuomotor task, if an error occurred—meaning the loop touched the wire—the participant would have needed additional time to adjust their head position and use motion parallax to refine their movements. This was impractical in the buzz-wire task because the buzzer that was set up to provide feedback about the errors also discouraged/penalised the participants with its high-intensity buzz. This would have created a rush and discouraged taking time to make any useful head movements. Each epoch of an error among the uniocular participants lasted for 0.55 ± 0.53 sec. Findings from the time titration experiment indicated that within 0.5 sec of the viewing interval, the detection sensitivity was close to chance level performance (Figure 5.2). A modified version of the task, where participants are not rushed and can freely make head movements, may provide more insights into whether long-term uniocular individuals develop an enhanced ability to use motion parallax in a visuomotor task. In the perceptual task, the participants were allowed to view the stimulus for 2 sec, giving enough time for head movements to be made, which might have been another reason for better performance. If the task was repeated by reducing the viewing duration to 0.5 sec, the uniocular participants would be expected to perform similarly to the monocular viewing condition.

The perceptual task does not require very accurate estimations of absolute or relative depth. The task can be easily completed with simple ordinal depth estimation. This helps in breaking camouflage, an ability that has been reported to be strongly related to evolution as it helps organisms to find their prey and avoid being one (Darwin &

Beer, 1951). Given this reasoning, there is a possibility that the perception of ordinal depth would be the first to be adapted to the absence of binocular disparity.

5.1.4.3 Is there any scope for monocular depth cues to improve with years of habituation?

One might expect that a good perception of depth would manifest in better motor action. However, it does not necessarily need to be true, and the Ebbinghaus illusion is an example where the perception is cheated by the visual information but the visuomotor action remains unaffected. Goodale and Milner (1992) suggested that the process of deriving inferences of the visual information for perception and motor action is through two separate processes, 1) a ventral stream of projections from the primary visual cortex to the temporal lobe and 2) a dorsal stream from the primary visual cortex (and the superior colliculus via the pulvinar) to the posterior parietal cortex. The ventral stream processes the characteristics of objects in space and the relations between each other, forming a perceptual representation of the world. The dorsal stream processes the characteristics of the objects and their location relative to egocentric coordinates and drives the goal-directed motor actions in prehension tasks (Cavina-Pratesi et al., 2007; Marotta et al., 1997). This dissociation in processing was first proposed through case studies, where individuals with visual agnosia, had compromised perception of the shape, size, orientation and depth of an object, but had accurate motor action (Goodale et al., 1991; Marotta et al., 1997). Later, fMRI studies confirmed the presence of two distinct streams responsible for coding the visual information for grasping and perceptual tasks (Cavina-Pratesi et al., 2007). To confirm if the ventral stream indeed changes in uniocular individuals, future studies can use neuroimaging studies to investigate whether the ventral stream shows any higher activity among uniocular individuals while performing a depth-related

perceptual task compared to the binocular individuals performing the task monocularly, however comparing absolute levels of BOLD signals from the fMRI across individuals is hard

5.2 Part 2

5.2.1 Introduction

Motion parallax refers to the relative motion between objects at different distances. It arises from the motion of the observer or the object in space. The successive stimulation of the retina over time is comparable to viewing the objects simultaneously with both eyes. Consequently, motion parallax and binocular disparity can provide similar depth estimates (Rogers & Graham, 1982). Motion parallax may have the potential to substitute for the absence of binocularity in the case of uniocular individuals (Gonzalez et al., 1989; Marotta et al., 1995).

Gonzalez et al. (1989) explored whether uniocular children made head movements spontaneously and if that was helpful in a task requiring the subjects to align two vertical plates on the same depth plane. They found that uniocular children did not move their heads spontaneously, and the error (distance between the two plates) was large compared to binocular viewing of age-matched controls. However, when they were asked to do so, the error was reduced. On the contrary, Marotta et al. (1995) showed that the uniocular adults moved their heads spontaneously in a task where they needed to grab objects. However, the authors did not provide any information regarding the accuracy of the task. Larger head movements do not necessarily mean that better estimation of depth (Figure 3.8 D and H). Evidence for this may be obtained from Mongolian gerbils. These animals are known to use motion parallax by moving their head up and down before jumping (Ellard et al., 1986). Ellard et al. (1986) created

lesions in the visual cortex of these animals and showed that the landing positions after a jump were highly variable, they over-jumped when the platform was closer and under-jumped when the platform was farther away. The group of gerbils with sham surgery could accurately jump onto the landing platform. Interestingly, the head motions were made in 55% of trials in the former group while the latter group made head movements in 38% of trials. This increase in the head motion with poor landing accuracy indicates that the head motions did not result in a better estimation of depth from motion parallax.

The resulting optic flow field from head motion includes both the motion parallax and dynamic occlusion information. The latter results in the farther objects undergoing gradual accretion/deletion of their features by the nearer object. The degree of motion parallax and the extent of accretion/deletion are influenced by the depth difference between the objects and the range of head movement – greater depth between the objects and greater extent of head movements will lead to larger accretion/deletion of information of the farther object. Ono et al. (1988) demonstrated that when dynamic occlusion and motion parallax cues contradict each other, the depth order is determined by the dynamic occlusion only when the two objects are separated by a greater distance, otherwise the depth order is determined by the motion parallax. While the depth order can still be derived from dynamic occlusion, the magnitude of depth was determined only by motion parallax.

Despite the similarities between binocular disparity and motion parallax, their depth thresholds differ. Rogers and Graham demonstrated that while the depth-sensitivity curves across spatial frequencies shared the same inverted U-shape, their absolute values were not identical. Of the three subjects, two were approximately twice as sensitive to depth from binocular disparity as from a comparable amount of motion

parallax (Ellard et al., 1986). While Rogers and Graham (1982) did not provide any possible reasons for the lower sensitivity to motion parallax among their two subjects, it might be attributed to the lack of practice in estimating depth from motion parallax. The present study aimed to test the hypothesis that uniocular subjects, with years of experience relying on motion parallax cues, would achieve a more accurate depth estimation in identifying a structure-from-motion than controls viewing monocularly.

5.2.2 Methods

5.2.2.1 Stimulus

The stimulus contained 14 continuous long rows of random white dots on a black background (**Figure 5.4**), extending beyond the 14" display screen. The random dots were presented at the centre of a gamma-calibrated LCD monitor (1680X1050 pixel resolution, 60 Hz refresh rate) and were controlled using the Psychtoolbox-3 interface of MATLAB (R2016a; The MathWorks, Natick, USA).

Motion parallax was generated by inducing relative velocity differentials among rows of random dots. To simulate the perspective change that would be produced by a single 3D triangular prism, the horizontal dot positions were carried by the product of a horizontally oriented, triangular wave. In the present experiment, a single cycle of triangular wave, corresponding to a spatial frequency of 0.3 cpd was used, such that a single apex of a triangular prism appeared to pop out of the screen, with its base fixed on the monitor screen. Figure 5.4 shows a cross-sectional view of the stimuli. To provide a stable depth sign (near vs far), a luminance gradient was applied that mimicked the same triangular wave, since brighter luminance is generally perceived as protruding forwards (O'Shea et al., 1994). With an assumption that the light source is on the observer's side and shining directly on the apex of the triangle, the brighter

luminance was at the rows representing the apex of the triangle with a gradual decrease in luminance towards the base.

Two characteristics of motion parallax stimulus were free to be manipulated. Firstly, depending on the viewing eye, the motion of the dots was either towards the right or left ensuring that the optic flow was always temporalward. This was done to ensure that the asymmetry in direction discrimination in motion as noted among uniocular individuals does not act as a confounding factor (Steeves et al., 2002). Second, a consistent luminance gradient alongside varying motion parallax signals across trials could create a cue-conflict situation. To mitigate this, we designed a condition where the luminance gradient changed in tandem with motion parallax. [Motion parallax video](#) provides a demo of the stimulus when the dots were moving rightward with a covarying luminance gradient.

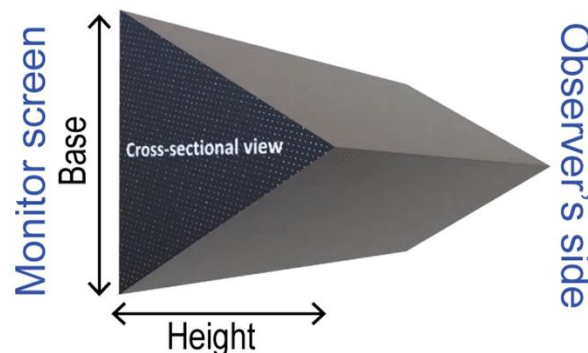


Figure 5.4 representative image showing a cross-sectional view of the triangular prism that would pop out of the monitor screen, when the stimulus starts to move. The base of the triangle was equivalent to the vertical width of the 14 rows of dots. The height of the triangle was based on depth seen with motion parallax.

5.2.2.2 Procedure

The participants were seated 1.88 m away from the monitor in a dark room so that the edge of the monitor was not visible. The psychophysical procedure was based on the method of adjustment, where the participants were asked to judge and compare the height (depth) with the base of the triangle. Every control participant performed the task monocularly, with the other eye occluded randomly. The subjects were asked to adjust the height to various sizes of the triangle as will be discussed in the next section. The start of each presentation was marked by a dull sound followed by the moving dot image and the end was marked by a sharper sound. After the sharp sound, the participant was asked to either increase or decrease the height by pressing the keys on the keyboard. Initially, the observers were presented with random dots with a random peak velocity level, based on which they were asked to increase or decrease the depth by pressing the assigned keys on a keyboard, to adjust the height (depth) of the triangle. The keys “P”, “L” and “M” increased the peak velocity in steps of 25%, 5%, and 1%, respectively, in increments based on the average horizontal distance between the dots divided by the reciprocal of the refresh rate (1/60th of a second). Conversely, the keys “Q,” “A,” and “Z” decreased the peak velocity by 25%, 5%, and 1%, respectively. The keys were attached with bump dots so that the participants could feel the keys in the darkness.

The criterion for which the participants adjusted the depth/height of the stimulus were:

Criterion 1. Just noticeable depth (the minimum speed difference required to see the depth) — seen as a bump and not necessarily as a triangle.

Criterion 2. Height of the triangle = Half the base

Criterion 3. Height of the triangle = Base

Criterion 4. Height of the triangle = Double the base

These 4 conditions along with the constant or covarying luminance gradient condition were repeated 3 times (4 conditions X 2 luminance gradient conditions X 3 repetitions = 24 trials), all randomly. Before the actual experiment, the stimulus was shown to the participants to confirm that the triangle was visible. Three-dimensional models of the three triangles were shown by placing them on the monitor screen to make the participant aware of what the stimulus would look like. Once they confirmed that they were able to see the triangle, at least 3 practice sessions were given, to get familiarised with the stimulus. The practice sessions were increased if the participants felt they wanted more practice.

5.2.3 Results

We enrolled 7 binocular controls and 5 uniocular individuals (20-30 years age group, with enucleation done at an early to late stage of life) for the study. The 7 binocular controls were recruited from the laboratory, out of which two were well acquainted with the stimulus having gone through the earlier versions of the stimuli. The rest of the 5 individuals were naïve with the experimental setup and the concept of depth from motion parallax. They never viewed the earlier versions of the stimulus during the developing process either and this was the first time they viewed the stimuli. However, they might be familiar with viewing 3D in random-dot stereograms as they might have participated in other experiments in the lab.

Out of the 7 control participants, 2 participants reported an absence of depth in the stimulus. As a quality check to know if the stimulus can generate the perception of depth, we expected to qualitatively see that the depth modulation increases as the

criterion for the height of the triangle increases. The five participants who were able to perceive the triangular structure were also able to demonstrate the expected trend. However, the absolute value of the depth modulation required to achieve that depth height varied substantially between participants (Figure 5.5 A-E). The depth modulations with a constant luminance gradient did not seem to be any different from the covarying luminance gradient (Figure 5.5 A-E).

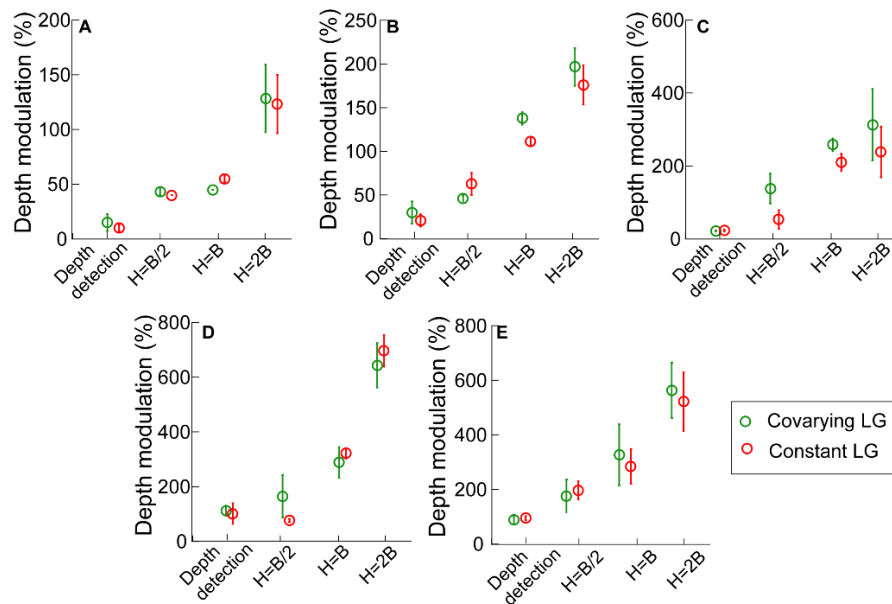


Figure 5.5 shows the depth modulation in percentage for the four depth criteria: depth detection, the height of the triangle = half the base of the triangle ($H=B/2$), the height of the triangle = base of the triangle ($H=B$), and height of triangle = double the base of the triangle ($H=2B$). Panel A-E, shows the results of the 5 control subjects. The y-axis limits are different to showcase the trend of increase in depth modulation with the increase in the depth criterion.

Interestingly, none of the 5 uniocular participants reported any presence of a triangular structure popping out of the monitor, nor any sort of depth in the stimulus. Instead, all participants noted that the rows of dots around the centre of the screen moved faster than the ones at the top and the bottom edges. Their ability to detect relative motion remained intact, as demonstrated through the two-finger test, where they correctly

identified the closer finger as the one moving faster. This analogy was used to explain that the faster-moving rows of dots would typically be perceived as projecting outward from the screen. Participants were given ample time to observe the stimulus and report any presence of depth perception. However, no such perception was reported!

5.2.4 Discussion

5.2.4.1 Summary

While the controls with one eye closed transiently could view the 3D structure depicted by the motion parallax, the uniocular individuals reported the absence of any sense of depth. We had hypothesised that if monocular depth cues were indeed functional and being used for performing perceptual depth-related tasks, it should lead to better identification of the height of the triangle compared to the monocular viewing of controls. Contrary to our expectations, the uniocular individuals denied the presence of a 3D structure, no matter what we did.

5.2.4.2 *Possible reason for uniocular individuals to not be able to view structure-from-motion*

There can be two possible reasons why the uniocular individuals did not report perceiving depth in the stimulus. Firstly, the uniocular participants were naïve to such tasks and may be unable to understand how the structure should appear and the “naïve” control may not be completely naïve. All the controls were enrolled from the laboratory and were all trained as an optometrist. So, most of them might be quite aware of words like “depth”, “3D”, and “pop-out”, which the uniocular individuals may not be acquainted with. However, to overcome this problem, the 3D models of the triangle were used to demonstrate and provide a visual representation of what the structure would appear to be. If the lack of experience and inability to understand the “pop-out” effect were a contributing factor to their difficulty in perceiving depth from

motion parallax, our keratoconic participants were also unfamiliar with random-dot stereograms, yet they understood the task and were able to perform it. However, before making a conclusive statement about the inability to use motion parallax for depth perception, when binocularity is completely lost, naïve controls need to be examined thoroughly, ideally, the uniocular participant's attendees to match for the same socio-economic and educational status. Also due to the lack of familiarity, it might be possible that the structure-from-motion was not visible on a virtual screen, but motion parallax might be helpful for familiar objects.

Secondly, depth estimations from motion parallax require the brain to assume some constraints like the rigidity of the structure. To perceive the 3D triangular shape on a virtual screen, the brain must assume that the random dots belong to a rigid structure and be able to bind all the visual features together (Todd, 1982). This task requires higher-order brain functioning that is shown to be permanently impaired if visual development is hampered in early infancy for a duration of 5 months or more (Putzar et al., 2007). While Gonzalez et al. (1989) reported global 2D shape discrimination is intact among the uniocular subjects, the perception of a 3D may require more complex higher visual functions. A similar impairment might exist due to long-term deprivation of binocular vision and provide a reason why the motion parallax might not support structure-from-motion.

Thirdly, the other reason can be that the uniocular individual really cannot derive any depth information from motion parallax cues. To derive estimates of depth from motion parallax, there are three key components in it. 1) Information related to the motion from the retina (Rogers & Graham, 1979). 2) Extra-retinal information from self-motion (e.g. Pursuits and vestibular information) (Nawrot, 2003b). 3) the neural integrity needs to be present to process and unify this information as a single-depth output (Nadler et

al., 2013). Uniocular individuals are noted to have higher thresholds for temporalward motion coherence relative to nasalward motion (Steeves et al., 2002). However, the thresholds for nasalward movement for both uniocular and control subjects are the same. Our stimulus also moved nasalward for both uniocular participants and controls. Thus, it does not seem to be a reason for the inability to perceive depth. Gonzalez et al. (2014) investigated the relative motion perception and pursuits among uniocular individuals. In their relative motion task, the top and bottom parts of a square were filled with random dots and were made to move at different speeds. Subjects were asked to respond to which section of dots moved faster while maintaining fixation at a red dot at the centre of the square. They found that the thresholds for detecting differences in speed were higher in uniocular compared to monocular and binocular viewing of controls. In their pursuit task, the subjects were asked to track a moving white dot. The pursuit gain remained unaffected between the three viewing conditions. However, relative speed detection and extra-retinal information are not necessary to perceive the presence of depth (Rogers & Graham, 1979), but they are necessary to derive a depth unambiguous estimate. Thus, this also does not completely explain why the uniocular reported no depth in our experiment. The last option is that the inactivation of neurons through binocular disparity, somehow also leads to inactivation by motion parallax. This seems to agree with the joint loss theory of Thompson and Nawrot (1999), where they demonstrated that higher thresholds for depth perception from retinal disparity also resulted in higher thresholds for depth perception from motion parallax. The current results along with our earlier finding of increased head movements without added advantage in the dynamic buzz-wire task may support the joint loss theory. However, these theories can only be assumed and will require future studies to confirm if the visual system undergoes a joint loss.

5.2.4.3 Effect of luminance gradient in the perception of structure-in-motion

In one of our earlier pilot studies using the same stimulus but without a luminance gradient, participants frequently reported perceiving the triangle as "popping in" rather than maintaining a stable "popping out" depth order. O'Shea et al. (1994) demonstrated that shading alone, or in combination with a conflicting relative size cue, served as a strong determinant of depth order. Based on this evidence, we introduced a luminance gradient to promote a stable "popping out" percept of the triangle. However, a constant luminance gradient introduces the potential for a cue-conflict scenario between the luminance gradient and motion parallax. To investigate this, we incorporated a covarying luminance condition.

The results indicate that none of the participants reported depth reversals in either stimulus condition. Additionally, there was no significant difference in depth modulation between the constant and covarying luminance gradient conditions (Figure 5.5, green and red dots), suggesting that luminance gradient and motion parallax cues were not additive in generating depth perception. However, since we did not test these five participants on motion parallax-only or luminance gradient-only stimuli, we cannot confirm whether any additive effect of the luminance gradient exists. If at all, the presence of a luminance gradient appeared to stabilize the depth order, which may suggest a modified weak fusion model of cue combination, wherein depth cues promote each other for veridical depth estimation. The previously ambiguous depth order became unambiguous in the presence of a luminance gradient.

5.2.4.4 Modifications to the experimental paradigm

The current experimental setup was developed based on the assumption that uniocular individuals can perceive depth from motion parallax. Consequently, the design focused on evaluating their ability to extract structure-from-motion. Since the

uniocular individuals failed to perceive any structure in the current study, we will have to first test our assumption that uniocular individuals can indeed perceive depth purely from motion parallax cues.

To address this, our initial step will be to recreate our stereo threshold stimuli described in Chapter 4, replacing binocular disparity cues with motion parallax cues. The stimuli will consist of random dot patterns, within which a bar will appear to pop out in depth. The depth will be modulated either by the observer's head movements or by programming the display to replicate the relative motion on the screen. The participant's task will be to identify the direction of the bar's displacement in depth.

Chapter 6 General summary and discussion

6.1 Summary of results

The 3D world is a composite of binocular and monocular depth cues. The usage of these depth cues is related to the task. The dissertation is based on the possibility of compensatory mechanisms of visual senses in particular by motion parallax for the perception of depth when binocularity is either absent or degraded. To test this, we explored depth perception for depth-related visuomotor tasks and perceptual tasks in case of absence and reduced binocularity. We opted for uniocular individuals and individuals with keratoconus as a model to study the impact of absence and reduced binocularity respectively. The results from the four experiments are summarised below.

Chapter 3:

- i) Error rates and speed of the uniocular participants in the buzz-wire task were no different from the monocular viewing of the binocular controls (Figure 3.3; Table 3-2; Sections 1 and 2).
- ii) The error rates significantly decreased with age and flattened after 16 years (Figure 3.4A – C; Table 3-3).
- iii) Error rates were not related to the duration of uniocularity (Figure 3.4D – E; Table 3-3).
- iv) Higher error rates were made when the participants had to transition from the straight to the curve section or vice-versa. The error rates decreased when the depth modulations were removed and the wire was straightened out (Figure 3.7).

- v) Larger translational head movements were made without additional benefit in the task and error rates remained similar upon restricting the head movements (Figure 3.6 and Figure 3.8 Table 3-2).

Chapter 4:

- i) Reduced binocularity resulted in higher error rates in the buzz-wire task, however, cases with relatively low monocular error rates showed a binocular advantage from binocular viewing and cases with high monocular error rates also had higher error rates when viewing the buzz wire binocularly (Figure 3A).
- ii) An improvement in the retinal image quality of cases with rigid contact lens wear reduced the binocular error rates in the buzz-wire task, relative to the spectacles (Figure 5B).
- iii) The stereo threshold was poorly correlated with the binocular advantage in error rate amongst the participants within each cohort and also poorly correlated with the reduction in error rate with the switch from spectacle to contact lenses (Figure 5C).
- iv) Controls, uncorrected myopes and cases executed the buzz-wire task faster under binocular than monocular conditions (Figures 3B and 6B). However, the magnitude of speed reduction from binocular to monocular viewing was smaller in cases than in the controls and uncorrected myopes (Figures 3B and 6B).

Chapter 5

- i) While the performance of uniocular participants was similar to the monocular viewing of controls, they were better in the perceptual task of detecting the same gap between the loop and the wire.

- ii) Uniocular cases spontaneously made larger head movements compared to the monocular viewing of controls.
- iii) The detection sensitivity was not correlated to the duration of uniocularity.
- iv) In the motion parallax experiment, the control participants were able to increase the depth modulations as the depth criteria increased.
- v) Uniocular individuals did not report seeing any depth in the stimuli but could report the presence of relative motion.

6.2 Contribution to science

The work done as a part of the PhD addresses the impact of absence and reduced binocularity on a visuomotor and a perceptually equivalent task requiring the estimation of depth. A pilot study on the perception of structure-from-motion experiment was also conducted to determine whether the absence of binocularity enhances the estimation of depth from motion parallax. Essentially the work tried to understand the role of monocular depth cues under different circumstances — dynamic depth-related visuomotor task, static perceptual depth-related task, and structure-from-motion.

Collectively, the findings provide evidence of impaired depth perception in visuomotor tasks for individuals with both absent and degraded binocularity when compared to binocular viewing of controls. However, while performance deficits were evident in the visuomotor task for those with absent binocularity, the same was not observed in the perceptual equivalent task. This suggests that monocular depth cues are insufficient for dynamic visuomotor tasks that require absolute and relative depth estimations and that the larger head movements exhibited by uniocular individuals did not compensate for their lack of binocular disparity. In contrast, monocular cues appeared to support ordinal depth estimations, allowing uniocular individuals to perform better than

binocular controls under monocular viewing conditions. The increased head movements observed in this task may have facilitated depth perception via dynamic occlusion, rather than motion parallax. The findings from the pilot study further suggest that in the absence of binocularity, the perception of structure-from-motion is also disrupted. This might challenge the conventional assumption that motion parallax can compensate for the loss of binocular disparity.

These findings lay an important foundation for rehabilitation strategies, starting from identifying the specific challenges faced by individuals with compromised binocularity, counselling patients and family regarding the surgery or the progression of the disease will have on their day-to-day life activities and guiding them for career choices based on functional abilities. Previous suggestions to train uniocular individuals to make larger head movements to extract depth information from motion parallax do not seem to be a useful suggestion as our pilot study indicates that motion parallax may be jointly impaired alongside binocular disparity, with other monocular cues potentially being enhanced over time as compensatory mechanisms.

Another key contribution is that in cases of reduced binocularity, neither disease severity nor conventional clinical measures such as high-contrast visual acuity or stereoacuity were reliable predictors of visuomotor limitations. This highlights the limitations of these standard assessments in capturing the real-world visual experience of patients. It also underscores the need to expand clinical evaluation protocols to include tasks that simulate complex activities of daily living.

6.3 Future direction

While the results address a few gaps in the literature, it opens Pandora's box of new questions. Two critical directions for future research are outlined below.

6.3.1 Neural Adaptation and Motion Parallax in the Absence of Binocularity

A fundamental question emerging from this work is related to the developmental timeline for depth perception through motion parallax. Firstly, if the absence of binocularity occurs during the critical period (e.g., in cases of microphthalmos or congenital cataract, enucleation etc), does the complete lack of experience with binocular disparity inherently lead to impaired depth perception from motion parallax?

Moreover, in cases where binocularity is later restored—such as through cataract surgery—does the ability to extract depth from motion parallax recover alongside improvements in stereoacuity? While an improvement in motion parallax will indicate that the neurons for binocular disparity and motion parallax are indeed linked, failure to see depth from motion parallax would indicate that prior experience of motion parallax is required to perceive depth from motion parallax.

6.3.2 Compensatory Monocular Cues and Training Strategies

If motion parallax does not effectively compensate for the absence of binocularity, identifying alternative monocular cues that could be trained or enhanced for depth estimation becomes crucial. However, the utility of different monocular cues may vary depending on the nature of the task. Future studies should investigate whether monocular cues (e.g., occlusion, texture, perspective etc) can be harnessed to improve functional depth perception in individuals with compromised binocularity. These findings could inform the development of targeted training strategies aimed at enhancing depth perception in unocular individuals.

6.4 Conclusion

While the mechanisms of depth perception from binocular and monocular cues have been extensively studied, the consequences of losing these depth cues and the compensatory adaptations of the visual system remain largely unexplored. We found no evidence to suggest that monocular depth cues alone can provide reliable absolute or relative depth estimates, as the addition of binocular depth cues provides. However, in tasks requiring only ordinal depth judgments—particularly those of a perceptual nature—monocular cues appear to undergo adaptation, allowing for some level of preserved depth perception. Our early findings suggest that when binocular depth cues are lost, motion parallax does not serve as a compensatory mechanism; rather, depth estimation from motion parallax appears to be jointly impaired.

To conclude, exactly 100 years ago, in 1925, Helmholtz described depth from motion parallax as being perceived “just as if he were looking at a good stereoscopic view of it”(Von Helmholtz, 1925). However, our pilot study suggests that this description does not hold for uniocular individuals. Or it does in the sense that they are equally poor in both!

References

- Aiello, F., Gallo Afflitto, G., Ceccarelli, F., Garziona, F., Pocobelli, G., Pinci, C., . . . Nucci, C. (2024). Keratoconus and personality traits: A case-control study. *Cornea*, 43(2), 237-244. <https://doi.org/10.1097/ICO.0000000000003284>
- Amos, B., Ludwiczuk, B., & Satyanarayanan, M. (2016). *Openface: A general-purpose face recognition library with mobile applications* (CMU-CS-16-118, Issue).
- Backus, B. T., Banks, M. S., van Ee, R., & Crowell, J. A. (1999). Horizontal and vertical disparity, eye position, and stereoscopic slant perception. *Vision Res*, 39(6), 1143-1170. [https://doi.org/10.1016/s0042-6989\(98\)00139-4](https://doi.org/10.1016/s0042-6989(98)00139-4)
- Barry, S. R., & Bridgeman, B. (2017). An Assessment of Stereovision Acquired in Adulthood. *Optometry and Vision Science*, 94(10). https://journals.lww.com/optvissci/fulltext/2017/10000/an_assessment_of_stereovision_acquired_in.10.aspx
- Bayes, T. (1991). An essay towards solving a problem in the doctrine of chances. 1763. *MD Comput*, 8(3), 157-171. <https://www.ncbi.nlm.nih.gov/pubmed/1857193>
- Bharadwaj, S. R., & Candy, T. R. (2009). Accommodative and vergence responses to conflicting blur and disparity stimuli during development. *J Vis*, 9(11), 4 1-18. <https://doi.org/10.1167/9.11.4>
- Bradshaw, M. F., Elliott, K. M., Watt, S. J., Hibbard, P. B., Davies, I. R., & Simpson, P. J. (2004). Binocular cues and the control of prehension. *Spat Vis*, 17(1-2), 95-110. <https://doi.org/10.1163/156856804322778288>
- Bradshaw, M. F., Parton, A. D., & Glennerster, A. (2000). The task-dependent use of binocular disparity and motion parallax information. *Vision Res*, 40(27), 3725-3734. [https://doi.org/10.1016/s0042-6989\(00\)00214-5](https://doi.org/10.1016/s0042-6989(00)00214-5)
- Bradshaw, M. F., & Rogers, B. J. (1996). The interaction of binocular disparity and motion parallax in the computation of depth. *Vision Res*, 36(21), 3457-3468. [https://doi.org/10.1016/0042-6989\(96\)00072-7](https://doi.org/10.1016/0042-6989(96)00072-7)
- Brainard, D. H. (1997). The Psychophysics Toolbox. *Spat Vis*, 10(4), 433-436. <https://www.ncbi.nlm.nih.gov/pubmed/9176952>
- Castiello, U. (2005). The neuroscience of grasping. *Nature Reviews Neuroscience*, 6(9), 726-736.
- Cavina-Pratesi, C., Goodale, M. A., & Culham, J. C. (2007). fMRI reveals a dissociation between grasping and perceiving the size of real 3D objects. *PLoS One*, 2(5), e424.
- Cheng, H., Barnett, J. K., Vilupuru, A. S., Marsack, J. D., Kasthurirangan, S., Applegate, R. A., & Roorda, A. (2004). A population study on changes in wave aberrations with accommodation. *J Vis*, 4(4), 272-280. <https://doi.org/10.1167/4.4.3>
- Chopin, A., Bavelier, D., & Levi, D. M. (2019). The prevalence and diagnosis of 'stereoblindness' in adults less than 60 years of age: a best evidence synthesis. *Ophthalmic Physiol Opt*, 39(2), 66-85. <https://doi.org/10.1111/opo.12607>
- Cohen, J. (1988). *Statistical power analysis for the behavioral sciences* (2 ed.). Hillsdale, NJ: Lawrence Erlbaum Associates, Publishers.
- Crawford, M. L., Blake, R., Cool, S. J., & von Noorden, G. K. (1975). Physiological consequences of unilateral and bilateral eye closure in macaque monkeys:

- some further observations. *Brain Res*, 84(1), 150-154. [https://doi.org/10.1016/0006-8993\(75\)90809-4](https://doi.org/10.1016/0006-8993(75)90809-4)
- Cutting, J. E., & Millard, R. T. (1984). Three gradients and the perception of flat and curved surfaces. *J Exp Psychol Gen*, 113(2), 198-216. <https://www.ncbi.nlm.nih.gov/pubmed/6242750>
- Dandapani, S. A., Padmanabhan, P., & Hussaindeen, J. R. (2020). Spectrum of binocular vision anomalies in keratoconus subjects. *Optom Vis Sci*, 97(6), 424-428. <https://doi.org/10.1097/OPX.0000000000001517>
- Darwin, C., & Beer, G. (1951). *The origin of species* (Vol. 71). Dent.
- Davis, L. J., Schechtman, K. B., Begley, C. G., Shin, J. A., & Zadnik, K. (1998). Repeatability of refraction and corrected visual acuity in keratoconus. The CLEK Study Group. Collaborative Longitudinal Evaluation of Keratoconus. *Optom Vis Sci*, 75(12), 887-896. <https://doi.org/10.1097/00006324-199812000-00011>
- de Vries, S. C., & Werkhoven, P. (1995). Cross-modal slant and curvature matching of stereo- and motion-induced surfaces. *Percept Psychophys*, 57(8), 1175-1186. <https://doi.org/10.3758/bf03208373>
- Deshmukh, R., Ong, Z. Z., Rampat, R., Alio Del Barrio, J. L., Barua, A., Ang, M., . . . Ting, D. S. J. (2023). Management of keratoconus: an updated review. *Front Med (Lausanne)*, 10, 1212314. <https://doi.org/10.3389/fmed.2023.1212314>
- Devi, P., Kumar, P., & Bharadwaj, S. R. (2023). Computational analysis of retinal image quality with different contact lens designs in keratoconus. *Cont Lens Anterior Eye*, 46(2), 101794. <https://doi.org/10.1016/j.clae.2022.101794>
- Devi, P., Kumar, P., Marella, B. L., & Bharadwaj, S. R. (2022). Impact of degraded optics on monocular and binocular vision: Lessons from recent advances in highly-aberrated eyes. *Semin Ophthalmol*, 37(7-8), 869-886. <https://doi.org/10.1080/08820538.2022.2094711>
- Ding, J., Lu, H. H., & Levi, D. M. (2024). Absolute and relative disparity mechanisms revealed by an equivalent noise analysis. *Sci Rep*, 14(1), 6863. <https://doi.org/10.1038/s41598-024-57406-2>
- Downie, L. E., & Lindsay, R. G. (2015). Contact lens management of keratoconus. *Clin Exp Optom*, 98(4), 299-311. <https://doi.org/10.1111/cxo.12300>
- Ellard, C. G., Goodale, M. A., Scorfield, D. M., & Lawrence, C. (1986). Visual cortical lesions abolish the use of motion parallax in the Mongolian gerbil. *Experimental Brain Research*, 64(3), 599-602. <https://doi.org/10.1007/BF00340498>
- Ernst, M. O. (2008). Multisensory integration: a late bloomer. *Curr Biol*, 18(12), R519-521. <https://doi.org/10.1016/j.cub.2008.05.002>
- Faul, F., Erdfelder, E., Lang, A.-G., & Buchner, A. J. B. r. m. (2007). G* Power 3: A flexible statistical power analysis program for the social, behavioral, and biomedical sciences. 39(2), 175-191.
- Ferdi, A. C., Nguyen, V., Gore, D. M., Allan, B. D., Rozema, J. J., & Watson, S. L. (2019). Keratoconus natural progression: A systematic review and meta-analysis of 11 529 eyes. *Ophthalmology*, 126(7), 935-945. <https://doi.org/10.1016/j.ophtha.2019.02.029>
- Fielder, A. R., & Moseley, M. J. (1996). Does stereopsis matter in humans? *Eye (Lond)*, 10(2), 233-238.
- Gibson, E. J., Gibson, J. J., Smith, O. W., & Flock, H. (1959). Motion parallax as a determinant of perceived depth. *J Exp Psychol*, 58(1), 40-51. <https://doi.org/10.1037/h0043883>

- Gillay, Z. (25 Aug 2022). Plot ellipse on scattered 2D data. <https://in.mathworks.com/matlabcentral/fileexchange/116610-plot-ellipse-on-scattered-2d-data> Accessed on 10 Sept 2024.
- Gonzalez, E., Steinbach, M., Ono, H., & Wolf, M. (1989). Depth perception in children enucleated at an early age. *Clinical Vision Sciences*, 4(2), 173-177.
- Gonzalez, E. G., Lillakas, L., Greenwald, N., Gallie, B. L., & Steinbach, M. J. (2014). Unaffected smooth pursuit but impaired motion perception in monocularly enucleated observers. *Vision Res*, 101, 151-157. <https://doi.org/10.1016/j.visres.2014.06.014>
- Goodale, M. A., Milner, A. D., Jakobson, L. S., & Carey, D. P. J. N. (1991). A neurological dissociation between perceiving objects and grasping them. 349(6305), 154-156.
- Goodale, M. A., & Milner, A. D. J. T. i. n. (1992). Separate visual pathways for perception and action. 15(1), 20-25.
- Gori, M., Del Viva, M., Sandini, G., & Burr, D. C. J. C. B. (2008). Young children do not integrate visual and haptic form information. 18(9), 694-698.
- Gothwal, V. K., Gujar, R., Sharma, S., Begum, N., & Pesudovs, K. (2022). Factors affecting quality of life in keratoconus. *Ophthalmic Physiol Opt*, 42(5), 986-997. <https://doi.org/10.1111/opo.13010>
- Grant, S., Melmoth, D. R., Morgan, M. J., & Finlay, A. L. (2007). Prehension deficits in amblyopia. *Investigative ophthalmology visual science*, 48(3), 1139-1148.
- Grant, S., Suttle, C., Melmoth, D. R., Conway, M. L., & Sloper, J. J. (2014). Age- and stereovision-dependent eye-hand coordination deficits in children with amblyopia and abnormal binocularity. *Invest Ophthalmol Vis Sci*, 55(9), 5687-57015. <https://doi.org/10.1167/iovs.14-14745>
- Haefner, R. M., Gerwinn, S., Macke, J. H., & Bethge, M. (2013). Inferring decoding strategies from choice probabilities in the presence of correlated variability. *Nat Neurosci*, 16(2), 235-242. <https://doi.org/10.1038/nn.3309>
- Hashemi, H., Beiranvand, A., Yekta, A., Maleki, A., Yazdani, N., & Khabazkhoob, M. (2016). Pentacam top indices for diagnosing subclinical and definite keratoconus. *J Curr Ophthalmol*, 28(1), 21-26. <https://doi.org/10.1016/j.joco.2016.01.009>
- Hell, W. (1978). Movement parallax: an asymptotic function of amplitude and velocity of head motion. *Vision Res*, 18(6), 629-635. [https://doi.org/10.1016/0042-6989\(78\)90142-6](https://doi.org/10.1016/0042-6989(78)90142-6)
- Hillis, J. M., Watt, S. J., Landy, M. S., & Banks, M. S. (2004). Slant from texture and disparity cues: optimal cue combination. *J Vis*, 4(12), 967-992. <https://doi.org/10.1167/4.12.1>
- Horton, J. C., & Hocking, D. R. (1998). Effect of early monocular enucleation upon ocular dominance columns and cytochrome oxidase activity in monkey and human visual cortex. *Vis Neurosci*, 15(2), 289-303. <https://doi.org/10.1017/s0952523898152124>
- Howard, I. P., & Rogers, B. J. (2002). *Seeing in depth, Vol. 2: Depth perception*. University of Toronto Press.
- Hubel, D. H. (1995). *Eye, brain, and vision*. Scientific American Library/Scientific American Books.
- Hubel, D. H., Wiesel, T. N., & LeVay, S. (1977). Plasticity of ocular dominance columns in monkey striate cortex. *Philos Trans R Soc Lond B Biol Sci*, 278(961), 377-409. <https://doi.org/10.1098/rstb.1977.0050>

- Jaskulski M, T. L., Bradley A, Kollbaum P. (2019). *IRIS – Indiana Retinal Image Simulator*. <https://blogs.iu.edu/corl/iris>.
- Jeannerod, M. (1986). Mechanisms of visuomotor coordination: a study in normal and brain-damaged subjects. *Neuropsychologia*, 24(1), 41-78. [https://doi.org/10.1016/0028-3932\(86\)90042-4](https://doi.org/10.1016/0028-3932(86)90042-4)
- Jinabhai, A., O'Donnell, C., & Radhakrishnan, H. (2012). Changes in refraction, ocular aberrations, and corneal structure after suspending rigid gas-permeable contact lens wear in keratoconus. *Cornea*, 31(5), 500-508. <https://doi.org/10.1097/ICO.0b013e31820f777b>
- Johnston, E. B., Cumming, B. G., & Landy, M. S. (1994). Integration of stereopsis and motion shape cues. *Vision Res*, 34(17), 2259-2275. [https://doi.org/10.1016/0042-6989\(94\)90106-6](https://doi.org/10.1016/0042-6989(94)90106-6)
- Johnston, E. B., Cumming, B. G., & Parker, A. J. (1993). Integration of depth modules: stereopsis and texture. *Vision Res*, 33(5-6), 813-826. [https://doi.org/10.1016/0042-6989\(93\)90200-g](https://doi.org/10.1016/0042-6989(93)90200-g)
- Jones, R. K., & Lee, D. N. (1981). Why two eyes are better than one: the two views of binocular vision. *J Exp Psychol Hum Percept Perform*, 7(1), 30-40. <https://doi.org/10.1037//0096-1523.7.1.30>
- Joy, S., Davis, H., & Buckkley, D. (2001). Is stereopsis linked to hand-eye coordination? *The British Orthoptic Journal*, 58, 38-41.
- Julesz, B. (1960). Binocular depth perception of computer-generated patterns. *Bell System Technical Journal*, 39(5), 1125-1162.
- Kandel, E. R., Schwartz, J. H., & Jessell, T. (2000). *Principles of neural science, Fourth Edition*. McGraw-Hill Companies, Incorporated. <https://books.google.co.in/books?id=yzEFK7Xc87YC>
- Keefe, B. D., Hibbard, P. B., & Watt, S. J. (2011). Depth-cue integration in grasp programming: no evidence for a binocular specialism. *Neuropsychologia*, 49(5), 1246-1257. <https://doi.org/10.1016/j.neuropsychologia.2011.02.047>
- Keefe, B. D., & Watt, S. J. (2017). Viewing geometry determines the contribution of binocular vision to the online control of grasping. *Exp Brain Res*, 235(12), 3631-3643. <https://doi.org/10.1007/s00221-017-5087-0>
- Kelly, K. R., Morale, S. E., Beauchamp, C. L., Dao, L. M., Luu, B. A., & Birch, E. E. (2020). Factors Associated with Impaired Motor Skills in Strabismic and Anisometropic Children. *Invest Ophthalmol Vis Sci*, 61(10), 43. <https://doi.org/10.1167/iovs.61.10.43>
- Kim, H. R., Angelaki, D. E., & DeAngelis, G. C. (2016). The neural basis of depth perception from motion parallax. *Philos Trans R Soc Lond B Biol Sci*, 371(1697). <https://doi.org/10.1098/rstb.2015.0256>
- Kivelä, T. (2009). The epidemiological challenge of the most frequent eye cancer: retinoblastoma, an issue of birth and death. 93(9), 1129-1131. <https://doi.org/10.1136/bjo.2008.150292> %J British Journal of Ophthalmology
- Knill, D. C. (2005). Reaching for visual cues to depth: the brain combines depth cues differently for motor control and perception. *Journal of Vision*, 5(2), 103-115. <https://doi.org/10.1167/5.2.2>
- Knill, D. C. (2007). Robust cue integration: a Bayesian model and evidence from cue-conflict studies with stereoscopic and figure cues to slant. *J Vis*, 7(7), 5 1-24. <https://doi.org/10.1167/7.7.5>

- Knill, D. C., & Saunders, J. A. (2003). Do humans optimally integrate stereo and texture information for judgments of surface slant? *Vision Res*, 43(24), 2539-2558. [https://doi.org/10.1016/s0042-6989\(03\)00458-9](https://doi.org/10.1016/s0042-6989(03)00458-9)
- Koenderink, J. J. (1986). Optic flow. *Vision Res*, 26(1), 161-179. [https://doi.org/10.1016/0042-6989\(86\)90078-7](https://doi.org/10.1016/0042-6989(86)90078-7)
- Kumano, H., & Uka, T. (2013). Neuronal mechanisms of visual perceptual learning. *Behav Brain Res*, 249, 75-80. <https://doi.org/10.1016/j.bbr.2013.04.034>
- Kumar, P., Campbell, P., Vaddavalli, P. K., Hull, C. C., & Bharadwaj, S. R. (2023). Structure-function relationship in keratoconus: Spatial and depth Vision. *Transl Vis Sci Technol*, 12(12), 21. <https://doi.org/10.1167/tvst.12.12.21>
- Landy, M. S., Maloney, L. T., Johnston, E. B., & Young, M. (1995). Measurement and modeling of depth cue combination: in defense of weak fusion. *Vision Res*, 35(3), 389-412. [https://doi.org/10.1016/0042-6989\(94\)00176-m](https://doi.org/10.1016/0042-6989(94)00176-m)
- Law, C. T., & Gold, J. I. (2008). Neural correlates of perceptual learning in a sensory-motor, but not a sensory, cortical area. *Nat Neurosci*, 11(4), 505-513. <https://doi.org/10.1038/nn2070>
- Levi, D. M., Knill, D. C., & Bavelier, D. (2015). Stereopsis and amblyopia: A mini-review. *Vision Res*, 114, 17-30. <https://doi.org/10.1016/j.visres.2015.01.002>
- MacLachlan, C., & Howland, H. C. (2002). Normal values and standard deviations for pupil diameter and interpupillary distance in subjects aged 1 month to 19 years. *Ophthalmic Physiol Opt*, 22(3), 175-182. <https://doi.org/10.1046/j.1475-1313.2002.00023.x>
- Mannis, M. J., Ling, J. J., Kyrillos, R., & Barnett, M. (2018). Keratoconus and personality-A Review. *Cornea*, 37(3), 400-404. <https://doi.org/10.1097/ICO.0000000000001479>
- Marella, B. L., Conway, M. L., Suttle, C., & Bharadwaj, S. R. (2021). Contrast rivalry paradigm reveals suppression of monocular input in keratoconus. *Invest Ophthalmol Vis Sci*, 62(2), 15. <https://doi.org/10.1167/iovs.62.2.12>
- Marella, B. L., Conway, M. L., Vaddavalli, P. K., Suttle, C. M., & Bharadwaj, S. R. (2024). Optical phase nullification partially restores visual and stereo acuity lost to simulated blur from higher-order wavefront aberrations of keratoconic eyes. *Vision Res*, 224, 108486. <https://doi.org/10.1016/j.visres.2024.108486>
- Marella, B. L., Vaddavalli, P. K., Reddy, J. C., Conway, M. L., Suttle, C. M., & Bharadwaj, S. R. (2023). Interocular contrast balancing partially improves stereoacuity in keratoconus. *Optom Vis Sci*, 100(4), 239-247. <https://doi.org/10.1097/OPX.0000000000002001>
- Marotta, J. J., Behrmann, M., & Goodale, M. A. (1997). The removal of binocular cues disrupts the calibration of grasping in patients with visual form agnosia. *Exp Brain Res*, 116(1), 113-121. <https://doi.org/10.1007/pl00005731>
- Marotta, J. J., Perrot, T. S., Nicolle, D., Servos, P., Servos, P., & Goodale, M. A. (1995). Adapting to monocular vision: grasping with one eye. *Exp Brain Res*, 104(1), 107-114. <https://doi.org/10.1007/BF00229860>
- Melmoth, D. R., Finlay, A. L., Morgan, M. J., & Grant, S. (2009). Grasping deficits and adaptations in adults with stereo vision losses. *Invest Ophthalmol Vis Sci*, 50(8), 3711-3720. <https://doi.org/10.1167/iovs.08-3229>
- Melmoth, D. R., & Grant, S. (2006). Advantages of binocular vision for the control of reaching and grasping. *Exp Brain Res*, 171(3), 371-388. <https://doi.org/10.1007/s00221-005-0273-x>

- Metlapally, S., Bharadwaj, S. R., Roorda, A., Nilagiri, V. K., Yu, T. T., & Schor, C. M. (2019). Binocular cross-correlation analyses of the effects of high-order aberrations on the stereoacuity of eyes with keratoconus. *J Vis*, 19(6), 12. <https://doi.org/10.1167/19.6.12>
- Milner, A. D. (1998). Neuropsychological studies of perception and visuomotor control. *Philos Trans R Soc Lond B Biol Sci*, 353(1373), 1375-1384. <https://doi.org/10.1098/rstb.1998.0291>
- Muftuoglu, O., Ayar, O., Hurmeric, V., Orucoglu, F., & Kilic, I. (2015). Comparison of multimetric D index with keratometric, pachymetric, and posterior elevation parameters in diagnosing subclinical keratoconus in fellow eyes of asymmetric keratoconus patients. *J Cataract Refract Surg*, 41(3), 557-565. <https://doi.org/10.1016/j.jcrs.2014.05.052>
- Murdoch, J., McGhee, C., & Glover, V. (1991). The relationship between stereopsis and fine manual dexterity: pilot study of a new instrument. *Eye*, 5(5), 642-643.
- Nadler, J. W., Barbash, D., Kim, H. R., Shimpi, S., Angelaki, D. E., & DeAngelis, G. C. (2013). Joint representation of depth from motion parallax and binocular disparity cues in macaque area MT. *J Neurosci*, 33(35), 14061-14074, 14074a. <https://doi.org/10.1523/JNEUROSCI.0251-13.2013>
- Nadler, J. W., Nawrot, M., Angelaki, D. E., & DeAngelis, G. C. (2009). MT neurons combine visual motion with a smooth eye movement signal to code depth-sign from motion parallax. *Neuron*, 63(4), 523-532. <https://doi.org/10.1016/j.neuron.2009.07.029>
- Nardini, M., Jones, P., Bedford, R., & Braddick, O. J. C. b. (2008). Development of cue integration in human navigation. 18(9), 689-693.
- Nawrot, M. (2003a). Depth from motion parallax scales with eye movement gain. *J Vis*, 3(11), 841-851. <https://doi.org/10.1167/3.11.17>
- Nawrot, M. (2003b). Eye movements provide the extra-retinal signal required for the perception of depth from motion parallax. *Vision Res*, 43(14), 1553-1562. [https://doi.org/10.1016/s0042-6989\(03\)00144-5](https://doi.org/10.1016/s0042-6989(03)00144-5)
- Nemanich, S. T., & Earhart, G. M. (2015). How do age and nature of the motor task influence visuomotor adaptation? *Gait Posture*, 42(4), 564-568. <https://doi.org/10.1016/j.gaitpost.2015.09.001>
- Niechwiej-Szwedo, E., Goltz, H. C., Chandrakumar, M., Hirji, Z., & Wong, A. M. (2011). Effects of anisometropic amblyopia on visuomotor behavior, III: Temporal eye-hand coordination during reaching. *Invest Ophthalmol Vis Sci*, 52(8), 5853-5861. <https://doi.org/10.1167/iovs.11-7314>
- Niechwiej-Szwedo, E., Goltz, H. C., Chandrakumar, M., & Wong, A. M. (2012). The effect of sensory uncertainty due to amblyopia (lazy eye) on the planning and execution of visually-guided 3D reaching movements. *PLoS One*, 7(2), e31075. <https://doi.org/10.1371/journal.pone.0031075>
- Nilagiri, V. K., Metlapally, S., Kalaiselvan, P., Schor, C. M., & Bharadwaj, S. R. (2018). LogMAR and stereoacuity in keratoconus corrected with spectacles and rigid gas-permeable contact lenses. *Optom Vis Sci*, 95(4), 391-398. <https://doi.org/10.1097/OPX.0000000000001205>
- Nilagiri, V. K., Metlapally, S., Schor, C. M., & Bharadwaj, S. R. (2020). A computational analysis of retinal image quality in eyes with keratoconus. *Sci Rep*, 10(1), 1321. <https://doi.org/10.1038/s41598-020-57993-w>

- O'Connor, A. R., Birch, E. E., Anderson, S., & Draper, H. (2010a). The functional significance of stereopsis. *Invest Ophthalmol Vis Sci*, 51(4), 2019-2023. <https://doi.org/10.1167/iovs.09-4434>
- O'Connor, A. R., Birch, E. E., Anderson, S., & Draper, H. (2010b). Relationship between binocular vision, visual acuity, and fine motor skills. *Optom Vis Sci*, 87(12), 942-947. <https://doi.org/10.1097/OPX.0b013e3181fd132e>
- O'Shea, R. P., Blackburn, S. G., & Ono, H. (1994). Contrast as a depth cue. *Vision Res*, 34(12), 1595-1604. [https://doi.org/10.1016/0042-6989\(94\)90116-3](https://doi.org/10.1016/0042-6989(94)90116-3)
- Ono, H., Rogers, B. J., Ohmi, M., & Ono, M. E. (1988). Dynamic occlusion and motion parallax in depth perception. *Perception*, 17(2), 255-266. <https://doi.org/10.1068/p170255>
- Ono, H., & Steinbach, M. J. (1990). Monocular stereopsis with and without head movement. *Percept Psychophys*, 48(2), 179-187. <https://doi.org/10.3758/bf03207085>
- Orban, G. A., Lagae, L., Verri, A., Raiguel, S., Xiao, D., Maes, H., & Torre, V. (1992). First-order analysis of optical flow in monkey brain. *Proc Natl Acad Sci U S A*, 89(7), 2595-2599. <https://doi.org/10.1073/pnas.89.7.2595>
- Pantanelli, S., MacRae, S., Jeong, T. M., & Yoon, G. (2007). Characterizing the wave aberration in eyes with keratoconus or penetrating keratoplasty using a high-dynamic range wavefront sensor. *Ophthalmology*, 114(11), 2013-2021. <https://doi.org/10.1016/j.ophtha.2007.01.008>
- Piano, M. E., & O'Connor, A. R. (2013). The effect of degrading binocular single vision on fine visuomotor skill task performance. *Invest Ophthalmol Vis Sci*, 54(13), 8204-8213. <https://doi.org/10.1167/iovs.12-10934>
- Putzar, L., Hotting, K., Rosler, F., & Roder, B. (2007). The development of visual feature binding processes after visual deprivation in early infancy. *Vision Res*, 47(20), 2616-2626. <https://doi.org/10.1016/j.visres.2007.07.002>
- Raasch, T. W., Schechtman, K. B., Davis, L. J., Zadnik, K., & Study, C. S. G. C. L. E. o. K. (2001). Repeatability of subjective refraction in myopic and keratoconic subjects: results of vector analysis. *Ophthalmic Physiol Opt*, 21(5), 376-383. <https://doi.org/10.1046/j.1475-1313.2001.00596.x>
- Rao, G., Massa, L., Schiavetti, I., Vagge, A., Nucci, P., Giorgia Perinelli, M., . . . Serafino, M. (2025). Relation between binocular vision alteration and prehension movements in children: a scoping review. *Graefes Arch Clin Exp Ophthalmol*, 263(1), 23-32. <https://doi.org/10.1007/s00417-024-06583-x>
- Read, J. C. (2015). Stereo vision and strabismus. *Eye (Lond)*, 29(2), 214-224. <https://doi.org/10.1038/eye.2014.279>
- Read, J. C., Begum, S. F., McDonald, A., & Trowbridge, J. (2013). The binocular advantage in visuomotor tasks involving tools. *Perception*, 42(2), 101-110. <https://doi.org/10.1068/i0565>
- Rogers, B. (2023). When is a disparity not a disparity? Toward an old theory of three-dimensional vision. *Perception*, 52(5), 20416695231202726. <https://doi.org/10.1177/20416695231202726>
- Rogers, B., & Graham, M. (1979). Motion parallax as an independent cue for depth perception. *Perception*, 8(2), 125-134. <https://doi.org/10.1068/p080125>
- Rogers, B., & Graham, M. (1982). Similarities between motion parallax and stereopsis in human depth perception. *Vision Res*, 22(2), 261-270. [https://doi.org/10.1016/0042-6989\(82\)90126-2](https://doi.org/10.1016/0042-6989(82)90126-2)

- Rogers, B. J., & Collett, T. S. (1989). The appearance of surfaces specified by motion parallax and binocular disparity. *Q J Exp Psychol A*, 41(4), 697-717. <https://doi.org/10.1080/14640748908402390>
- Roy, J. P., Komatsu, H., & Wurtz, R. H. (1992). Disparity sensitivity of neurons in monkey extrastriate area MST. *J Neurosci*, 12(7), 2478-2492. <https://doi.org/10.1523/JNEUROSCI.12-07-02478.1992>
- Ruitenbergh, M. F. L., Koppelmans, V., Seidler, R. D., & Schomaker, J. (2023). Developmental and age differences in visuomotor adaptation across the lifespan. *Psychol Res*, 87(6), 1710-1717. <https://doi.org/10.1007/s00426-022-01784-7>
- Rushton, S. K., Bradshaw, M. F., & Warren, P. A. (2007). The pop out of scene-relative object movement against retinal motion due to self-movement. *Cognition*, 105(1), 237-245. <https://doi.org/10.1016/j.cognition.2006.09.004>
- Sakata, H., Taira, M., Kusunoki, M., Murata, A., & Tanaka, Y. (1997). The TINS Lecture. The parietal association cortex in depth perception and visual control of hand action. *Trends Neurosci*, 20(8), 350-357. [https://doi.org/10.1016/s0166-2236\(97\)01067-9](https://doi.org/10.1016/s0166-2236(97)01067-9)
- Santodomingo-Rubido, J., Carracedo, G., Suzaki, A., Villa-Collar, C., Vincent, S. J., & Wolffsohn, J. S. (2022). Keratoconus: An updated review. *Cont Lens Anterior Eye*, 45(3), 101559. <https://doi.org/10.1016/j.clae.2021.101559>
- Saunders, J. A., & Chen, Z. (2015). Perceptual biases and cue weighting in perception of 3D slant from texture and stereo information. *J Vis*, 15(2). <https://doi.org/10.1167/15.2.14>
- Scheiman, M., & Wick, B. (2008). *Clinical management of binocular vision: heterophoric, accommodative, and eye movement disorders*. Lippincott Williams & Wilkins.
- Stanislaw, H., & Todorov, N. (1999). Calculation of signal detection theory measures. *Behav Res Methods Instrum Comput*, 31(1), 137-149. <https://doi.org/10.3758/bf03207704>
- Steeves, J. K., Gonzalez, E. G., Gallie, B. L., & Steinbach, M. J. (2002). Early unilateral enucleation disrupts motion processing. *Vision Res*, 42(1), 143-150. [https://doi.org/10.1016/s0042-6989\(01\)00270-x](https://doi.org/10.1016/s0042-6989(01)00270-x)
- Stevenson, S. B., Cormack, L. K., & Schor, C. M. (1989). Hyperacuity, superresolution and gap resolution in human stereopsis. *Vision Res*, 29(11), 1597-1605. [https://doi.org/10.1016/0042-6989\(89\)90141-7](https://doi.org/10.1016/0042-6989(89)90141-7)
- Suttle, C. M., Melmoth, D. R., Finlay, A. L., Sloper, J. J., & Grant, S. (2011). Eye-hand coordination skills in children with and without amblyopia. *Invest Ophthalmol Vis Sci*, 52(3), 1851-1864. <https://doi.org/10.1167/iovs.10-6341>
- Thibos, L. N., Wheeler, W., & Horner, D. (1997). Power vectors: an application of Fourier analysis to the description and statistical analysis of refractive error. *Optom Vis Sci*, 74(6), 367-375. <https://doi.org/10.1097/00006324-199706000-00019>
- Thompson, A. M., & Nawrot, M. (1999). Abnormal depth perception from motion parallax in amblyopic observers. *Vision Res*, 39(7), 1407-1413. [https://doi.org/10.1016/s0042-6989\(98\)00235-1](https://doi.org/10.1016/s0042-6989(98)00235-1)
- Todd, J. T. (1982). Visual information about rigid and nonrigid motion: a geometric analysis. *J Exp Psychol Hum Percept Perform*, 8(2), 238-252. <https://doi.org/10.1037//0096-1523.8.2.238>

- Todorovic, D. (2008). Is pictorial perception robust? The effect of the observer vantage point on the perceived depth structure of linear-perspective images. *Perception*, 37(1), 106-125. <https://doi.org/10.1068/p5657>
- Tyler, C. W. (1975). Spatial organization of binocular disparity sensitivity. *Vision Res*, 15(5), 583-590. [https://doi.org/10.1016/0042-6989\(75\)90306-5](https://doi.org/10.1016/0042-6989(75)90306-5)
- Tyler, C. W. (1989). Two processes control variations in flicker sensitivity over the life span. *J Opt Soc Am A*, 6(4), 481-490. <https://doi.org/10.1364/josaa.6.000481>
- Tyler, C. W. (2019a). Accelerated Cue Combination for Multicue Depth Perception. *Perception*,
- Tyler, C. W. (2019b). Depth cue combination: A quantitative critique. *Perception*, 48(9), 765-768. <https://doi.org/10.1177/0301006619865899>
- Tyler, C. W. (2020). The Intersection of Visual Science and Art in Renaissance Italy. *Perception*, 49(12), 1265-1282. <https://doi.org/10.1177/0301006620974973>
- Ujike, H., & Ono, H. (2001). Depth thresholds of motion parallax as a function of head movement velocity. *Vision Res*, 41(22), 2835-2843. [https://doi.org/10.1016/s0042-6989\(01\)00164-x](https://doi.org/10.1016/s0042-6989(01)00164-x)
- Vemuganti, G. K., Jalali, S., Honavar, S. G., & Shekar, G. C. (2001). Enucleation in a tertiary eye care centre in India: prevalence, current indications and clinicopathological correlation. *Eye (Lond)*, 15(Pt 6), 760-765. <https://doi.org/10.1038/eye.2001.245>
- Verghese, P., Tyson, T. L., Ghahghaei, S., & Fletcher, D. C. (2016). Depth perception and grasp in central field loss. *Invest Ophthalmol Vis Sci*, 57(3), 1476-1487. <https://doi.org/10.1167/iovs.15-18336>
- Vishwanath, D. (2014). Toward a new theory of stereopsis. *Psychol Rev*, 121(2), 151-178. <https://doi.org/10.1037/a0035233>
- Von Helmholtz, H. (1925). *Helmholtz's treatise on physiological optics* (Vol. 3). Optical Society of America.
- Wani, M. A. (2018). Interpretation of stepwise multiple linear regression analysis in behavioral sciences in APA format. *Remarking: An Analisation*(3), 144-149.
- Watson, A. B. (1979). Probability summation over time. *Vision Res*, 19(5), 515-522. [https://doi.org/10.1016/0042-6989\(79\)90136-6](https://doi.org/10.1016/0042-6989(79)90136-6)
- Watt, S. J., & Bradshaw, M. F. (2003). The visual control of reaching and grasping: binocular disparity and motion parallax. *J Exp Psychol Hum Percept Perform*, 29(2), 404-415. <https://doi.org/10.1037/0096-1523.29.2.404>
- Watt, S. J., Bradshaw, M. F., Clarke, T. J., & Elliot, K. M. (2003). Binocular vision and prehension in middle childhood. *Neuropsychologia*, 41(4), 415-420. [https://doi.org/10.1016/s0028-3932\(02\)00174-4](https://doi.org/10.1016/s0028-3932(02)00174-4)
- Wheatstone, C. (1838). On some remarkable and hitherto unobserved phenomena of binocular vision. *Phil Trans Roy Soc, London*, 128, 371-394. <https://www.ncbi.nlm.nih.gov/pubmed/14000225>
- Yuille, A., & Bülthoff, H. (1996). Bayesian Decision Theory and Psychophysics. *Perception as Bayesian Inference*.

Appendix 1

A1. Demographic details

Table A1 Demographic details of the 30 keratoconic participants along with their corneal topographic outcomes (maximum keratometry and D-index) and visual functions (logMAR visual acuity and stereo thresholds) with spectacles and contact lens.

Sub No.	Age (yrs)	Sex	Maximum Keratometry (D)		D-index (unitless)		Visual acuity with spectacles (logMAR)		Stereo threshold with spectacles (arc sec)	Visual acuity with contact lens (logMAR)		Stereo threshold with contact lens (arc sec)
			RE	LE	RE	LE	RE	LE		RE	LE	
1	19	M	45.5	70.8	2.96	16.77	0.00	0.60	841.97	*	0.10	820.65
2	18	M	44.6	79.3	2.13	22.05	0.00	1.10	3372.25	*	0.40	1032.86
3	19	M	55.5	44.1	8.06	0.53	1.40	0.00	800.18	0.00	0.00	62.03
4	19	M	58.5	51.4	7.97	5.51	0.30	0.18	462.70	0.30	0.00	142.78
5	22	M	56.7	48.8	7.94	4.29	0.40	0.00	222.54	0.18	0.00	33.94
6	22	F	67.6	50.7	14.2	6.44	0.70	0.00	1159.30	0.00	*	233.76
7	20	F	44.9	43.0	9.41	4.12	0.18	0.00	63.31	0.10	0.00	56.88
8	25	M	56.6	57.0	7.19	7.89	0.00	0.30	281.38	*	0.00	127.48
9	26	F	48.6	55	3.87	6.89	0.00	0.10	60.62	0.00	0.00	192.58
10	17	M	60.1	52.6	11.09	5.89	0.30	0.18	278.80	0.00	0.00	401.12
11	26	F	61.3	57.1	14.96	16.32	0.30	0.18	584.58	0.00	0.00	145.83
12	32	M	48.5	64.6	7.27	12.8	0.18	0.48	251.90	*	0.00	138.43
13	18	M	62.4	75.5	8.38	16.95	0.18	0.30	1390.05	0.00	0.00	1115.27
14	21	F	53.6	41.4	10.12	3.36	0.70	0.10	1997.88	0.00	*	601.26
15	18	M	56.8	49.8	11.96	6.83	0.40	0.18	855.42	0.00	0.00	169.57
16	24	M	56.1	61.9	9.03	8.7	0.00	0.40	717.63	0.10	0.00	296.03
17	24	M	49.7	50	6.99	6.52	0.18	0.10	200.85	0.00	0.10	134.62
18	25	F	54.4	52.7	4.85	4.63	0.18	0.18	666.34	NA	NA	NA
19	17	M	48.5	55.6	3.38	7.67	0.30	0.30	1855.71	NA	NA	NA
20	34	F	53.2	53.1	4.99	3.58	0.30	0.30	1773.45	NA	NA	NA
21	22	M	63.6	60.2	11.29	10.2	0.18	0.10	146.20	NA	NA	NA
22	28	M	52.9	42.8	5.31	1.35	0.48	0.48	250.76	NA	NA	NA
23	19	M	63.3	55.2	14.44	8.33	0.48	0.18	601.53	NA	NA	NA
24	22	M	44	46	2.27	5.17	0.30	0.18	139.60	NA	NA	NA
25	19	F	65.9	44.6	NA	4	1.10	0.00	4596.21	NA	NA	NA
26	24	F	71.3	50.8	24.6	16.3	0.90	0.18	1118.56	NA	NA	NA
27	20	M	62.4	53.5	11.67	11.24	0.60	0.48	1720.88	NA	NA	NA
28	18	M	62.4	52.5	27.13	10.17	1.60	0.80	1269.90	NA	NA	NA
29	28	F	46.9	54.4	8.09	10.71	0.30	0.40	1927.61	NA	NA	NA
30	17	M	48.9	52.3	9.89	12.49	0.70	1.10	1048.99	NA	NA	NA

Abbreviations: max K: maximum keratometry reading, stereo: stereo threshold, RE: right eye, LE: left eye, SP: spectacle, CL: contact lens, NA: not applicable (these participants were not tested with contact lens correction). Participants 1 – 17 performed the task with both spectacles and contact lenses. The asterisk symbol indicates participants wore contact lens only in one eye, for which the visual acuity is reported. The fellow eye's refractive error was corrected with spectacles, if any. The fellow eye's acuity thus equalled what is reported in columns 8 and 9 of this table. Participants 18 – 30 performed the task with only their spectacles.

Appendix 2

A2.1 Ethic certificate (LVPEI)

Hyderabad Eye Research Foundation

L V Prasad Eye Institute Ethics Committee
Kallam Anji Reddy Campus, Banjara Hills, Hyderabad
Registration No: ECR/468/Inst./AP/2013/RR-19
NABH Registration No: EC-CT-2019-0126

October 23, 2021

Ethics Ref. No. LEC-BHR-P-10-21-766

To:

Ms Preetirupa Devi

Dr Shrikant R Bharadwaj

Principal Investigator

L V Prasad Eye Institute, L V Prasad Marg, Banjara Hills

Hyderabad- 500 034, Telangana

Subject: Ethics Committee Approval Letter for Prospective Study

Protocol Entitled: "Perception of 3D depth in individuals with one functional eye"

Dear Ms Preetirupa Devi, Dr Shrikant R Bharadwaj:

With reference to your Submission for the approval of above prospective proposal, the Institutional Review Board Committee of L V Prasad Eye Institute held on October 23, 2021 had reviewed and discussed in detail the below submitted documents.

1	Protocol
2	Informed Consent Form

It is understood that the study will be conducted under your direction at L.V. Prasad Eye Institute, Hyderabad

It is hereby confirmed that neither you nor any of the members of the study team participated in the decision making/voting procedures.

After consideration, the committee has approved the study for a period of one year (Until closing hour of October 22, 2022)

We hereby confirm that, the Institutional Review Board, L V Prasad Eye Institute is organized and operates as per GCP (Good Clinical Practice) and applicable Indian regulations.

Ethics Committee
L.V. Prasad Eye Institute
Kallam Anji Reddy Campus,
Banjara Hills, Hyderabad-500 034.
Reg.No.ECR/468/Inst./AP/2013/RR-19



L V Prasad Eye Institute, Kallam Anji Reddy Campus, L V Prasad Marg, Banjara Hills, Hyderabad 500034, India
Tel: +91 40 68102020, Fax: +91 40 23548339, Email: info.hyd@lvpei.org, Website: www.lvpei.org

Hyderabad Eye Research Foundation

L V Prasad Eye Institute Ethics Committee
Kallam Anji Reddy Campus, Banjara Hills, Hyderabad
Registration No: ECR/468/Inst./AP/2013/RR-19
NABH Registration No: EC-CT-2019-0126

Please note:

- a. In the events of any protocol amendments, Ethics Committee must be informed and the amendments should be highlighted. All approval of amendments in the projects must be obtained prior to implementation of changes. The amendment is unlikely to be approved by the Ethics Committee unless all the required information is provided.
- b. Any advertisement placed in the newspapers, magazines must be submitted for approval.
- c. The results of the study should be presented in any of the academic forums of the Institute.
- d. Any SAE, which could affect any study, must be communicated to Ethics Committee within 24 hours of their occurrence and evaluate the rate of complications if any.
- e. Any protocol deviation/ waiver in the protocol must be informed to the Ethics Committee
- f. At the time of PI's retirement/intention to leave the institute, the study responsibility should be transferred to a colleague with an approval from the Ethics Committee
- g. For extension of your study you are requested to submit the status (ongoing / closed etc) and progress reports (how many recruited, how many followed up and how many left the study etc.) by mail or hard copy to the Ethic Committee one month before completion of one year of the study period as given above. The decision for extensions would be taken by the Ethics Committee Members and conveyed to PIs in hard copies. Lack of response from PI's regarding the status/inadequate progress reports or no responses beyond deadline would be deemed as closure of the study by the EC and conveyed to the PI who would now have to present the study afresh in the next EC meeting. The EC would also take a decision for PI's who fail to submit progress reports on time and refrain the PI from presenting any further study to the EC until further notice or until reports are submitted and presented in person with reason for delay/ non-response.



LV Prasad Eye Institute, Kallam Anji Reddy Campus, LV Prasad Marg, Banjara Hills, Hyderabad-500034, India
Tel: +91 40 68102020, Fax: +91 40 23548339, Email: info.hyd@lvpei.org Website: www.lvpei.org

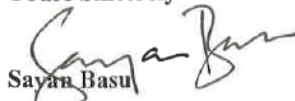
Hyderabad Eye Research Foundation

L V Prasad Eye Institute Ethics Committee
Kallam Anji Reddy Campus, Banjara Hills, Hyderabad
Registration No: ECR/468/Inst./AP/2013/RR-19
NABH Registration No: EC-CT-2019-0126

The following members of the Ethics Committee were present at the meeting held on October 23, 2021 at 5pm in BHERC Conference Room, L V Prasad Eye Institute, KAR Campus, Hyderabad 500034

Name	Qualification	Designation/Title	Gender	Affiliations as to the Institution Yes/No
Mr Vijay Kumar Chejerla	M A.,LLM,FIIL,DPM	Chairperson and Social Scientist	Male	No
Dr Sayan Basu	MBBS, M.S	Member Secretary	Male	Yes
Dr Dilip Kumar Mishra	MBBS, MD	Basic Medical Scientist	Male	Yes
Dr Santosh Kumar B	MBBS, MD Pharmacology	Basic Medical Scientist	Male	No
Ms Aarti Rawat	BA, PG Diploma in Public Relations	Layperson	Female	Yes
Dr Arjun Srirampur	MS Ophthalmology, FRCA, FCAS	Clinician	Male	No
Mrs Amita Desai	MA. M.Ed.	Social Scientist	Female	No
Ms Renuka Rao Donthineni	B Sc , BED, LLB	Legal Expert	Female	No

Yours Sincerely


Sayan Basu

Member Secretary

Ethics Committee
L.V. Prasad Eye Institute
Kallam Anji Reddy Campus,
Banjara Hills, Hyderabad-500 034.
Reg.No.ECR/468/Inst./AP/2013/RR-19

L V Prasad Eye Institute Ethics Committee

L V Prasad Eye Institute, Banjara Hills

Hyderabad- 500 034



LV Prasad Eye Institute, Kallam Anji Reddy Campus, LV Prasad Marg, Banjara Hills, Hyderabad 500034, India
Tel: +91 40 68102020, Fax: +91 40 23548339, Email: info.hyd@lvpei.org, Website: www.lvpei.org

A2.2 Ethic certificate (City St. George's University of London)



Dear Preetirupa

Reference: ETH2122-0689

Project title: Perception of 3D depth in individuals with one-eye

Start date: 15 Jun 2022

End date: 1 Jan 2024

I am writing to you to confirm that the research proposal detailed above has been granted formal approval from the Optometry Proportionate Review Committee. The Committee's response is based on the protocol described in the application form and supporting documentation. Approval has been given for the submitted application only and the research must be conducted accordingly. You are now free to start recruitment.

Please ensure that you are familiar with [City's Framework for Good Practice in Research](#) and any appropriate Departmental/School guidelines, as well as applicable external relevant policies.

Please note the following:

Project amendments/extension

You will need to submit an amendment or request an extension if you wish to make any of the following changes to your research project:

- Change or add a new category of participants;
- Change or add researchers involved in the project, including PI and supervisor;
- Change to the sponsorship/collaboration;
- Add a new or change a territory for international projects;
- Change the procedures undertaken by participants, including any change relating to the safety or physical or mental integrity of research participants, or to the risk/benefit assessment for the project or collecting additional types of data from research participants;
- Change the design and/or methodology of the study, including changing or adding a new research method and/or research instrument;
- Change project documentation such as protocol, participant information sheets, consent forms, questionnaires, letters of invitation, information sheets for relatives or carers;
- Change to the insurance or indemnity arrangements for the project;
- Change the end date of the project.

Adverse events or untoward incidents

You will need to submit an Adverse Events or Untoward Incidents report in the event of any of the following:



- a) Adverse events
- b) Breaches of confidentiality
- c) Safeguarding issues relating to children or vulnerable adults
- d) Incidents that affect the personal safety of a participant or researcher

Issues a) and b) should be reported as soon as possible and no later than five days after the event. Issues c) and d) should be reported immediately. Where appropriate, the researcher should also report adverse events to other relevant institutions, such as the police or social services.

Should you have any further queries relating to this matter, please do not hesitate to contact me. On behalf of the Optometry Proportionate Review Committee, I do hope that the project meets with success.

Kind regards

Michael Powner

Optometry Proportionate Review Committee

City, University of London